UNIVERSITY OF ALBERTA

THE RESPONSE OF HEMATOPOIETIC PROGENITOR CELLS TO TREHALOSE-LOADED LIPOSOMES FOR APPLICATIONS IN CRYOBIOLOGY

by

KIRBY LYNNE SCOTT 

A thesis submitted to the Faculty of Graduate Studies and Research
in partial fulfillment of the requirements for the degree of

Master of Science

in

Medical Sciences – Laboratory Medicine and Pathology

Edmonton, Alberta
Fall 2006

Your file Votre référence
ISBN: 978-0-494-22367-3
Our file Notre référence
ISBN: 978-0-494-22367-3

ABSTRACT

Trehalose is a disaccharide of glucose that has been shown to exhibit protective properties at relatively low concentrations during freezing, when available on both sides of the cell membrane. The major challenge to utilizing trehalose as an intracellular cryoprotectant is that trehalose cannot move passively across biological membranes and mammalian cells do not contain the proper machinery to actively transport this molecule. The human cell line TF-1 was used as a model system to explore the use of liposomes as a vehicle for the intracellular delivery of trehalose. Parameters which influence the interaction between liposomes and TF-1 cells were identified and applied to assess the freezing response of cells following liposomal treatment. Under the conditions tested, a positive correlation between liposomal treatment and post-thaw survival was observed. For this approach to have a significant influence on cryobiology at a clinical level, further investigation is required to increase intracellular trehalose concentrations.

ACKNOWLEDGEMENTS

I wish to express my sincere appreciation to the following individuals, without whom this thesis could not have been completed.

To Dr. Jason Acker, my supervisor, for having faith in me and pushing me beyond what I believed I was capable of.

To Dr. Locksley McGann, my co-supervisor, whose guidance made the road to completion a great experience.

To Dr. Maria Gyongyossy-Issa, our collaborator on this project, whose 'eureka' this work grew from. Her love for life and passion for research is contagious.

To Jelena Holovati, my friend and colleague, whose work ethic and dedication I admire.

To Lisa Purdy, my teaching mentor and committee member. She has been an excellent role model.

To Dr. Judy Hannon, for serving as a committee member, and helping me stay focused on the 'big picture'.

To Dr. Janet Elliot, for her thorough review of this work.

To Dr. Judith Hugh, for serving as my examining committee chairperson.

To Lisa Ross-Rodriguez, who always made time for me, and shared her skills and knowledge.

To Iren Constantinescu, Sandra Marcus and Dorothy Rutkowski, for their technical expertise.

To the members of the Acker and McGann-Elliot Cryolabs, for many good times and the sharing of ideas.

To all of my family and friends who have provided me with love and support throughout my life.

Thank you.

This thesis is dedicated to my family.

Thank you for your love, support and encouragement,

and most of all . . . for believing in me.

TABLE OF CONTENTS

LIST OF TABLES

LIST OF FIGURES

LIST OF ABBREVIATIONS

ABBREVIATIONS

CPA	cryoprotectant
DMSO	dimethyl sulfoxide
HPC	hematopoietic progenitor cells
LUV	large unilamellar vesicle
IIF	intracellular ice formation
E_a	activation energy
L_p	hydraulic conductivity
P_s	cryoprotectant permeability parameter
R	universal gas constant
σ	reflection coefficient
V_b	osmotically-inactive fraction
$[KCl]_i$	intracellular potassium chloride concentration
CR	cooling rate
SC	supercooling
T_g	glass transition temperature
T_m	membrane phase transition temperature
DPPC	1,2-dipalmitoyl-*sn*-glycero-3-phosphocholine
CL	cholesterol
SFM	serum free media (RPMI-1640)
MLV	multi lamellar vesicle
LUVET	large unilamellar vesicle extrusion technique

HBSI	HEPES buffered saline intracellular
KCl	potassium chloride
NaCl	sodium chloride
CF	5(6)-carboxyfluorescein
RT	room temperature (22 ˚C)
7-AAD	7-amino-actinomycin D
PerCP	peridinin chlorophyll protein
PE	R-phycoerythrin
APC	allophycocyanin
FITC	fluorescein isothyocyanate
TG	treatment group
FBS	fetal bovine serum
BSA	bovine serum albumin
dH_20	distilled water
CFU	colony forming unit
GM-CSF	granulocyte-macrophage colony-stimulating factor
EPO	erythropoietin
IL-3	interleukin-3

CHAPTER 1

INTRODUCTION

1.1 GENERAL INTRODUCTION

Mother Nature has given birth to millions of species with biological capabilities which were acquired out of necessity through adaptation and evolution. Scientists often study natural systems to find answers to complex questions which cannot be explained using conventional methods. The study of freeze-tolerant and desiccation-tolerant species is a prime example of how nature has influenced advances in medicine. Cryobiologists are scientists dedicated to the study of life at low temperatures and they play an increasingly important role in transfusion, transplantation and regenerative medicine. With the development of engineered tissues and the growing demand for blood and tissue banks, preservation of biological structure and function *ex vivo* is a crucial requirement for the successful utilization of these biological components in medicine. Cryopreservation prevents significant changes to the physicochemical properties of the system by suppressing molecular motions and in some cases arresting metabolic and biochemical reactions all together. Although cryopreservation is not a requirement for autologous transfusion or transplantation, degradation of structure and function during hypothermic storage is a problem. Freezing and storage at low (< -135 °C) temperatures is currently the only technology available which facilitates long term storage of

biological materials while maintaining functional, structural and biological characteristics.

The primary challenge to developing a successful freezing protocol is minimizing the damage associated with the formation of ice crystals and the resulting change in solution properties that occur in the intra- and extracellular environment. Cryopreservation was first made possible after the serendipitous discovery of the cryoprotective properties of glycerol in 1949 (1). Since that time a number of other cryoprotective chemicals have been identified. Commonly used cryoprotectants (CPA) are classified as either non-permeating or permeating. Non-permeating CPAs include sugars, large polymers such as polyvinyl pyrrolidone and polyethylene glycol, and starches such as hydroxyethyl starch. Lower molecular weight compounds such as dimethyl sulfoxide (DMSO) and alcohols like glycerol and propylene glycol readily diffuse across the plasma membrane and fall in the class of permeating CPAs. The mechanism of action of these CPAs differs depending on their classification within the two groups (2-4). In general, CPAs act colligatively to alter intra- and extracellular solution properties, reduce the amount of ice formed at any given temperature, and buffer the concentration of other solutes during dehydrating stresses such as freezing (5, 6). One major concern with most conventional CPAs is their associated toxicity, especially at ambient temperatures (7) and at increasing concentrations as ice forms during freezing at low temperatures (8-10). Formulations which combine permeating and non-permeating CPAs and freezing protocols designed to limit the amount of time cells are exposed to

increasing solute concentrations are common approaches to confer cryoprotection while reducing toxicity (11-13).

1.2 CRYOPRESERVATION OF STEM CELLS

Autologous or allogeneic "stem" cells collected from the bone marrow, peripheral blood, or umbilical cord blood are used for reestablishing hematopoiesis in patients following chemotherapy or irradiation therapy. Due to a progressive loss of hematopoietic progenitor cells (HPC) during non-frozen storage, sources of stem cells used in cancer treatment are often cryopreserved and stored at low temperatures until required. Regardless of the cryopreservation protocol, all existing methods for stem cell cryopreservation require DMSO as the primary CPA.

A successful cryopreservation protocol utilizing DMSO requires a fine balance between protection from freeze damage, and the occurrence of cryoprotectant-induced toxicity. The toxicity of DMSO has been attributed to poor cell viability and clonogenic activity (14), a loss of mature blood cells, as well as numerous transient and dose-dependent infusion-related reactions (15-20). While post-thaw cell processing reduces the amount of DMSO infused (14), processing may contribute to a decrease in myeloid precursor cells necessary for successful engraftment (21). Manual processing and open systems also increase the risk of bacterial contamination (18). Attempts to reduce the cost and complexity of HPC cryopreservation processes using mechanical freezers for freezing and storage may increase the rate of cell loss due to degradative

biochemical activity at higher storage temperatures (15). The risk of DMSO toxicity at higher storage temperatures may also contribute to cell loss. Considering the growing number of clinical applications for both hematopoietic and non-hematopoietic stem cells, there is a renewed interest in improving the outcome for cryopreservation of stem cells (22).

1.3 NOVEL CPAs

In order to address the limitations associated with current cryopreservation practices, a major focus of biopreservation research has been on the development of alternative cryopreservation methods including investigation into novel, non-toxic CPAs. A number of freeze-tolerant and desiccation tolerant organisms, including vertebrates, insects, fungi, plants, and micro-organisms, respond to environmental stress by accumulating low molecular weight carbohydrates, such as glucose, trehalose and polyols (23-26). These carbohydrates help provide colligative resistance to cell volume changes, relieving osmotic stress and the cellular toxicity resulting from increased intracellular osmolality during freezing (26). Glycogen reserves in the liver get converted to glucose which can be transported across the cell membrane into the intracellular spaces, however utilization of trehalose, a membrane impermeable non-reducing disaccharide of glucose, requires specialized enzymatic pathways for synthesis and degradation (27, 28).

Trehalose is primarily found in high concentrations (up to 20 % dry weight) in desiccation tolerant organisms (25, 29-31) and as a result has gained attention

as a potential agent that may confer protection on biological materials during freezing and freeze-drying. Trehalose has the ability to stabilize the structure of biological membranes during dehydration, inhibiting morphological and functional changes associated with exposure to low temperatures (29, 32-34), and helps to maintain the native conformation of proteins during freezing and freeze-drying (35-39). In addition, trehalose exhibits a number of thermophysical properties in aqueous solutions which may contribute to its efficacy at low temperatures (39, 40) and relatively low concentrations (< 200 mmol/L) (41-43).

The major impediment to utilizing trehalose as the primary constituent of biopreservation solutions is the membrane impermeable nature of this molecule which has been shown to be required on both sides of the cell membrane for optimal protection (41, 42, 44-47). The protective capabilities of trehalose have been demonstrated during cryopreservation or lyophilization in a number of biological systems including liposomes (47), bacteria (48, 49), yeast (44, 46), islets (50), keratinocytes (42), fibroblasts (41, 42, 51), stem cells (43, 52), platelets (53), and red blood cells (45, 54). Techniques used to permeabilize cells for loading trehalose include electroporation (55, 56), gene transfection (57), controlled loading using a genetic mutant of the pore forming protein α-hemolysin from *Staphylococcus aureus* (42, 43, 58), thermal shock (50, 53, 59), cellular fluid-phase endocytosis (60) and more recently, laser-induced pore formation (61) and transient permeabilization using the ATP-dependent P2Z receptor channel (52). Each technique has its own limitations, primarily with

regard to the low concentrations of trehalose that can be achieved intracellularly. In the case of the bacteria-derived pore-forming protein, while quite successful at loading cryoprotective concentrations of trehalose into various human cell types, this method cannot be transferred to clinical use. Reversible cell permeabilization using the P2Z receptor is a promising approach which has led to the successful cryopreservation of HPCs in a single study (52) but its use is limited to cells that express this protein.

1.4 A NEW LOADING METHOD

The focus of several projects in our lab is to look at an alternative approach to loading trehalose into mammalian cells. Liposomes are microscopic structures composed of one or more concentric lipid bilayers (lamellae) with an aqueous compartment separating each lamella. The bilayer membrane is composed of discrete lipid molecules which separate the internal compartment from the external medium (62). Liposomes can be synthesized to conform to a variety of sizes, shapes and compositions, depending on the application. Liposomes were originally used as model membrane systems to study the structural elements of the lipid bilayer such as membrane fluidity, permeability, and molecular and physicochemical organization, as well as the interaction of membrane-active drugs with lipids (63, 64). More recently liposomes have been used to promote cell-cell fusion, alter membrane content and transfer water-soluble impermeant molecules into cells (64). Liposomes can be used to entrap both lipophilic and hydrophilic compounds for a number of applications including

microencapsulation of therapeutic agents such as drugs and enzymes as well as the delivery of genetic material for gene therapy and protein targeting (65, 66). Liposomal delivery of biologically active compounds is attractive due to their versatility and because liposomes are a relatively non-toxic vector which could potentially reduce host inflammatory and immune responses (67). Applications involving liposomes have been applied to a wide range of disciplines and liposomes are currently FDA-approved for drug delivery in the pharmaceutical industry (68).

1.5 HYPOTHESIS[1]

Liposomes can be used as a vehicle for the delivery of trehalose to the intracellular compartment of nucleated mammalian cells, which would then provide protection to the cells during freezing and thawing.

1.6 OBJECTIVES AND APPROACH

The extensive use of lipid vesicles over a diverse range of disciplines is possible primarily because of their versatility which allows a variety of materials to be entrapped in the aqueous compartment and inserted into the vesicle membrane. Additional characteristics include the synthesis of liposomes from natural, biodegradable, nontoxic, and non-immunogenic lipid molecules. Combined, these characteristics make liposomes an attractive vehicle for the delivery of intracellular trehalose which has potential applications in cryobiology.

[1] The concept of using liposomes as a delivery vehicle for intracellular trehalose is a direct result of collaborative work between Dr. Maria Gyongyossy-Issa and Dr. Jason Acker.

In order to prove the hypothesis, it will be necessary to demonstrate the delivery of liposomal contents into the target cell population, and show that a direct correlation exists between liposomal treatment and cell survival during low temperature exposure. Four studies have been designed to investigate the feasibility of utilizing liposomes to overcome the permeability barrier of trehalose to nucleated human cells.

1. ***To explore the osmotic response of cells to freezing in the presence of low concentrations of intra- and/or extracellular trehalose.***

   The design of condition-specific cryopreservation protocols is required to minimize cell volume changes during CPA addition and removal, and to limit the time cells are exposed to concentrated solutes. Both of these conditions are governed by the cellular osmotic responses during cooling, which depends on the type of CPA and cell-specific membrane properties. The osmotic responses of cells to low temperature exposure under variable conditions can be predicted theoretically using computer modeling. Due to the impermeable nature of trehalose it is difficult to determine the extent of its ability to protect against cryoinjury. Computer modeling will be used to explore the role of trehalose as a cryoprotective agent by studying cellular osmotic changes that occur during cooling in the presence of low concentrations of intra- and/or extracellular trehalose.

2. ***To develop a reliable and reproducible technique for the synthesis of trehalose-loaded liposomes, that can be well characterized.***

   A number of techniques have been established to synthesize liposomes of variable sizes (69-74). The liposome synthesis technique selected for this study will be based on the method of extrusion which has been shown to produce a relatively homogenous population of large unilamellar vesicles (LUVs) (69, 74). The reliability and reproducibility of this technique will be assessed by developing methods to characterize the final liposomal product. Characterization will help to define measurable properties which can then be compared from one preparation to the next as a method of quality control to reduce experimental variability.

3. ***To identify the parameters which influence liposome-cell interaction.***

   An assessment of biological compatibility between cells and liposomes, and the identification of parameters which influence liposomal-cell interaction will be explored. Liposomes containing a membrane impermeable fluorescent marker will be combined with cells under variable experimental conditions. Flow cytometric assessment of cellular fluorescence will be used as an indirect indicator of liposome-cell association. Immunophenotyping will be performed to determine the effect liposomes have on the expression of surface antigens involved in cell proliferation and differentiation. These two approaches combined will help to determine the interaction between liposomes and cells and identify conditions which influence this interaction.

4. ***To determine the response of cells to freezing conditions following liposomal treatment.***

The parameters identified to influence the intracellular delivery of liposomal contents will be applied to explore the potential of this approach for applications in cryobiology. The response of cells to freezing following exposure to trehalose-loaded liposomes, either in the presence or absence of extracellular trehalose, will be compared to cells frozen without cryoprotection. The results of this study will be used to assess the utility of liposomes in the delivery of cryoprotective concentrations of intracellular trehalose.

1.7 REFERENCES

1. Polge C, Smith AU, Parkes AS. Revival of spermatozoa after vitrification and dehydration at low temperatures. Nature 1949;164:666.
2. Meryman HT. Cryoprotective agents. Cryobiology 1971;8(2):173-183.
3. McGann LE. Differing actions of penetrating and nonpenetrating cryoprotective agents. Cryobiology 1978;15:382-390.
4. Meryman H. Freezing injury and its prevention in living cells. Ann Rev Biophys Bioeng 1974;3:341-63.
5. Connor W, Ashwood-Smith MJ. Cryoprotection of mammalian cells in tissue culture with polymers; possible mechanisms. Cryobiology 1973;10(6):488.

6. Farrant J. Is there a common mechanism of protection of living cells by polyvinylpyrrolidone and glycerol during freezing? Nature 1969;222(5199):1175.

7. Arakawa T, Carpenter J, Kita Y, Crowe J. The basis for toxicity of certain cryoprotectants: A hypothesis. Cryobiology 1990;27:401-415.

8. Fahy GM. The relevance of cryoprotectant "toxicity" to cryobiology. Cryobiology 1986;23(1):1.

9. Fahy GM, Lilley TH, Linsdell H, Douglas MSJ, Meryman HT. Cryoprotectant toxicity and cryoprotectant toxicity reduction: In search of molecular mechanisms. Cryobiology 1990;27(3):247.

10. Fahy GM, MacFarlane DR, Angell CA, Meryman HT. Vitrification as an approach to cryopresevation. Cryobiology 1984;21:407-26.

11. Ross-Rodriguez LU, Elliot JAW, McGann LE. Experimental correlation and optimization of a theoretically-designed cryopreservation protocol. Cryobiology 2006 (*submitted*).

12. Ross-Rodriguez LU. Using simulations to design a cryopreservation procedure for hematopoietic stem cells without DMSO, Master of Science, Medical Sciences - Laboratory Medicine and Pathology. Edmonton: University of Alberta; 2003.

13. Boutron P, Peyridieu J. Reduction in toxicity for red blood cells in buffered solutions containing high concentrations of 2,3-butanediol by trehalose, sucrose, sorbitol, or mannitol. Cryobiology 1994;31:367-373.

14. Rubinstein P, Dobrila L, Rosenfield RE, Adamson JW, Migliaccio G, Migliaccio AR, et al. Processing and cryopreservation of placental/umbilical cord blood for unrelated bone marrow reconstitution. Proc Natl Acad Sci U S A 1995;92:10119-10122.

15. Hubel A. Cryopreservation of HPCs for clinical use. Transfusion 2001;41:579-580.

16. Davis JM, Rowley SD, Braine HG. Clinical toxicity of cryopreserved bone marrow graft infusion. Blood 1990;75(3):781-786.

17. Rowley SD. Hematopoietic stem cell cryopreservation: A review of current techniques. J Hematother 1992;1:233-250.

18. Stroncek DF, Fautsch SK, Lasky LC, Hurd DD, Ramsay NKC, McCullough J. Adverse reactions in patients transfused with cryopreserved marrow. Transfusion 1991;31:521-526.

19. Lopez-Jimenez J, Cervero C, Munoz A, Hdez-Madrid A, Fernandez Pineda J, Garcia Larana J, et al. Cardiovascular toxicities related to the infusion of cryopreserved grafts: Results of a controlled study. Bone Marrow Transplant 1994;13:789-793.

20. Alessandrino EP, Bernasconi P, Caldera D, Colombo A, Bonfichi M, Malcovati L, et al. Adverse events occurring during bone marrow or peripheral blood progenitor cell infusion: analysis of 126 cases. Bone Marrow Transplant 1999;23:533-537.

21. O'Donnell J, Burnett A, Sheehan T, Tansey P, McDonald G. Safety of dimethyl sulphoxide. Lancet North Am Ed 1981:498.

22. Fleming KK, Hubel A. Cryopreservation of hematopoietic and non-hematopoietic stem cells. Transf Apher Sci 2006;34:309-315.

23. Storey KB. Living in the cold: freeze-induced gene responses in freeze-tolerant vertebrates. Clin Exp Pharmacol Physiol 1999;26:57-63.

24. Potts M. Desiccation tolerance of prokaryotes. Microbiol Rev 1994;58(4):755-805.

25. Crowe JH, Hoekstra FA, Crowe LM. Anhydrobiosis. Annu Rev Physiol 1992;54:579-99.

26. Storey KB, Storey JM. Physiology, biochemistry and molecular biology of vertebrate freeze tolerance: The wood frog. In: Fuller BJ, Lane N, Benson EE, editors. Life in the frozen state. 1 ed: CRC Press; 2004. p. 243-74.

27. Elbein AD. The metabolism of alpha, alpha-trehalose. Adv Carbohydr Chem Biochem 1974;30:227-256.

28. Birch GG. Trehaloses. Adv Carbohydr Chem 1963;18:201-225.

29. Crowe LM, Mouradian R, Crowe JH, Jackson SA, Womersley C. Effects of carbohydrates on membrane stability at low water activities. Biochim Biophys Acta 1984;769:141-150.

30. Clegg JS. The origin of trehalose and its significance during the formation of encysted dormant embryos of Artemia Salina. Comp Biochem Physiol 1965;14:135-143.

31. Crowe JH, Crowe LM. Preservation of mammalian cells-learning nature's tricks. Nature Biotechnol 2000;18:145-146.

32. Womersley C, Uster PS, Rudolph AS, JH C. Inhibition of dehydration-induced fusion between liposomal membranes by carbohydrates as measured by fluorescence energy transfer. Cryobiology 1986;23:245-255.

33. Crowe JH, Crowe LM, Chapman D. Preservation of membranes in anhydrobiotic organisms: The role of trehalose. Science 1984;223:701-703.

34. Crowe JH, Crowe LM, Carpenter JF, Rudolph AS, Wistrom CA, Spargo BJ, et al. Interactions of sugars with membranes. Biochim Biophys Acta 1988;947:367-384.

35. Carpenter JF, Crowe LM, Crowe JH. Stabilization of phosphofructokinase with sugars during freeze-drying: Characterization of enhanced protection in the presence of divalent cations. Biochim Biophys Acta 1987;923:109-115.

36. Crowe JH, Crowe LM, Carpenter JF, Aurell Wistrom C. Stabilization of dry phospholipid bilayers and proteins by sugars. Biochem J 1987;242:1-10.

37. Crowe JH, Crowe LM, Jackson SA. Preservation of stuctural and functional activity in lyophilized sarcoplasmic reticulum. Arch Biochem Biophys 1983;220(2):477-484.

38. Allison SD, Chang B, Randolph TW, Carpenter JF. Hydrogen bonding between sugar and protein is responsible for inhibition of dehydration-induced protein unfolding. Arch Biochem Biophys 1999;365(2):289-298.

39. Xie G, Timasheff SN. The thermodynamic mechanism of protein stabilization by trehalose. Biophys Chem 1997;64:25-43.

40. Miller DP, de Pablo J, Corti H. Thermophysical properties of trehalose and its concentrated aqueous solutions. Pharm Res 1997;14(5):578-590.

41. Chen T, Acker JP, Eroglu A, Cheley S, Bayley H, Fowler A, et al. Beneficial effect of intracellular trehalose on membrane integrity of dried mammlian cells. Cryobiology 2001;43:168-181.

42. Eroglu A, Russo MJ, Bieganski R, Fowler A, Cheley S, Bayley H, et al. Intracellular trehalose improves the survival of cryopreserved mammalian cells. Nature Biotechnol 1999;18:163-167.

43. Buchanan S, Gross S, Acker J, Toner M, Carpenter J, Pyatt D. Cryopreservation of stem cells using trehalose: Evaluation of the method using a human hematopoietic cell line. Stem Cells Dev 2004;13:295-305.

44. Cerrutti P, Segovia de Huergo M, Galvagno M, Schebor C, del Pilar Buera M. Commercial baker's yeast stability as affected by intracellular content of trehalose, dehydration procedure and the physical properties of external matrices. Appl Microbiol Biotechnol 2000;54:575-580.

45. Goodrich RP, Sowemimo-Coker SO. Freeze-drying of red blood cells. Adv Low Temp Biol 1993;2:53-99.

46. Leslie S, Israeli E, Lighthart B, Crowe J, Crowe L. Trehalose and sucrose protect both membranes and proteins in intact bacteria during drying. Appl Environ Microbiol 1995;61(10):3592-3597.

47. Crowe LM, Crowe JH, Rudolph A, Womersley C, Appel L. Preservation of freeze-dried liposomes by trehalose. Arch Biochem Biophys 1985;242(1):240.

48. Conrad P, Miller D, Cielenski P, de Pablo J. Stabilization and preservation of *Lactobacillus acidophilus* in saccharide matrices. Cryobiology 2000;41:17-24.

49. Israeli E, Shaffer B, Lighthart B. Protection of freeze-dried *Escherichia coli* by trehalose upon exposure to environmental conditions. Cryobiology 1993;30:519-523.

50. Beattie G, Crowe J, Lopez A, Cirulli V, Ricordi C, Hayek A. Trehalose: A cryoprotectant that enhances recovery and preserves function of human pancreatic islets after long-term storage. Diabetes 1997;46:519-523.

51. Acker JP, Fowler A, Lauman B, Cheley S, Toner M. Survival of desiccated mammalian cells: Beneficial effects of isotonic media. Cell Preserv Technol 2002;1(2):129-140.

52. Buchanan SS, Menze MA, Hand SC, Pyatt DW, Carpenter JF. Cryopreservation of human hematopoietic stem and progenitor cells loaded with trehalose: Transient permeabilization via the adenosine triphophate-dependent P2Z receptor channel. Cell Preserv Technol 2005;3(4):212-222.

53. Wolkers W, Walker N, Tablin F, Crowe J. Human platelets loaded with trehalose survive freeze-drying. Cryobiology 2001;42:79-87.

54. Goodrich RP, Sowemimo-Coker SO, Zerez CR, Tanaka KR. Preservation of metabolic activity in lyophilized human erythrocytes. Proc Natl Acad Sci U S A 1992;89:967-971.

55. Mussauer H, Sukhorukov, VL., Zimmermann U. Trehalose improves survival of electrotransfected mammalian cells. Cytometry 2001;45:161-169.

56. Shirikashi R, Kostner CM, Muller KJ, Kurschner M, Zimmerman U, Sukhorukov VL. Intracellular delivery of trehalose into mammalian cells by electropermeabilization. J Membr Biol 2002;189:45-54.

57. Guo Ning PI, Brown D, Mansbridge J, Levin F. Trehalose expression confers desiccation tolerance on human cells. Nature Biotechnol 2000;18:168-71.

58. Acker JP, Lu X, Young V, Cheley S, Bayley H, Fowler A, et al. Measurement of trehalose loading of mammalian cells porated with a metal-actuated switchable pore. Biotechnol Bioeng 2003;82(5):525-532.

59. Satpathy GR, Torok Z, Bali R, Dwyre DM, Little E, Walker NJ, et al. Loading red blood cells with trehalose: a step towards biostabilization. Cryobiology 2005;51(3):290-305.

60. Oliver AE, Jamil K, Crowe JH, Tablin F. Loading human mesenchymal stem cells with trehalose by fluid-phase endocytosis. Cell Preserv Technol 2004;2(1):35-49.

61. Kohli V, Acker JP, Elezzabi AY. Reversible permeabilization using high-intensity femtosecond laser pulses: Applications to biopreservation. Biotechnol Bioeng 2005;92(7):889-899.

62. Philippot JR, Schuber F. Liposomes as tools in basic research and industry. Boca Raton: CRC Press; 1994.

63. Pagano RE. Interactions of liposomes with mammalian cells. Ann Rev Biophys Bioeng 1978;7:435-68.

64. Poste G, Papahadjopoulos D, Vail WJ. Lipid vesicles as carriers for introducing biologically active materials into cells. In: Methods in Cell Biology: Academic Press; 1976. p. 33-71.

65. Aksentijevich I, Pastan I, Lunardi-Iskandar Y, Gallo RC, Gottesman MM, Thierry AR. In vitro and in vivo liposome-mediated gene transfer leads to human MDR1 expression in mouse bone marrow progenitor cells. Hum Gene Ther 1996;7:1111-1122.

66. Tari A, Khodadadian M, Ellerson D, Deisseroth A, Lopez-Berestein G. Liposomal delivery of oligodeoxynucleotides. Leuk Lymphoma 1996;21:93-97.

67. Colin M, Maurice M, Trugnan G, Kornprobst M, Harbottle RP, Knight A, et al. Cell delivery, intracellular trafficking and expression of an integrin-mediated gene transfer vector in tracheal epithelial cells. Gene Ther 2000;7:139-152.

68. Lian T, Ho RJY. Trends and developments in liposome drug delivery systems. J Pharm Sci 2001;90(6):667-680.

69. Hope MJ, Bally MB, Webb G, Cullis PR. Production of large unilamellar vesicles by a rapid extrusion procedure. Characterization of size distribution, trapped volume and ability to maintain a membrane potential. Biochim Biophys Acta 1985;812:55-65.

70. Barenholzt Y, Amselem S, Lichtenberg D. A new mothod for preparation of phospholipid vesicles (liposomes) - French press. FEBS Lett 1979;99(1):210-214.

71. Batzri S, Korn ED. Single bilayer liposomes prepared without sonication. Biochim Biophys Acta 1973;298(4):1015-1019.

72. Enoch HG, Strittmatter P. Formation and properties of 1000-A-diameter, single-bilayer phospholipid vesicles. Proc Natl Acad Sci U S A 1979;76(1):145-149.

73. Kagawa Y, Racker E. Partial resolution of the enzymes catalyzing oxidative phosphorylation. IX. Reconstruction of oligomycin-sensitive adenosine triphosphatase. J Biol Chem 1966;241(10):2467-2474.

74. Olson F, Hunt CA, Szoka FC, W.J. V, Papahadjopoulos D. Preparation of liposomes of defined size and distribution by extrusion through polycarbonate membranes. Biochim Biophys Acta 1979;557:9-23.

CHAPTER 2

COMPUTER MODELING OF CELLULAR OSMOTIC RESPONSES TO FREEZING IN THE PRESENCE OF TREHALOSE

2.1 INTRODUCTION

When cells are exposed to low temperatures, a number of physical processes take place. Ice forms as water freezes in the extracellular environment and solutes concentrate in the unfrozen fraction of the extracellular solution. An efflux of water from the cell, with a corresponding decrease in cell volume, occurs in response to the changing extracellular environment and the resulting difference in chemical potential across the cell membrane. The magnitude of change in cell volume is dependent on the cooling rate, the permeability of the cell membrane to water and the temperature dependence of the permeability. Rapid cooling inhibits water movement out of the cell due to the changing kinetics and decreased permeability of the plasma membrane to water at low temperatures (1, 2). With a large volume of intracellular water remaining, the cell becomes increasingly supercooled as temperature continues to decrease (2). Supercooling (SC) is defined as the number of degrees below its freezing point that a solution has cooled before ice nucleation occurs. As the cell becomes increasingly supercooled, there is an increased probability of intracellular ice nucleation followed by the spontaneous formation of small ice crystals in the cell cytoplasm, referred to as intracellular ice formation (IIF) (3). IIF has been associated with cell death (4-6) therefore cooling protocols are

generally designed to prevent IIF by limiting the degree of intracellular SC the cell is subjected to during low temperature exposure.

When cooling rates are sufficiently low, cells are able to maintain equilibrium with the increasingly concentrated extracellular environment by exosmosis, resulting in cellular dehydration (1, 2). The combined effects of slow cooling include cell shrinkage (7), biochemical damage on lengthy exposure to high solute concentrations (8, 9) and cellular deformations due to the constraining forces of ice crystals which confine cells in the diminishing unfrozen fraction (4), defined as slow cooling injury or otherwise referred to as 'solution effects' (3).

The osmotic response of cells to low temperature exposure can be predicted theoretically using computer modeling. As a result, computer modeling has become a valuable tool in cryobiology for the purpose of aiding in the design of protocols for CPA addition and removal which minimize osmotic stresses on the cell and limit exposure time to CPAs (10, 11) or to correlate theoretical approaches in cryobiology with biological outcomes (12). Due to the impermeable nature of trehalose it is difficult to experimentally determine the extent of its ability to protect against cryoinjury. With the aid of computer modeling the outcome of conditions which are not easily tested experimentally can be predicted theoretically.

Accurately predicting the osmotic response of a cell to low temperatures using computer modeling requires a number of osmotic parameters that can be calculated from cell volume measurements and solution properties specific to the cell system in question. The first two parameters, hydraulic conductivity (L_p)

and the cryoprotectant permeability parameter (P_s), describe water and solute movement across the cell membrane, respectively and are calculated based on the model of Johnson and Wilson (13):

$$\frac{dV}{dt} = L_p \cdot A \cdot R \cdot T(\pi_i - \pi_e) \qquad \text{(Eq 2.1)}$$

$$\frac{dS}{dt} = P_s \cdot A(\Delta C_s) + (1-\sigma)\frac{\bar{c}_s}{2} \cdot \frac{dV}{dt} \qquad \text{(Eq 2.2)}$$

where V is the water volume in the cell (μm^3), t is the time (min), L_p is the hydraulic conductivity, A is the cell surface area (μm^2), R is the universal gas constant (kcal/mol/K), T is the absolute temperature (K), π_e is the extracellular osmolality (osmoles/kg water), π_i is the intracellular osmolality (osmoles/kg water), and ΔC_s is the difference between the intracellular and extracellular solute concentration.

The reflection coefficient (σ) is used to account for the interaction of water and solutes in the cell membrane. The activation energies (E_a) for L_p and P_s are temperature dependent parameters which describe the energy required for a permeant molecule to diffuse across the cell membrane. The Arrhenius equation represents the linear relationship between the logarithm of the membrane permeability parameter and the inverse of the absolute temperature and is used to calculate E_a (14). The osmotically-inactive fraction (V_b) of the cell is the fraction of the isotonic cell volume not involved in the osmotic activities of the cell. V_b is calculated from equilibrium cell volume measurements in response to anisotonic environments using the Boyle van't Hoff relationship (15). Phase diagrams are the final required element and are used to calculate

temperature related concentrations of intra- and extracellular components present in the simulated environment (2, 16, 17). Based on these equations, a computer simulation program was developed by Dr. Locksley McGann, which enables theoretical predictions of cell volume changes in response to low temperatures.

A user interface of the program is shown in Figure 2.1, indicating the input required for operating the program. Cellular osmotic permeability parameters were taken from the thesis of Lisa Ross-Rodriguez (12, 18) and are summarized in Table 2.1(a), (b) and (c). The cellular osmotic parameters which include the isotonic cell volume (V_o), V_b, L_p and E_a for L_p, were for the human cell line TF-1 (American Type Culture Collection (ATCC), CRL-2003, VA, USA) which is used as a model cell system for HPCs in this and subsequent studies, to test the hypothesis outlined in Chapter 1.

Mazurs' two-factor hypothesis of freezing injury (3) which uses intracellular solute concentrations and supercooling as predictors of cryoinjury, was used to interpret simulation results. The maximum degree of intracellular supercooling (SC) was used as an indicator of IIF. When the cytoplasm is supercooled greater than 10 °C there is an increased probability of ice nucleation followed by IIF (19) therefore 10 °C was used as the upper limit to tolerable intracellular supercooling. Maximum intracellular potassium chloride concentration ($[KCl]_i$) was used as an indicator of solution effects injury where 'tolerable' concentrations of $[KCl]_i$ are defined as $\leq$1 mol/kg. This limit was selected based on experimental observations by Mazur and colleagues that cell survival

dropped to below 20 % for salt concentrations ≥2 mol/kg but remained above 80 % for salt concentrations < 1 mol/kg (4).

2.2 THEORETICAL METHODOLOGY

Computer simulations were used to predict the osmotic response of TF-1 cells exposed to low temperatures at variable cooling rates from 1 °C/min – 100 °C/min in the presence of (i) no CPA, (ii) extracellular trehalose (0.1, 0.2, and 0.3 mol/kg), (iii) intracellular trehalose (0.1, 0.2, and 0.3 mol/kg), (iv) intra- and extracellular trehalose (0.1, 0.2, and 0.3 mol/kg), and (v) 10 % or 1.559 mol/kg DMSO (standard conditions for cryoprotection). The cooling protocol for each condition involved cooling from 25 °C to 0 °C at 100 °C/min followed by cooling to -40 °C at controlled rates varying from 1 °C/min to 100 °C/min. Conditions (ii) (iii) and (v) required an initial hold step, determined by the time required for osmotic equilibrium, allowing cells to reach equilibrium cell volume. This ensured that cells were in osmotic equilibrium at the onset of cooling. Hold times were 3 minutes and 4 minutes for trehalose and DMSO, respectively.

2.3 RESULTS

Low Temperature Exposure in the Absence of a CPA

Predicted osmotic responses of TF-1 cells cooled to -40 °C at cooling rates (CR) ranging from 1 °C/min to 100 °C/min without a CPA is shown in Figure 2.2. As CR increases maximum supercooling increases. At cooling rates < 20 °C/min, maximum SC of the cell cytoplasm does not exceed the tolerable upper limit of

10 °C. At CRs > 20 °C/min, maximum SC would exceed 10 °C, increasing the probability of IIF. Increasing CRs have the opposite effect on maximum $[KCl]_i$. At CRs < 50 °C/min, there is a marked increase in $[KCl]_i$. With no CR where both SC and intracellular solute concentrations can be maintained within tolerable limits, the simulations predict low cell survival over the entire range of CRs in the absence of a CPA.

Osmotic Response to Freezing with Extracellular Trehalose

When trehalose is restricted to the extracellular environment, the cell is shrunken below isotonic cell volume prior to cooling (Figure 2.8). The result of simulations of TF-1 cells cooled at different rates in the presence of extracellular trehalose is shown in Figure 2.3. The cellular response in the absence of a CPA is included for comparison. Extracellular trehalose decreases the maximum degree of SC over the entire range of CRs but has the opposite effect on $[KCl]_i$. The addition of extracellular trehalose increases the maximum tolerable CR up to 30 °C/min with 0.3 mol/kg trehalose. With no CR that maintains SC and $[KCl]_i$ within tolerable limits, the simulations predict that extracellular trehalose, at the concentrations examined, will not provide cryoprotection for these cells.

Osmotic Response to Freezing with Intracellular Trehalose

When trehalose is restricted to the intracellular environment, the cell is swollen above isotonic cell volume prior to cooling (Figure 2.8) and the osmotic response (Figure 2.4) is opposite to that seen with extracellular trehalose. Intracellular trehalose increases the maximum SC and reduces $[KCl]_i$ in a

concentration dependent manner. In the presence of 0.3 mol/kg trehalose, SC exceeds 10 °C at CRs above 10 °C/min. Maximum $[KCl]_i$ is reduced over the entire range of CRs when intracellular trehalose is present, but exceeds the tolerable limit at CRs > 50 °C/min. The effect of intracellular trehalose on maximum $[KCl]_i$ becomes more pronounced as CR decreases. As the trehalose concentration increases, the degree of SC increases and $[KCl]_i$ decreases. The response is shown by a left shift of the graph with respect to cells frozen without a CPA. Cell survival is predicted to be low because no CR maintains both SC and $[KCl]_i$ within tolerable limits.

Osmotic Response to Freezing in the Presence of Intra- and Extracellular Trehalose

When trehalose is present in the intra- and extracellular environment, the cell is at isotonic cell volume prior to cooling (Figure 2.8). The predicted osmotic response of TF-1 cells to low temperature exposure over a range of linear CRs in the presence of low ($\leq$ 0.3 mol/kg) concentrations of both intra- and extracellular trehalose is shown in Figure 2.5. Under these conditions the maximum SC exceeds 10 °C at CRs > 20 °C/min and $[KCl]_i$ is reduced at lower CRs, with little change seen at CRs higher than 50 °C/min. The CRs predicted to avoid IIF are the same as without a CPA (< 20 °C/min) while CRs > 50 °C are most effective for maintaining low concentrations of intracellular KCl. Based on these results the simulations do not identify a CR that is optimal for reducing both the maximum SC and $[KCl]_i$ therefore survival of TF-1 cells is predicted to

be low over the entire range of CRs when trehalose is present at low concentrations in both the intra- and extracellular spaces.

Osmotic Response to Freezing with DMSO

When a cell is exposed to the permeating CPA DMSO, at concentrations used during routine cryopreservation (10 % or 1.559 mol/kg), the cell is at isotonic cell volume prior to cooling. The osmotic response of TF-1 cells to low temperatures under these conditions is shown in Figure 2.6. The maximum SC increases with CR in the presence of 10 % DMSO when compared to cooling without a CPA. However, $[KCl]_i$ is substantially reduced over the entire range of CRs. While high CRs are still optimal for minimizing solution effects, $[KCl]_i$ remains relatively low compared to cells frozen without a CPA, even at CRs < 10 °C/min. A CR of ~ 7 °C/min is predicted to maintain SC below the tolerable upper limit while substantially reducing $[KCl]_i$, hence cell survival is likely at this CR.

Osmotic Response to Freezing with High Concentrations of Trehalose

When concentrations of trehalose in the intra- and extracellular spaces are increased to match DMSO concentrations used during routine cryopreservation (1.559 mol/kg) the cellular osmotic response under these two conditions can be compared (Figure 2.7). When high concentrations (1.559 mol/kg) of trehalose are present on both sides of the cell membrane during cooling, the magnitude of the osmotic response and the trend seen with respect to SC are similar to that seen when equimolar concentrations of DMSO (1.559 mol/kg) are present. The simulations predict a CR of < 10 °C would be required to maintain SC within the

tolerable range in the presence of 1.559 mol/kg trehalose. At CRs < 10 °C, $[KCl]_i$ is at the threshold of the tolerable maximum concentration, predicting that cell survival may be tolerated at a CR of 10 °C/min.

Cell Volume Response

The cell volume (as a function of the isotonic volume) in response to decreasing temperatures at low (1 °C/min), intermediate (50 °C/min) and high (100 °C/min) CRs in the presence of low concentrations (0.3 mol/kg) of trehalose inside the cell, outside the cell, or on both sides of the cell membrane, is illustrated in Figure 2.8. The cell volume response to low and high CRs in the absence of a CPA and with 10 % DMSO is also included for reference. The cell initially responds to extracellular trehalose by shrinking, so the cell volume is below the isotonic volume at the onset of cooling. Similarly, the cell responds to intracellular trehalose by swelling, so the cell volume is higher than the isotonic volume at the onset of cooling. When intra- and extracellular trehalose is available during low temperature exposure, the cell volume is at isotonic at the onset of cooling. At slow CRs the cell volume decreases rapidly at high subzero temperatures (> 5 °C) and the cell volume at low temperatures is similar regardless of the starting condition. As the CR increases the cell volume at low temperatures differs depending on the starting condition because variable amounts of water remain inside the cell.

2.4 DISCUSSION

The combined effects of IIF (4-6), osmotic stress (20, 21), and lengthy exposure to high salt concentrations in the unfrozen fraction (8, 22, 23), result in cryoinjury when cells are exposed to low temperatures in the absence of cryoprotective additives. The simulations demonstrate how non-permeating and permeating cryoprotective additives help reduce the probability of IIF or exposure to toxic solute concentrations, respectively, which would otherwise result in cryoinjury (9, 24-26).

Effect of Extracellular Trehalose

Non-permeating agents such as large polymers, starches and sugars generally act by dehydrating the cell at high subzero temperatures, allowing rapid cooling to minimize exposure to damaging concentrations of solutes, while avoiding IIF (26). The simulations predict a similar response with low concentrations of extracellular trehalose. During initial equilibration at 20 °C, extracellular trehalose causes the cell to shrink as water moves out of the cell in response to the increased osmotic pressure (Figure 2.8). With the cell in a shrunken state prior to cooling, less water is inside the cell which explains the decrease in the degree of SC at any CR (Figure 2.3). This decrease in intracellular water also accounts for the higher $[KCl]_i$ at each CR. Cell survival is predicted to be low under these conditions due mostly to high concentrations of $[KCl]_i$ which can only be avoided at high cooling rates (100 °C/min). The right shift of the graph in Figure 2.3 illustrates how one condition is improved (maximum SC) at the expense of the other (maximum [KCl]i). Since the concentrations of trehalose

are relatively low outside, a large volume of intracellular water would still be available to freeze at high CRs and cell death from IIF would result (1). Increasing the concentration of extracellular trehalose would remove a larger volume of cell water prior to cooling. While this would decrease the probability of IIF at high CRs, increased intracellular solute concentrations may be injurious. The osmotic response predicts that even low concentrations of trehalose promote cellular dehydration prior to slow cooling thereby reducing the likelihood of IIF (1). However, because the cell is in a pre-shrunken state at the onset of cooling and there is no compatible solute inside the cell to reduce solute concentrations during cooling, there is an increased probability of lethal cell injury from solution effects (1, 3, 4, 20, 27, 28).

Effect of Intracellular Trehalose

Simulating the cellular osmotic response with an impermeant molecule inside the cell provides us with a tool to look at a unique scenario that cannot be easily achieved experimentally. The osmotic response is opposite to that seen with extracellular trehalose. With trehalose confined to the intracellular space, the cell will swell in a concentration dependent manner in response to the osmotic pressure difference as water moves into the cell at 20 °C. With an increased volume of cell water at the onset of cooling, the degree of SC will increase with increasing CR (1). This decreases the range of tolerable CRs, with respect to SC, to < 10 °C/min in order to avoid ice nucleation and IIF. Increased intracellular water at the onset of cooling has the opposite effect on $[KCl]_i$, allowing for lower CRs before solute concentrations become harmful. The

overall effect is a leftward shift of the graph, once again illustrating how an improvement in one condition ($[KCl]_i$) gets cancelled out by the impairment of the other condition (SC) (Figure 2.4). When trehalose is limited to the confines of the intracellular environment the cell is subjected to osmotic stress as the cell volume increases above isotonic prior to cooling, then decreases below isotonic during cooling (Figure 2.8). Furthermore, even though the cell is swollen above isotonic at the onset of cooling when low concentrations of intracellular trehalose are present, the overall effect on solute concentrations at slow CRs is small, and the increased volume of intracellular water during cooling makes the cell more susceptible to IIF (1).

Effect of Intra- and Extracellular Trehalose

The predicted response of TF-1 cells to freezing in the presence of intra- and extracellular trehalose demonstrates how this condition is most effective at reducing cell volume excursions. The equilibrium cell volume is isotonic so the cell is neither shrunken nor swollen at the onset of cooling (Figure 2.8). At slow CRs (< 20 °C), low equimolar concentrations of trehalose inside and out have little effect on the maximum SC in response to trehalose concentration or relative to cells frozen without a CPA (Figure 2.5). Maximum $[KCl]_i$ decreases in response to increasing CRs and trehalose concentrations when trehalose is available on both sides of the cell membrane. The concentration dependence is more pronounced at lower CRs (< 50 °C/min). At CRs < 20 °C/min, there is no change in the degree of SC but $[KCl]_i$ is reduced bringing the CR that is tolerable for each parameter of cryoinjury closer together. The probability of

survival would still be low because in the presence of low concentrations of trehalose there is not a single CR that is optimal for maintaining SC below the upper tolerable limit of 10 °C while reducing $[KCl]_i$ below 1 mol/kg. While low equimolar concentrations of trehalose inside and outside the cell do not appear to provide substantial protection against solution effects injury or IIF it does reinforce the importance of a compatible solute on both sides of the cell to minimize osmotic stress on the cell prior to cooling (Figure 2.8) (20).

Comparing Trehalose to DMSO

During low temperature exposure in the presence of the permeating CPA DMSO, cell volume changes are reduced with respect to isotonic (Figure 2.8) and $[KCl]_i$ is substantially decreased over the entire range of CRs (Figure 2.6) in comparison to that achieved in the presence of low concentrations of intra- and extracellular trehalose (Figure 2.5). The efficacy of DMSO compared to intra- and extracellular trehalose is attributed to the high concentration of DMSO (10 % or 1.559 mol/kg) in comparison to trehalose (0.3 mol/kg). The concentration dependence becomes obvious when comparing Figure 2.5 to Figure 2.7 because a similar osmotic response to that seen with DMSO is predicted when high (1. 559 mol/kg) equimolar concentrations of trehalose are present on both sides of the cell membrane during cooling. While DMSO substantially reduces $[KCl]_i$, the degree of SC over the entire range of CRs increases. When a compatible solute is available on both sides of the cell membrane during cooling, it is apparent that the osmotic response with respect to both the degree

of SC and $[KCl]_i$ is primarily a result of the concentration of the CPA and not specific to the type of CPA used (Figure 2.7).

Predictive Capabilities of Computer Modeling

In general, the simulations reflect the expected osmotic response of the cells during low temperature exposure under various conditions. This provides validity to the design of the modeling program and our interpretation of the results when consideration is given to the two-factor hypothesis of freezing injury (3). Results of the simulations reinforce the importance of a compatible solute inside the cell to limit intracellular solute concentrations and associated biochemical damage a cell experiences during slow cooling (9, 24). Despite the fact that the cell model used in the simulations does not reflect the complexity of a living cell, the simulations predicted an optimal CR for TF-1 cells exposed to 10 % DMSO to be about 7 °C/min which agrees well with experimental evidence that 3 °C/min is an optimal cooling rate for human hematopoietic stem cells isolated from peripheral blood (29). Nucleated cells contain organelles and undergo complex intra- and intercellular interactions.

Since the two-factor hypothesis of cryoinjury was used to interpret the simulation results a number of assumptions related to this interpretation must be addressed. The chosen upper tolerable limit for SC and $[KCl]_i$ may be conservative and overstate the conditions that result in cryoinjury. The simulations of cellular osmotic responses capture SC well. Our indicator for solution effects injury, maximum $[KCl]_i$, is one limiting assumption as damage resulting from solution effects is not only dependent on the concentration of

solutes but also on the relative toxicity of the CPA and the temperature and time of exposure.

One other consideration which must be addressed is that by focusing only on the osmotic response of TF-1 cells during cooling in the presence of trehalose we did not take into account some additional characteristic properties of trehalose. The thermophysical properties of trehalose (30, 31) and experimental observations that trehalose forms stabilizing interactions with biological structures (32-35) may in part account for the efficacy of trehalose at relatively low concentrations (< 200 mmol/L) during freezing (36-38) and freeze-drying (39) that have been observed using different loading techniques.

Trehalose has a very high glass transition temperature (T_g) (40, 41) defined as the temperature at which a supercooled liquid vitrifies (42). It is the high glass transition temperature of trehalose that has led to the suggestion that solutions containing trehalose become vitrified during dehydrating stresses thereby preserving membrane structure (40). Vitrification is the solidification of a liquid to an amorphous solid resulting from increasing viscosity (42). Additional benefits related to vitrification are the avoidance of ice crystallization and its associated change in solution properties (42). By looking at the osmotic response alone, glass transformation was not taken into account during this study. However, because the simulations use phase diagrams to calculate the intra- and extracellular trehalose concentrations as a function of temperature during cooling, simulations could be used to determine conditions where glass transformation has been shown to occur (41).

Another proposed mechanism by which trehalose produces stabilizing effects has come to be known as the water replacement hypothesis and refers to the ability of sugars to replace the hydrogen bonds of water on phospholipids (43). Membrane cooling causes thermotropic phase transitions from the liquid crystalline to solid gel phase and water permeability decreases. It is believed that direct interaction of trehalose with membrane phospholipids prevents the liquid crystalline-gel phase transition that occurs in response to a loss of intracellular water (44, 45). Trehalose depresses the membrane phase transition temperature (T_m) so that membranes remain fluid even at low temperatures. This helps to stabilize membrane proteins, including soluble proteins, by conserving their native conformation during dehydrating stresses such as those associated with freezing (32, 33, 44) (46). Trehalose is found to be superior to other glass forming polymers such as HES and dextran because it interacts directly with membrane phospholipids (47).

The ability of trehalose to prevent membrane phase transitions at low temperatures (44, 45) would effect water movement across the membrane and the associated osmotic parameters. A change in TF-1 cell osmotic parameters in the presence of trehalose was not accounted for in the modeling and could potentially alter the cellular osmotic response. Discrepancies between empirically derived data and theoretical predictions resulting from deviations in the osmotic permeability parameters at lower temperatures have been observed in sperm (48). Trehalose also effects ice nucleation and growth as shown by the change in position of the cell in the growing ice front during directional

solidification (49). These results are consistent with that observed by Shirakashi *et al.* that trehalose prevented the mechanical suppression of cells in extracellular ice grains and reduced the occurrence of flashing which is correlated with IIF (50). Trehalose has a number of characteristic properties which need to be considered when designing a cryopreservation protocol and when using theoretical modeling to predict outcomes following cryopreservation. By doing so this will enable predictions to be made which capture the response seen in living systems and help strengthen our understanding of cryoinjury, including mechanisms of protection.

2.5 CONCLUSION

Simulations of cellular osmotic responses at low temperatures clearly have predictive capabilities with respect to the events that influence cell recovery during cryopreservation. Computer modeling is a valuable tool for identifying conditions where experimental validation is necessary, reducing experimentation based exclusively on empirical observations. Data generated from computer simulations should be interpreted with caution nevertheless, when designed and executed appropriately and used congruently with experimentation the results can provide valuable information about a biological system. In addition, modeling allows us to test our theoretical understanding of cryoinjury and how it fits with experimental outcomes, which may in fact help improve our approach to both theoretical modeling and experimentation.

2.6 REFERENCES

1. Mazur P. Kinetics of water loss from cells at subzero temperatures and the likelihood of intracellular freezing. J Gen Physiol 1963;47:347-69.
2. Schwartz G, Diller, KR. Osmotic response of individual cells during freezing. Cryobiology 1983;20:61-77.
3. Mazur P, Leibo SP, Chu EHY. A two-factor hypothesis of freezing injury. Exp Cell Res 1972;71:345-55.
4. Mazur P. Freezing of living cells: Mechanisms and implications. Am J Physiol 1984;247(3):C125-C142.
5. Karlsson JOM, Cravalho EG, Toner M. Intracellular ice formation: Causes and consequences. Cryo Letters 1993;14:323-334.
6. Muldrew K, McGann LE. Mechanisms of intracellular ice formation. Biophys. J. 1990;57:525-532.
7. Meryman HT. Modified model for the mechanism of freezing injury in erythrocytes. Nature 1968;218:333-336.
8. Lovelock JE. The haemolysis of human red blood cells by freezing and thawing. Biochim Biophys Acta 1953;10:414-26.
9. Lovelock JE. The mechanism of the protective action of glycerol against haemolysis by freezing and thawing. Biochim Biophys Acta 1953;11:28-36.
10. Hunt CJ, Armitage SE, Pegg DE. Cryopreservation of umbilical cord blood: 2. Tolerance of CD34+ cells to multimolar dimethyl sulphoxide and

the effect of cooling rate on recovery after freezing and thawing. Cryobiology 2003;46:76-87.

11. Woods EJ, Liu J, Derrow CW, Smith FO, Williams DA, Critser JK. Osmometric and permeability characteristics of human placental/umbilical cord blood CD34+ cells and their application to cryopreservation. J Hematother Stem Cell Res 2000;9(2):161-73.
12. Ross-Rodriguez LU. Using simulations to design a cryopreservation procedure for hematopoietic stem cells without DMSO, Master of Science, Medical Sciences - Laboratory Medicine and Pathology. Edmonton: University of Alberta; 2003.
13. Johnson JA, Wilson TA. Osmotic volume changes induced by a permeable solute. J Theor Biol 1967;17(2):304-311.
14. McGrath JJ. Membrane transport properties. In: McGrath JJ, Diller KR, editors. Low temperature biotechnology emerging applications and engineering contributions. New York: American Society of Mechanical Engineers; 1988. p. 273-330.
15. Lucke B, McCutcheon M. The living cell as an osmotic system and its permeability to water. Phys Rev 1932;12:68-139.
16. Wolf AV, Brown MG, Prentiss PG. Concentrative properties of aqueous solutions. Weast, R.C. ed. Boca Raton, FL: CRC Press, Inc.; 1982.
17. Freedman C, Hoffman JF. Ionic and osmotic equilibria of human red blood cells treated with nystatin. J Gen Physiol 1979;74:157-185.

18. Ross-Rodriguez LU, Elliot JAW, McGann LE. Experimental correlation and optimization of a theoretically-designed cryopreservation protocol. Cryobiology 2006 (*submitted*).

19. Mazur P. The role of cell membranes in the freezing of yeast and other cells. Ann N Y Acad Sci 1965;125:658-76.

20. Meryman H. Osmotic stress as a mechanism of freezing injury. Cryobiology 1971;8:489-500.

21. Muldrew K, Mcgann LE. The osmotic rupture hypothesis of intracellular freezing injury. Biophys J 1994;66(2):532-541.

22. Mazur P RN. Contributions of unfrozen fraction and of salt concentration to the survival of slowly frozen human erythrocytes: Influence of warming rate. Cryobiology 1983;20:274-289.

23. Pegg DE, Diaper MP. On the mechanism of injury to slowly frozen erythrocytes. Biophys J 1988;54:471-488.

24. Lovelock JE. The protective action of neutral solutes against haemolysis by freezing and thawing. Biochem J 1954;56:265-70.

25. Meryman HT. Cryoprotective agents. Cryobiology 1971;8(2):173-183.

26. McGann LE. Differing actions of penetrating and nonpenetrating cryoprotective agents. Cryobiology 1978;15:382-390.

27. Mazur P. Cryobiology: The freezing of biological systems. Science 1970;168:939-49.

28. Meryman H. Freezing injury and its prevention in living cells. Ann Rev Biophys Bioeng 1974;3:341-63.

29. McGann LE, Turner AR, Allalunis MJ, Turc JM. Cryopreservation of human peripheral blood stem cells: Optimal cooling and warming conditions. Cryobiology 1981;18:469-472.

30. Miller DP, de Pablo J, Corti H. Thermophysical properties of trehalose and its concentrated aqueous solutions. Pharm Res 1997;14(5):578-590.

31. Aldous BJ, Auffret AD, Franks F. The crystallization of hydrates from amorphous carbohydrates. Cryo Letters 1995;16:181-186.

32. Xie G, Timasheff SN. The thermodynamic mechanism of protein stabilization by trehalose. Biophys Chem 1997;64:25-43.

33. Crowe JH, Crowe LM, Carpenter JF, Rudolph AS, Wistrom CA, Spargo BJ, et al. Interactions of sugars with membranes. Biochim Biophys Acta 1988;947:367-384.

34. Crowe JH, Crowe LM, Chapman D. Preservation of membranes in anhydrobiotic organisms: The role of trehalose. Science 1984;223:701-703.

35. Carpenter JF, Crowe LM, Crowe JH. Stabilization of phosphofructokinase with sugars during freeze-drying: Characterization of enhanced protection in the presence of divalent cations. Biochim Biophys Acta 1987;923:109-115.

36. Eroglu A, Russo MJ, Bieganski R, Fowler A, Cheley S, Bayley H, et al. Intracellular trehalose improves the survival of cryopreserved mammalian cells. Nature Biotechnol 1999;18:163-167.

37. Buchanan S, Gross S, Acker J, Toner M, Carpenter J, Pyatt D. Cryopreservation of stem cells using trehalose: Evaluation of the method using a human hematopoietic cell line. Stem Cells Dev 2004;13:295-305.

38. Buchanan SS, Menze MA, Hand SC, Pyatt DW, Carpenter JF. Cryopreservation of human hematopoietic stem and progenitor cells loaded with trehalose: Transient permeabilization via the adenosine triphophate-dependent P2Z receptor channel. Cell Preserv Technol 2005;3(4):212-222.

39. Chen T, Acker JP, Eroglu A, Cheley S, Bayley H, Fowler A, et al. Beneficial effect of intracellular trehalose on membrane integrity of dried mammlian cells. Cryobiology 2001;43:168-181.

40. Green JL, Angell CA. Phase relations and vitrification in saccharide-water solutions and the trehalose anomaly. J Phys Chem 1988;93:2880-2882.

41. Chen T, Fowler A, M T. Literature review: Supplemented phase diagram of the trehalose-water binary mixture. Cryobiology 2000;40:277-282.

42. Fahy GM, MacFarlane DR, Angell CA, Meryman HT. Vitrification as an approach to cryopresevation. Cryobiology 1984;21:407-26.

43. Crowe LM, Crowe JH. Anhydrobiosis: A strategy for survival. Adv Space Res 1992;12(4):239-247.

44. Crowe LM, Womersley C, Crowe JH, Reid DS, Appel L, Rudolph A. Prevention of fusion and leakage in freeze-dried liposomes by carbohydrates. Biochim Biophys Acta 1986;861:131-40.

45. Clegg JS. The physical properties and metabolic status of artemia cysts at low water contents: The water replacement hypothesis. Membranes, Metabolism, and Dry Organisms 1986:169-87.

46. Crowe JH, Spargo BJ, Crowe LM. Preservation of dry liposomes does not require retention of residual water. Proc Natl Acad Sci U S A 1987;84:1537-1540.

47. Crowe LM, Reid DS, Crowe JH. Is trehalose special for preserving dry biomaterials? Biophys J 1996;71:2087-2093.

48. Gilmore JA, Liu J, Woods EJ, Peter AT, Critser JK. Cryoprotective agent and temeprature effects on human sperm membrane permeabilities: Convergence of theoretical and empirical approaches for optimal cryopreservation methods. Hum Reprod 2000;15(2):335-343.

49. Hubel A, Darr TB, Chao A, Dantzig JA. Cell partitioning during the directional solidification of trehalose solutions. Cryobiology 2006;53 (*in press*).

50. Shirikashi R, Muller KJ, Sukhorukov VL, Zimmermann U. Effects of saccharide on living cells during the freezing-thawing process and effects of their uptake by electroporation. In; CryoBiomol 2003. p. 156.

Table 2.1: Solution composition and osmotic parameters. Isotonic solution composition (a) and osmotic parameters for TF-1 cells used in trehalose simulations (b) and in DMSO simulations (c).

(a) Isotonic solution composition

osm/kg	Intracellular	Extracellular
KCl	0.160	0.005
NaCl	0.010	0.171
Protein	0.004	0.000
Total Osmolality	0.301	0.301

(b) Osmotic parameters – trehalose simulations

Isotonic Volume	776 μm^3
Inactive Fraction	0.353
Lp (20°C)	0.342 µm/min/atm
Activation Energy for Lp	13.4 kcal/mol

(c) Osmotic parameters – DMSO simulations

Isotonic Volume	776 μm^3
Inactive Fraction	0.353
Lp (20 °C)	0.4444 µm/min/atm
Activation Energy for Lp	14.884 kcal/mol
Isotonic Osmolality	0.301 osm/kg
Activation Energy for Ps	10.637 kcal/mol
Ps (20 °C)	7.0145 µm/min/atm
Reflection coefficient (σ)	0.8095

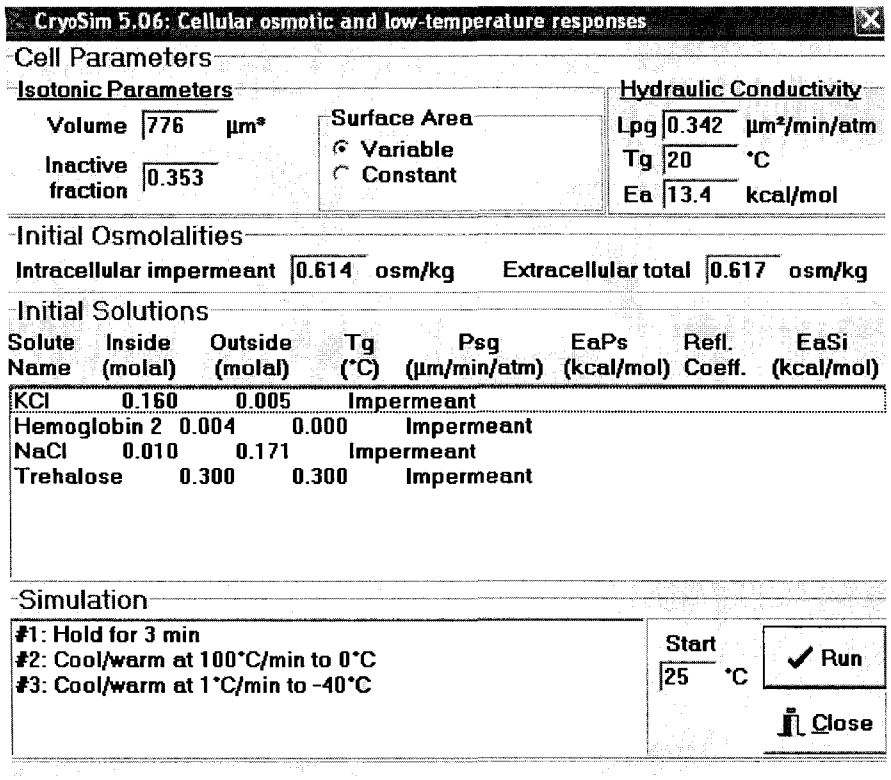

Figure 2.1: CryoSim Interface. User interface of the CryoSim V5.06 demonstrating the required input for modeling the osmotic response of TF-1 cells cooled at 1 °C/min in the presence of 0.3 mol/kg intra- and extracellular trehalose.

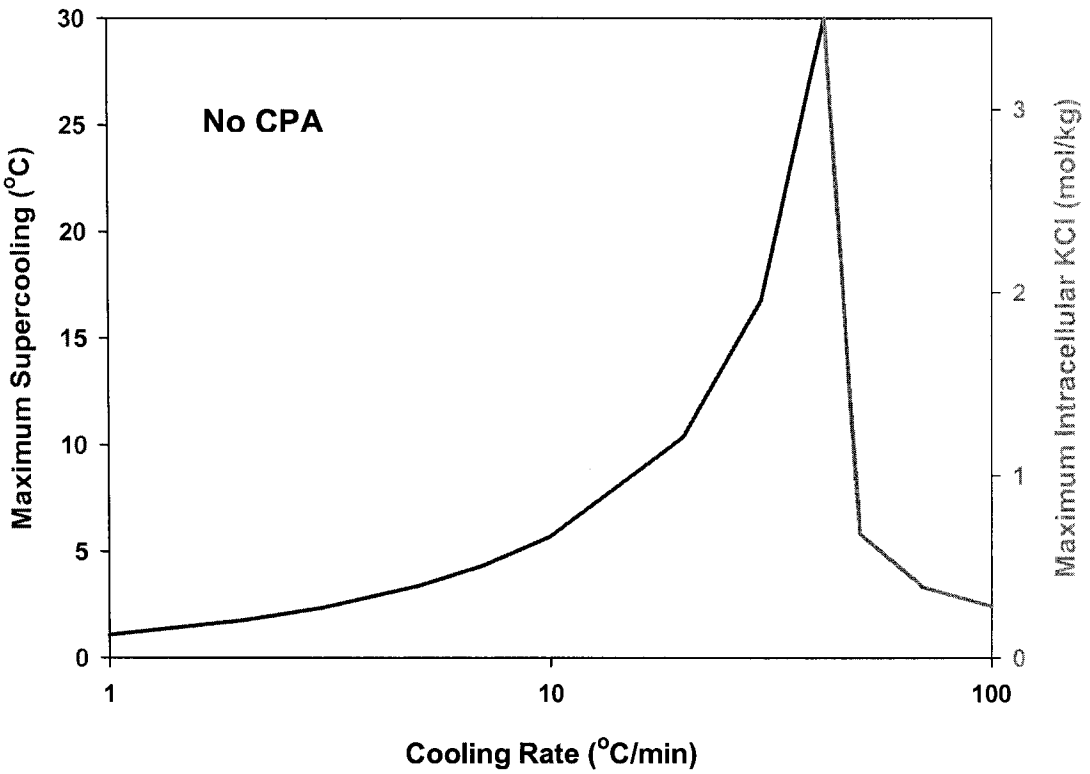

Figure 2.2: No CPA. The predicted osmotic response of TF-1 cells to low temperatures in the absence of a CPA.

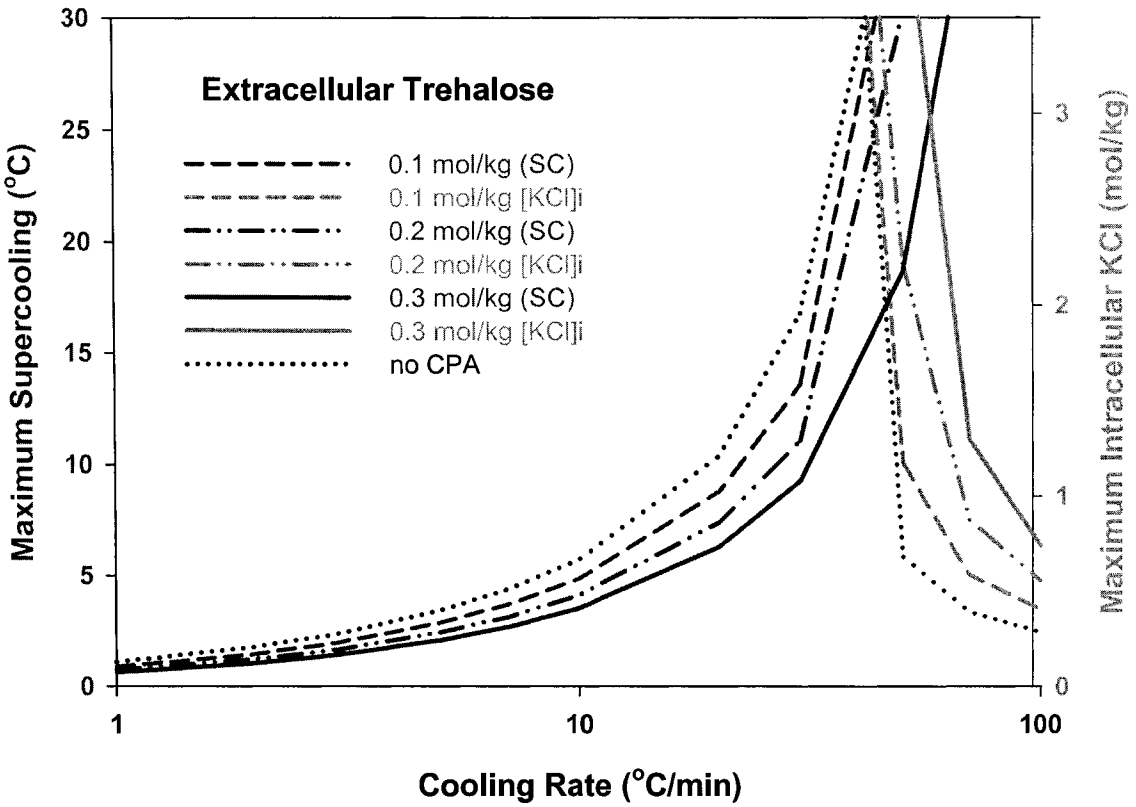

Figure 2.3: Extracellular trehalose. The predicted osmotic response of TF-1 cells to low temperatures in the presence of low concentrations (0.1-0.3 mol/kg) of extracellular trehalose. Dotted lines represent the cellular osmotic response in the absence of a CPA.

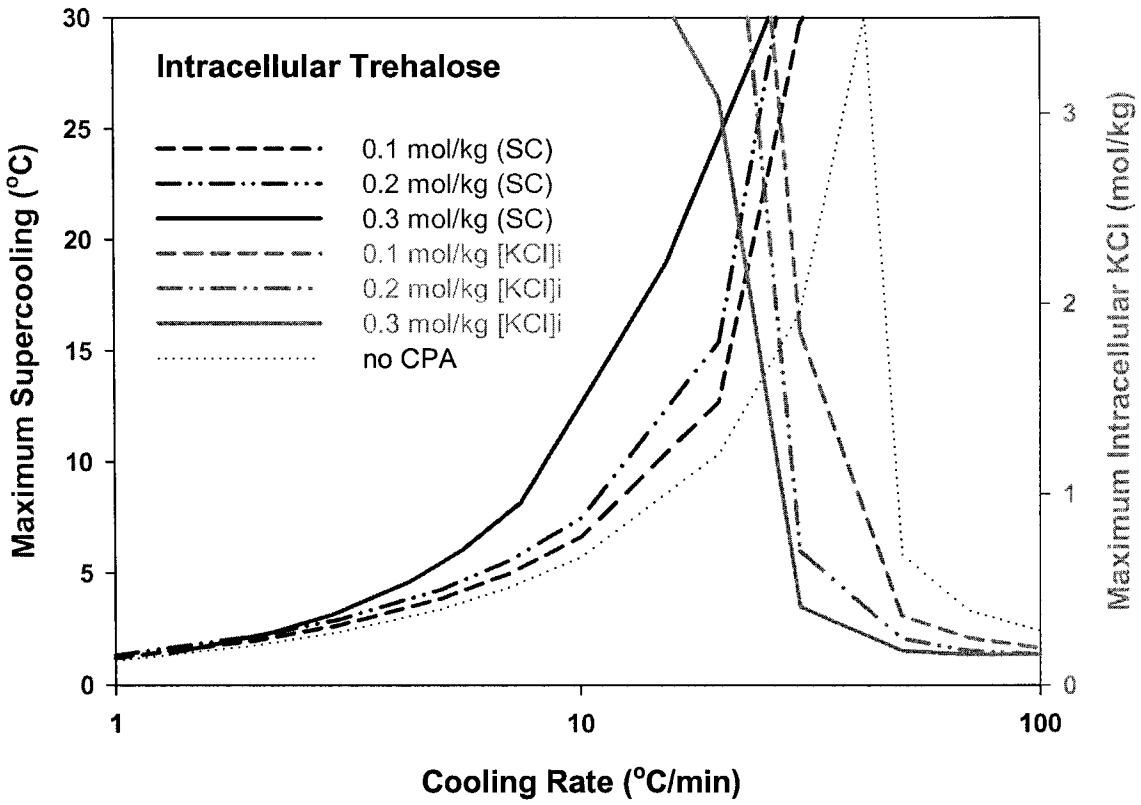

Figure 2.4: Intracellular trehalose. The predicted osmotic response of TF-1 cells to low temperatures in the presence of low concentrations (0.1-0.3 mol/kg) of intracellular trehalose. Dotted lines represent the cellular osmotic response in the absence of a CPA.

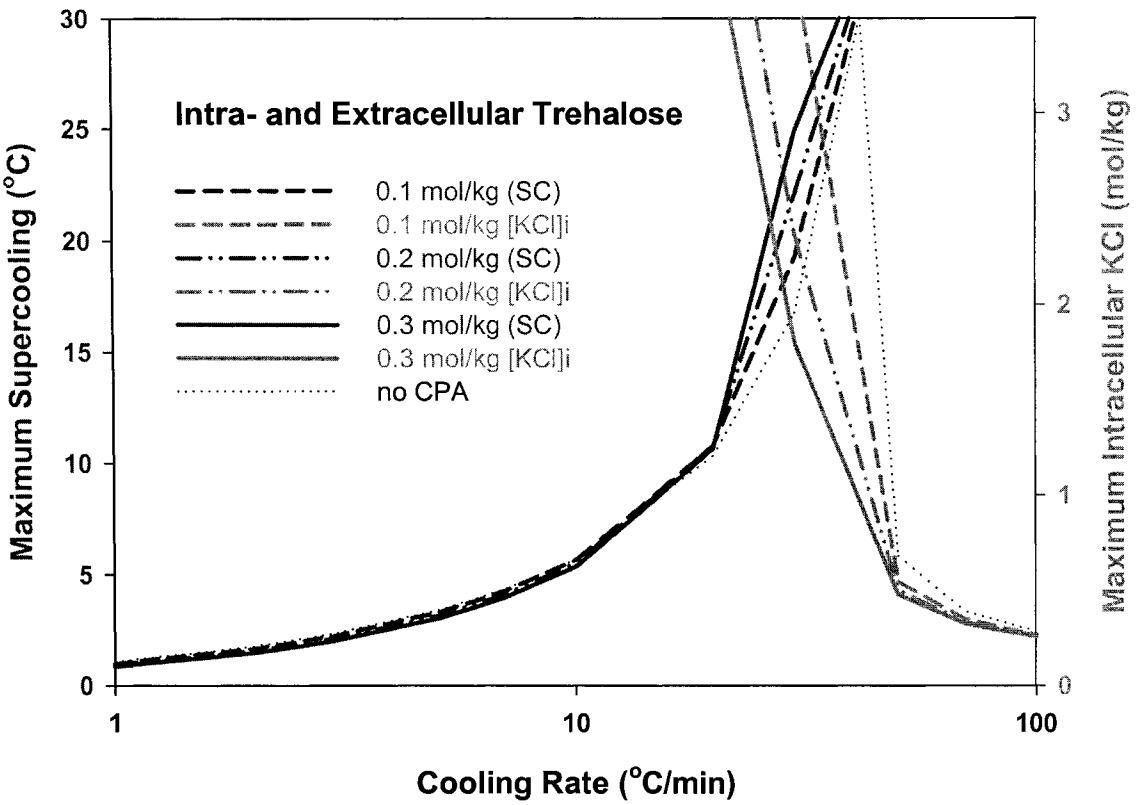

Figure 2.5: Intra- and extracellular trehalose. The predicted osmotic response of TF-1 cells to low temperatures in the presence of low concentrations (0.1-0.3 mol/kg) of intra- and extracellular trehalose. Dotted lines represent the cellular osmotic response in the absence of a CPA.

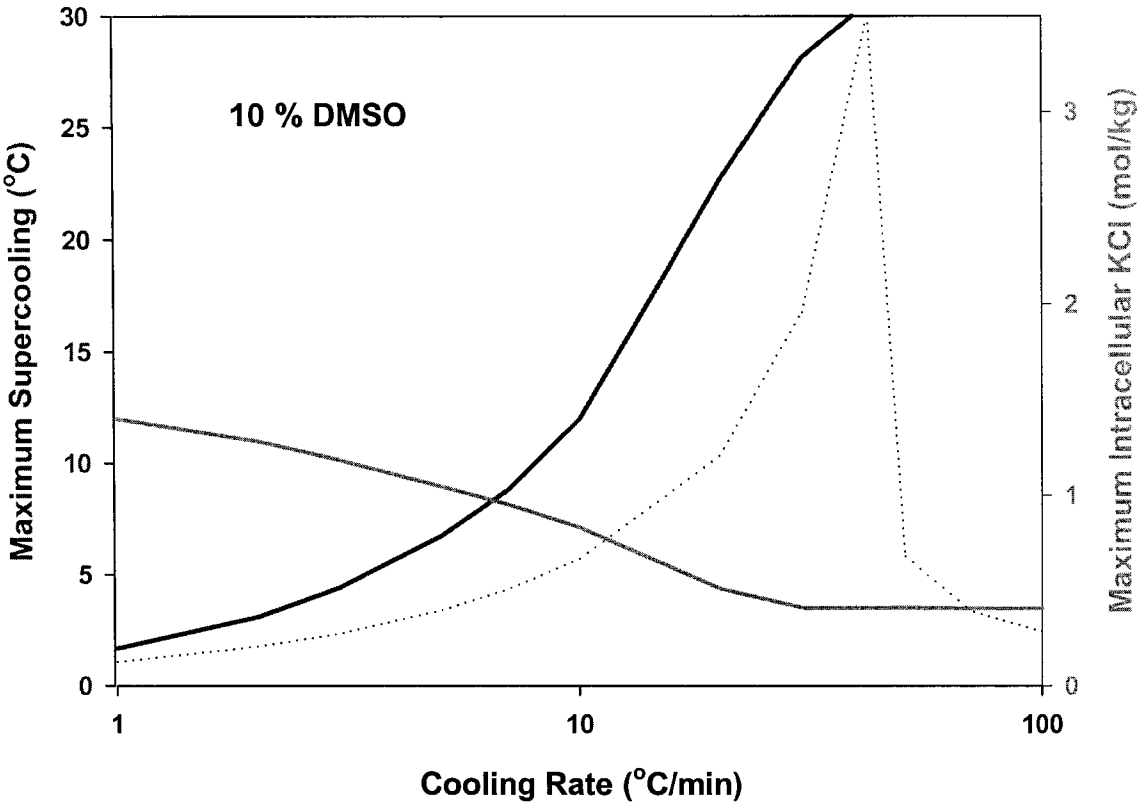

Figure 2.6: 10 % DMSO. The predicted osmotic response of TF-1 cells to low temperatures in the presence of the permeating CPA DMSO (10 % or 1.559 mol/kg). Dotted lines represent the cellular osmotic response to cooling in the absence of a CPA.

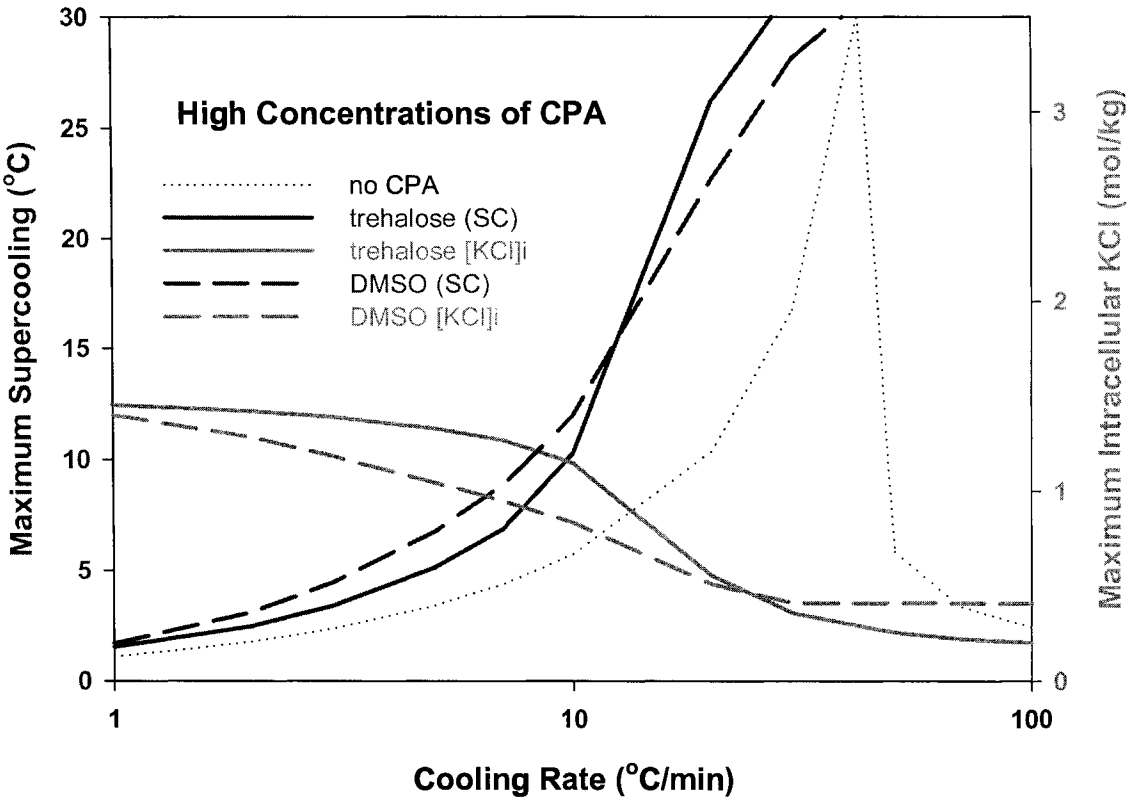

Figure 2.7: High concentrations of CPA. Predicted osmotic response of TF-1 cells to low temperatures in the presence of (i) high concentrations of intra- and extracellular trehalose (1.559 mol/kg) or (ii) DMSO (1.559 mol/kg). Dotted lines represent the cellular osmotic response in the absence of a CPA.

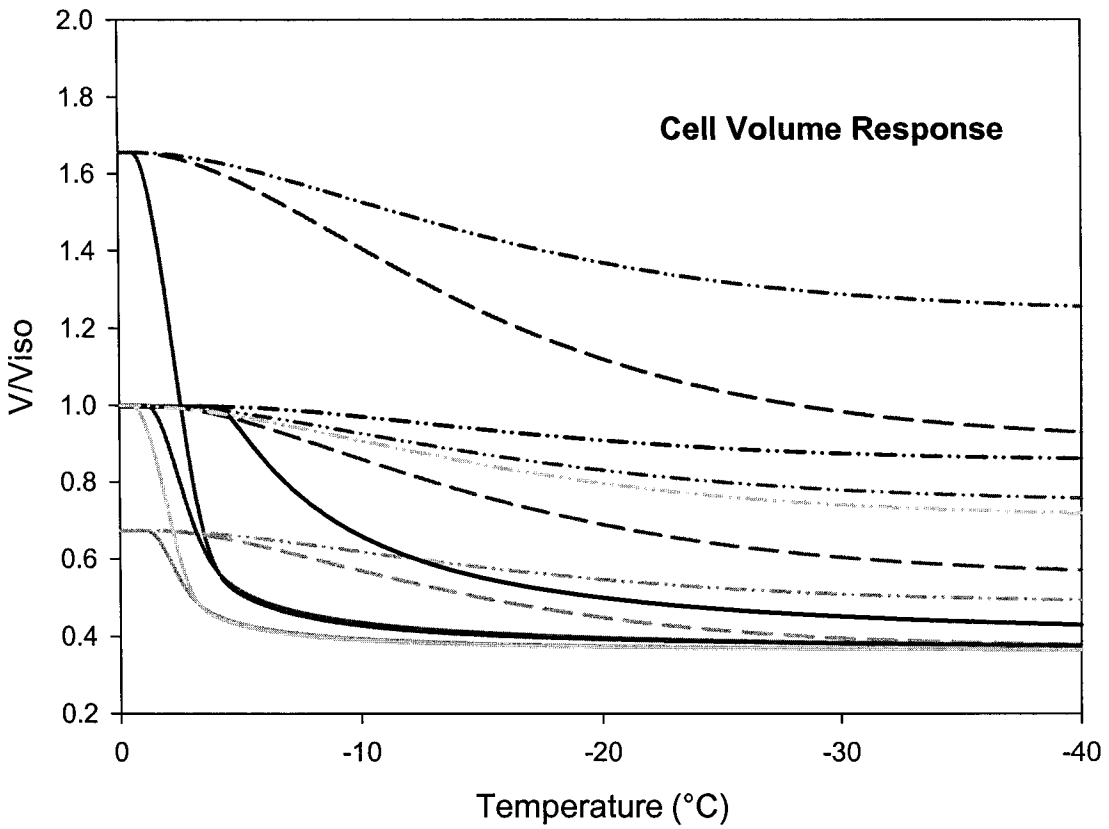

Figure 2.8: Cell volume response. Predicted equilibrium cell volume (V/Viso) at the onset of cooling and during cooling to -40 °C at different CRs (1, 50, 100 °C/min), in the presence of 0.3 mol/kg intra- and extracellular trehalose, (ii) 10 % DMSO and (iii) no CPA.

CHAPTER 3

LIPOSOME SYNTHESIS AND CHARACTERIZATION[1]

3.1 INTRODUCTION

Computer modeling provided theoretical predictions as to the osmotic response of TF-1 cells to cooling in the presence of intra- and extracellular trehalose at variable cooling rates (Chapter 2). The simulations play a valuable role in defining the importance of a compatible solute on both sides of the cell membrane in order to prevent cell volume changes at the onset of cooling which cause detrimental increases in either the degree of supercooling or the concentration of solutes. With that in mind we are faced with the challenge of loading trehalose into the intracellular compartment in order to maximize the cryoprotective benefits of this molecule. In an attempt to do so, we will focus on the use of liposomes as a delivery vehicle for intracellular trehalose.

Methods of Liposome Formation

Liposomes are microscopic structures composed of one or more concentric lipid bilayers (lamellae) with an aqueous compartment separating each lamella. Multilamellar vesicles (MLV) consist of multiple lipid bilayers that form during dispersal in aqueous solutions by self-closing to prevent the hydrophobic hydrocarbon core of the bilayer from interacting with water. MLVs are obtained by techniques involving organic solvents (1) and freeze-thaw procedures (2).

[1] Training to develop the methods and techniques of liposome synthesis and characterization were provided by Dr. Maria Gyongyossy-Issa and Iren Constantinescu at the University of British Columbia. Kirby Scott and Jelena Holovati made an equal contribution to the development of these techniques in the Acker Laboratory. All of the results and interpretation of the data presented herein is the independent work of Kirby Scott.

The resulting vesicles are heterogeneous in size (1-20 μm), shape and number of lamellae per vesicle. Large unilamellar vesicles (LUV) can be produced from MLV suspensions by disrupting the multiple bilayers and essentially decreasing the final size of the particle. This process is analogous to peeling off the layers of an onion and requires energy input. The type of energy required to reduce the particle size depends on the desired final product. Small unilamellar vesicles (SUV) ranging in size between 15-50 nm can be produced by sonication (3-5) or French press (6) techniques. LUVs are between 0.1-1 μm in size and can be synthesized from MLVs by dilution from organic solvent (7), detergent dialysis (8, 9) or extrusion (10, 11). The focus of this paper will be on the synthesis and characterization of LUV's using the mechanical method of extrusion. LUVs were chosen for this study because of their size, which allows entrapment of an appreciable volume while avoiding problems associated with very small, highly curved systems (11, 12).

Characteristics of Liposomes

Liposomes have a number of favorable characteristics that make them compatible with biological specimens. Liposomes are very versatile and can be easily manipulated to alter the size, charge, and composition of the lipid bilayer and aqueous compartment. Altering the lipid composition and charge is an approach used to facilitate specific interactions between liposomes and the target cell population (13). The stability of liposomes, which is defined as the ability to retain structural integrity of the lipid bilayer and prevent leakage of their aqueous contents, is also influenced by the composition (14, 15). Often the

components are biodegradable and found in natural membrane systems, preventing cytotoxicity and immunogenic responses *in vivo* (16).

Purpose

The purpose of this study is to develop a technique for the controlled synthesis of liposomes encapsulating a trehalose-rich buffer which will then be used to test the hypothesis that liposomes can be used as a delivery vehicle to load trehalose into the nucleated mammalian cell line TF-1 (CRL-2003, American Type Culture Collection (ATCC)). The development of methods for characterizing the final liposome product will be another crucial element which is necessary to test the reproducibility of the selected synthesis technique and allow for experimental comparison between batches of liposomes. This will ensure a standard of quality between preparations and reduce experimental variability. It is important that the techniques established can be applied to the synthesis of liposomes of variable composition and size so that if alteration of these characteristics is required it can be accomplished with ease.

3.2 METHODS

Liposome Synthesis

Phospholipids are the building blocks of natural membrane systems. The bulk of the liposome structure is formed by 1,2-dipalmitoyl-*sn*-glycero-3-phosphocholine (DPPC), a synthetic, neutral phospholipid. DPPC is composed of long saturated fatty acid chains that help to stabilize the liposome structure by increasing the lipid membrane phase transition temperature (T_m) (17). In addition, DPPC is

fluid at room temperature and therefore pliable, which makes selection and manufacturing of liposomes with a defined size possible. Cholesterol (CL) is combined with DPPC to help stabilize the membrane. CL, which can be added up to 50 mol % for maximum stability, has a condensing effect which reduces membrane permeability to aqueous solutes above the T_m and also increases membrane fluidity in the gel phase (17). Stock solutions between 100-200 mg/ml of DPPC (Avanti polar Lipids Inc., Alabaster, AL) and CL (Sigma Aldrich, ON, Canada) were prepared by dissolving dry commercial preparations in chloroform. The lipid formulation was prepared from the stock solutions and was composed of 25 mmol/L DPPC and 25 mmol/L CL, combined at a ratio of 70 to 30, respectively. Liposomes were prepared by a modification of the technique of Bangham *et al.* (18). The lipid formulation was agitated by vortexing to ensure a homogenous mixture of lipids followed by evaporation of the chloroform solvent using a light stream of nitrogen gas. Residual chloroform was removed by lyophilization overnight in a freeze-dryer (Flexi-Dry MP™, FTS Systems, Inc., NY, USA).

The dry lipid film was hydrated using one of the following aqueous solutions: HEPES buffered salt solution (150 mmol/L KCl or NaCl, 10 mmol/L HEPES), a modification referred to as HBSI containing 120 mmol/L KCl, 20 mmol/L HEPES, 10 mmol/L NaCl, and 5 mmol/L glucose, or modified cell culture medium (RPMI-1640 serum free media (SFM), ATCC, VA, USA); with or without the addition of sucrose or trehalose (0.20-0.29 mol/L). Hydration buffers used for each liposome preparation are summarized in Table 3.3. All buffers were

filter sterilized and prepared to physiological pH (7.4) and osmolality (~280 mOsm/kg). SFM was decreased in volume by 2/3 prior to the addition of 200 mmol/L trehalose and then returned to the starting volume with distilled water in order to maintain physiological osmolality. Inclusion of the fluorescent marker 5(6)-carboxyfluorescein ((CF), Molecular Probes, Invitrogen Canada Inc., ON, Canada), at concentrations ranging from 10 µmol/L-800 µmol/L permitted labeling of the liposomal vesicles. CF was selected based on its molecular weight (376 g/mol), which is similar to that of the dihydrate form of trehalose (378.3 g/mol), and the fact that it is retained in the liposomes following synthesis due to the lack of ionizable moieties which makes it membrane impermeable. Hydration involved dispersal of the dry lipid film by repeated vortexing and heating of the sample near 70 °C to form MLVs, which are composed of between 5 and 20 bilayers (17), encapsulating water soluble compounds. Heating above the T_m of the lipid membrane (> 55°C) (19), ensures the membrane is in a fluid state during hydration, helping to improve encapsulation efficiency (16). Batches were left to stand overnight, referred to as aging, which is suggested to improve the homogeneity of the MLV population.

Following hydration and aging, MLV suspensions were frozen in liquid nitrogen then thawed in a 70 °C water bath. The freeze-thaw cycle was repeated five times. Freeze-thawing helps to increase the interlamellar spaces reducing osmotic imbalances between the interior and exterior environments caused by decreased solute concentrations in the trapped buffer (2). In addition, the freeze-thaw procedure results in an appreciable increase in trapped volume,

improved trapping efficiencies and homogeneity of the size distribution of the final suspension (2, 11). The MLV suspensions were reduced in size and number of lamellae using the large unilamellar vesicle extrusion technique (LUVET) (2, 10, 11, 20). MLVs were injected into the extrusion chamber (Lipex™, Northern lipids Inc., BC, Canada) attached to a nitrogen gas cylinder fitted with a high pressure regulator. Nitrogen pressure was applied at 100-400 lb/in^2 forcing the MLVs through the extrusion chamber which was fitted with two stacked 25 mm polycarbonate filters (Nuclepore Corp., CA, USA) with a 0.4 µm pore size. The vesicles were collected from the outlet port and re-injected. Extrusion was repeated between 6 and 10 times in order to obtain a log normal size distribution. The extruder and buffers were warmed to 70 °C prior to extrusion to increase membrane fluidity and ease of passage through the filter pores to prevent clogging. Unencapsulated CF molecules were removed by repeated centrifugation at 13 362 x g for 15 minutes and washing in buffer devoid of marker and sugars. Washing in sugar free buffers was required for separation due to the increased buoyancy of liposomes in the presence of sugars. Final re-suspension of all liposome samples was in unmarked buffer (no 5(6)-CF) but otherwise of equal composition to the entrapped buffer.

Liposome Characterization

Phosphate Assay

The phosphorus assay method of Fiske and Subbarow (21) was developed as a modification of the methods of Bell and Doisy (22), Briggs (23) and Benedict and Theis (24). It was used to determine total phosphate in the lipid formulation

which was then used to calculate total lipid concentration based on the ratio of DPPC to CL. In summary, reduction of phosphomolybdic acid by the catalyst 1-amino-2-napthol-4-sulphonic acid and sulfite produces a blue substance in the presence of phosphate that can be measured spectrophotometrically at 815 nm. Fiske-Subbarow (21) reagent was prepared by the addition of 95 % 0.5 g of 4-amino-3-hydroxy-1-naptholenesulfonic acid (Sigma Aldrich, ON, Canada), over medium heat with mechanical stirring, to 200 ml of 15 % anhydrous sodium bi-sulfite containing 1 g of anhydrous sodium sulfite. The solution was stored in a borosilicate bottle and filtered prior to use to remove formed crystals. Ammonium molybdate (2.2 g) was dissolved in concentrated sulfuric acid (20 ml) and diluted with distilled water to a final concentration of 0.22 %. Standard solutions of sodium phosphate (3 mmol/L) ranging from 0-500 µl were prepared in 20 ml PYREX round bottom test tubes. Depending on the final concentration, 5 -100 µl of liposome sample was used in the analysis of total phosphate, while 10 µl of DPPC stock solution diluted 1 in 100 followed by evaporation of the organic solvent, was used as a control. For liposome samples synthesized with SFM, a measured volume of SFM was run along with the samples to correct for the presence of phosphates in the media. All other buffers used were devoid of phosphates. Whenever possible, duplicates of DPPC stock solutions and liposomes were prepared for the assay. Standards and controls were always run in duplicate and the average absorbance calculated. Hydrolysis of the phosphates was achieved by addition of 0.7 ml perchloric acid (70 %) to standard, stock and sample preparations followed by heating to 190 °C for 1.5

hours in an aluminium test tube rack using a dry heating block (DB·3A Techne, Dri-Block, NJ, USA). Fiske-Subbarrow reagent (0.9 ml) and molybdate solution (7 ml) were added to the cooled samples followed by heating in a boiling water bath for 15-20 minutes. Heating develops the blue color of the phosphomolybdic acid complex (24) which is stable at room temperature for several hours (25, 26). Samples were contained within a perchloric acid waterfall hood during the heating process due to the explosive nature of perchloric acid in the presence of organics. The cooled samples were read directly at an absorbance of 815 nm in 1.5 ml cuvettes using a spectrophotometer (384 SpectraMax Plus, Molecular Devices Corp., CA, USA). The phosphate concentration of liposome samples and DPPC stock solutions were calculated from the absorbance reading using the linear regression equation generated form the standard curve. The total lipid concentration (mM) was then calculated from the phosphate concentration based on the percentage of DPPC in the lipid formulation or DPPC stock solution (Eq 3.1):

$$\text{total lipid concentration (mM)} = (([P0_4] / V_s) / \%\ P0_4) \times 100 \qquad \text{(Eq 3.1)}$$

where $[PO_4]$ is the phosphate concentration (nmol) calculated from the absorbance, V_s is the volume (µl) of liposomes, DPPC stock or control used in the assay and $\%\ P0_4$ is the percent of DPPC in the sample which is 70 for liposomes and 100 for DPPC stock solutions.

Sizing

The size and homogeneity of the final liposome preparation was determined using a particle sizing system capable of submicron to millimetre measurements

(Mastersizer Hydro 2000 SM, Malvern Instruments Ltd., Worcestershire, UK). Liposomes suspended in their respective buffers were passed through a focused laser beam (λ=633 nm) and the angular intensity of scattered light was measured by a series of photosensitive detectors. The scattering information was processed by the Malvern software based on the principle of Mie scattering, whereby the angle of scattered light is inversely proportional to particle size, to produce a size distribution for the particles. Polystyrene (0.2 µm and 0.4 µm) and silica (0.8 µm) uniform microsphere size standards were used for instrument calibration (Bangs Laboratories Inc., IN, USA) where the observed and expected mean size of the microsphere distribution curves were used to generate a standard curve. The regression equation from the standard curve and the measured mean liposome size was then used to calculate the actual liposome size by correcting for the error in the instrument. The refractive index (RI) for the particles being measured and their dispersion buffers was required to relate fluctuations in intensity to particle size and the RI depends on the excitation wavelength. Because the dispersant solutions were very dilute, the RI value for water (1.33) was used for all dispersion buffers (27), while 1.34 was used as the particle RI for liposome samples, 1.59 for the 0.2 and 0.4 µm polystyrene bead standards (28) and 1.5 for the silica bead standard. SPSS ® 12.0 for Windows ® (SPSS Inc., IL, USA) was the analytical software used for the statistical analysis. Levene's Test for Equality of Variance was used to compare the mean of the liposome size distributions between batches of liposomes while One Way Analysis of Variance using Bonferroni to test for

multiple comparisons was used to compare the mean size distribution of liposomes synthesized with and without sugars.

Flow Cytometry

The physical characteristics of dilute liposome particles were measured using flow cytometry (FACSCanto, Becton Dickinson, NJ, USA). Relative size and granularity based on forward scatter and side scatter, respectively, were used as indicators of liposome population distribution and homogeneity. Relative fluorescence intensity of liposomes synthesized with CF, verified entrapment of the hydration buffer within the aqueous core. Concentrated liposomes diluted with filter sterilized unmarked buffers were used for the analysis.

3.3 RESULTS

Phospholipid Content

There is a strong linear relationship between phosphate concentration and absorbance (Figure 3.1), with some deviation in the slope of the curve between assays (Table 3.1). The absorbance was linear over the entire range tested (0-1500 nmol PO_4). The variability between measured and expected lipid stock concentrations is represented by the standard error of the average (Table 3.2). Calculated lipid concentrations for liposome samples are summarized in Table 3.3.

Size Analysis

Eight batches of liposomes were synthesized in total over the course of the study with a total of 30 individual samples. Representative microsphere size

standard distribution curves generated from the Mastersizer are depicted in Figure 3.2. The mean size of the distribution, referred to as the volume weighted mean, for each standard is smaller than the expected mean (Table 3.4). Measured and corrected volume weighted means for each liposome sample and the group average are summarized in Table 3.6(a), (b) and (c). Refer to Figure 3.3 for the standard curve and regression equation used to calculate the actual mean liposome size of the distribution from the measured mean. The size distribution between batches of liposomes synthesized without sugars and with trehalose or sucrose is illustrated in Figure 3.4. There is no significant difference ($p = 0.308$, $\alpha = 0.05$) in the mean liposome size from one batch to the next when comparing size distributions between liposomes of the same type. The size distribution of different types (sucrose, trehalose, no sugar) of liposomes is illustrated in Figure 3.5. When comparing size distributions between different types of liposomes, liposomes synthesized with sugars have a mean size which is significantly smaller ($p < 0.001$, $\alpha = 0.05$) than liposomes synthesized without sugars. The results of the statistical analysis are summarized in Table 3.5.

Flow Cytometric Analysis

The flow histograms and scatter plots for liposomes devoid of CF and synthesized with 200 µmol/L CF are shown in Figures 3.6 and 3.7, respectively. The scatter plot illustrates that there is a single distinct population. The histograms confirm that the population is homogeneous with a normal distribution (Figure 3.6(b) and 3.7(b)) and indicates entrapment of the CF

marker (Figure 3.7(c)) in washed liposome samples. Figure 3.8 illustrates that liposome fluorescence intensity increases with increasing CF concentration but not lipid concentration. There is about a ten fold increase in the fluorescence intensity of liposomes synthesized with 200 µmol/L CF compared to liposomes synthesized with 20 µmol/L CF. When the lipid concentration for each sample is increased from 0.5 mmol/L to 1 mmol/L the fluorescence intensity does not increase.

3.4 DISCUSSION

The techniques used to characterize liposomes demonstrate sample reproducibility, confirm encapsulation and allow quantitative measure of the final product. There is a strong positive linear correlation between phosphate concentration and absorbance indicated by the high R^2 values generated from the phosphate assay standard curve. Deviations in the slope of the curve reiterates the importance of running a new set of standards for preparation of a new standard curve, along with controls, each time the assay is performed. The good linear fit of the curve ensures accuracy of the sample absorbance in relation to phosphate concentration. The difference between expected and measured DPPC stock solutions indicates there is variability, represented by the standard error, resulting either from the preparation of the stock solution or the phosphate assay itself (Table 3.2). Concentrated stock solutions are solubilized with concentrated chloroform which is subject to fast evaporation. Evaporation may explain the deviation from the expected starting concentrations. Similarly,

volume measurement error during preparation of stocks or dilution to working concentrations as well as loss of lipid during experimental setup, may contribute to the observed variability. Stock concentrations are an important factor due to the built in assumption for the calculation of total lipid, which assumes a lipid composition consisting of 70 % DPPC (Eq 3.1). As a result there is some variability associated with total lipid estimates based on the phosphate assay. Variability between liposome samples (Table 3.3) is expected because total lipid will be influenced by the final concentration on re-suspension of the washed product in outside buffer and measured volumes are not used for re-suspension. While the phosphate assay does not allow direct measure of liposome concentration, it does provide a method that can be used experimentally to control the amount of lipid, a measure which is determined based on the amount of lipid required to see the desired effect. A concentration value would be the preferred measurement however, determining the concentration of nanoparticles is difficult due to the lack of sensitivity of instrumentation in the nanometer scale range where background interference is a problem.

Size characterization validates the size reproducibility of the LUVET technique between batches of liposomes. By synthesizing liposomes of a reproducible size we can assume that the encapsulation volume is also consistent between batches, an important factor when looking at dose response. This is also important when considering lipid concentrations for experimental procedures because with a reproducible size, lipid concentration measurements would correlate better with respect to the number of liposomes and make experimental

comparisons possible. The corrected values for liposome size are considered to be a more accurate measurement than those calculated by the instrument because the size of the microsphere beads used in the calibration are based on certificates of analysis. Statistical analysis of the sizing results show that inclusion of low concentrations of sugars in the hydrating buffer produces liposomes with an average size close to that expected using extruder membranes with a pore size of 400 nm. Liposomes synthesized without sugars are on average significantly larger than expected. Trehalose in particular has been shown to increase the packing density of polar headgroups of phospholipids in unilamellar vesicles (29) which may account for this size difference. It is not known if increasing the concentration of sugars has any influence on size but the size variability of liposomes prepared with different hydration buffers is of notable importance when developing procedures to maximize the intraliposomal concentration of trehalose and the volume entrapped. The size histograms also provide information about the liposome population confirming that the extrusion technique produces a homogenous population with a log normal distribution.

Flow cytometric analysis of the liposome population was the final technique used to characterize the synthesized product. The liposome flow histograms (Figure 3.6(b) and 3.7(b)) and the scatter plots (Figure 3.6(a), 3.7(a)) re-confirm the homogeneity and normal distribution of the liposome population. The fluorescence intensity of the histogram (Figure 3.7(c)) confirms encapsulation of the CF marker. Furthermore, Figure 3.8 confirms that increasing the CF

concentration of the hydrating buffer results in an increase in fluorescence intensity of the liposome population that is detectable by flow cytometry. An increase in fluorescence intensity is not detectable as the lipid concentration increases, indicating that the instrument is capable of detecting single particles in the nanoscale size range (Figure 3.8).

The relatively low trapped volumes ($\leq$30 %) that can be achieved using the extrusion synthesis technique have been detailed elsewhere (11, 30) and are a source of concern. Although liposomes used in previous studies were smaller (100 nm) than liposomes synthesized in this study, low encapsulation efficiencies could be problematic when considering our application. Additional concerns are the use of chloroform to solubilize DPPC and CL and producing sterile liposomes of the required size. While the lyophilization step should ensure the removal of residual chloroform, the use of organic solvents runs the risk of being potentially toxic. Sterile filtering of liposomes > 150 nm is not possible therefore aseptic techniques would be required (16). Autoclaving may be an option however lipid degradation may occur. The sterility factor along with the high cost of commercially available lipids has poor economic feasibility. These are all issues which need to be addressed when developing a clinically acceptable process and require early consideration.

3.5 CONCLUSION

The LUVET technique for liposome synthesis is a relatively straightforward procedure that results in a reproducible product that helps to ensure a standard

of quality between samples. The phosphate assay, although indirect, provides a method of quantitative measure to control the amount of liposomes used experimentally. The size reproducibility combined with the phosphate assay allows some degree of experimental comparison. The flow cytometric and sizing methods ensure that the synthesis technique produces a single normally distributed population of liposomes. The ability of the flow cytometer to detect nanometer size particles and discern between particles of increasing intensity makes it a powerful tool for looking at transfer of liposomal contents into cells. This is a promising outcome because flow cytometry will be the method used to evaluate the interaction between cells and liposomes. Overall, the LUVET technique combined with the versatility of liposomes, allows easy alteration of the aqueous composition without changing the methods of characterization. This may prove to be important when it comes to optimizing the delivery of liposomal contents.

The generality and reproducibity of the LUVET approach to liposome synthesis will allow one to take full advantage of the versatility of liposomes, enabling alteration of the lipid composition and aqueous contents if required. Increasing the intraliposomal concentration of trehalose and changing the surface charge and composition of the membrane may be required for application purposes. Lipid membrane charge and composition influence the ease with which liposomes and cells interact and even the mechanism of interaction, both factors which need to be considered when trying to maximize intracellular delivery (14, 31).

The development of methods to measure intraliposomal trehalose concentration and trapping efficiency would also be of considerable value and are techniques which are currently being developed in our laboratory by Jelena Holovati (32). A direct measure of liposome concentration would assist in this goal and provide a more accurate measure of trapping efficiency and intraliposomal trehalose concentrations than the theoretical calculations which are usually employed. The accuracy of measuring liposome concentration and entrapment is further complicated by the log normal distribution of the liposome population. While numerous factors need to be taken into consideration, the establishment of a reliable and reproducible liposome synthesis technique provides a firm foundation for conducting investigations into the interaction between liposomes and cells *in vivo*.

3.6 REFERENCES

1. Gruner SM, Lenk RP, Janoff AS, Ostro MJ. Novel multilayered lipid vesicles: Comparison of physical characteristics of multilamellar liposomes and stable plurilamellar vesicles. Biochemistry 1984;24:2833-2842.
2. Mayer LD, Hope HJ, Cullis PR, Janoff AS. Solute distributions and trapping efficiencies observed in freeze-thawed multilamellar vesicles. Biochim Biophys Acta 1985;817:193-196.
3. Abramson MB, Katzman R, Gregor HP. Aqueous dispersions of phosphatidylserine. J Biol Chem 1964;239:70-76.

4. Saunders L, Perrin J, Gammack DB. Ultrasonic irradiation of some phospholipid sols. J Pharm Pharmacol 1962;14:567-572.

5. Huang C. Studies on phosphatidylcholine vesicles. Formation and physical characteristics. Biochemistry 1969;8(1):344-352.

6. Barenholzt Y, Amselem S, Lichtenberg D. A new mothod for preparation of phospholipid vesicles (liposomes) - French press. FEBS Lett 1979;99(1):210-214.

7. Batzri S, Korn ED. Single bilayer liposomes prepared without sonication. Biochim Biophys Acta 1973;298(4):1015-1019.

8. Enoch HG, Strittmatter P. Formation and properties of 1000-A-diameter, single-bilayer phospholipid vesicles. Proc Natl Acad Sci U S A 1979;76(1):145-149.

9. Kagawa Y, Racker E. Partial resolution of the enzymes catalyzing oxidative phosphorylation. IX. Reconstruction of oligomycin-sensitive adenosine triphosphatase. J Biol Chem 1966;241(10):2467-2474.

10. Olson F, Hunt CA, Szoka FC, W.J. V, Papahadjopoulos D. Preparation of liposomes of defined size and distribution by extrusion through polycarbonate membranes. Biochim Biophys Acta 1979;557:9-23.

11. Hope MJ, Bally MB, Webb G, Cullis PR. Production of large unilamellar vesicles by a rapid extrusion procedure. Characterization of size distribution, trapped volume and ability to maintain a membrane potential. Biochim Biophys Acta 1985;812:55-65.

12. Schuh JR, Banerjee U, Muller U, Chan SI. The phospholipid packing arrangement in small bilayer vesicles as revealed by proton magnetic resonance studies at 500 MHz. Biochim Biophys Acta 1982;687(2):219-225.

13. Eytan GD, Broza R, Notsani B, Dachir D, Gad AE. Interaction of acidic liposomes with red blood cells induction of endocytosis and shedding of particles. Biochim Biophys Acta 1982;689:464-474.

14. Poste G, Papahadjopoulos D. The influence of vesicle membrane properties on the interaction of lipid vesicles with cultured cells. Ann N Y Acad Sci 1978;308:164-184.

15. Lelkes PI, Tandeter HB. Studies on the methodology of the carboxyfluorescein assay and on the mechanism of liposome stabilization by red blood cells. Biochim Biophys Acta 1982;716:410-419

16. Lasic D. Novel applications of liposomes. Tibtech 1998;16:307-321.

17. Philippot JR, Schuber F. Liposomes as tools in basic research and industry. Boca Raton: CRC Press; 1994.

18. Bangham AD, Standish MM, Watkins JC. Diffusion of univalent ions across the lamellae of swollen phospholipids. J Mol Biol 1965;13(1):238-252.

19. McMullen TPW, McElhaney RN. New aspects of the interaction of cholesterol with dipalmitoylphosphatidylcholine bilayers as revealed by high-sensitivity differential scanning calorimetry. Biochim Biophys Acta 1994;1234:90-98.

20. Mayer LD, Hope MJ, Cullis PR. Vesicles of variable sizes produced by a rapid extrusion procedure. Biochim Biophys Acta 1986;858:161-168.

21. Fiske CH, Subbarow Y. The calorimetric determination of phosphorous. J Biol Chem 1925;66(2):375-400.

22. Bell RD, Doisy EA. Rapid calorimetric methods for the determination of phosphates in urine and blood. J Biol Chem 1920;44:55-67.

23. Briggs AP. A modification of the Bell-Doisy phosphate method. J Biol Chem 1922;53:13-16.

24. Benedict SR, Theis RC. A modification of the molybdic method for the determination of inorganic phosphorus in serum. J Biol Chem 1924;61:63-66.

25. Horecker BL, Ma TS, E. H. Note on the determination of microquantities of organic phosphorus.

26. Bartlett GR. Phosphorus assay in column chromatography. 1959;234(3):466-468.

27. Tuchin V. Optical propreties of tissues with strong (multiple) scattering: Refractive index measurements. In: O'Shea DC, editor. Tissue Optics Light Scattering Methods and Instruments for Medical Diagnostics. Bellingham: SPIE-The International Society for Optical Engineering; 2000. p. 40-44.

28. Ma X, Lu JQ, Brock RS, Jacobs KM, Yang P, Hu X. Determination of complex refractive index of polystyrene microspheres from 370 to 1610 nm. Phys Med Biol 2003;48:4165-4172.

29. Luzardo MdC, Amalfa F, Nunez AM, Diaz S, Biondi de Lopez AC, Disalvo EA. Effect of trehalose and sucrose on the hydration and dipole potential of lipid bilayers. Biophys J 2000;78:2452-2458.

30. Szoka F, Olson F, Heath F, Vail T, Mayhew E, Papahadjopoulos D. Preparation of unilamellar liposomes of intermediate size (0.1-0.2 umol) by a combination of reverse phase evaporation and extrusion through polycarbonate membranes. Biochim Biophys Acta 1980;601(3):559-571.

31. Poste G, Papahadjopoulos D. Lipid vesicles as carriers for introducing materials into cultured cells: Influence of vesicle lipid composition on mechanism(s) of vesicle incorporation into cells. Proc Natl Acad Sci U S A 1976;73(5):1603-1607.

32. Holovati JL, Acker JP. Spectrophotometric measurement of intra-liposomal trehalose. Cryobiology 2006;53 (*in press*).

Table 3.1: Phosphate assay standard curve linear regression results.

Liposome Batch #	R^2 Value	Regression Equation
L5-L7	0.9995	y = 0.0024x + 0.0125
L8	0.9939	y = 0.0023x + 0.0093
L9	0.9956	y = 0.0022x + 0.0088
L10	0.9997	y = 0.003x + 0.0144
L11	0.9954	y = 0.0021x + 0.1265
L12	0.9977	y = 0.003x + 0.0224

Table 3.2: Average DPPC lipid stock solution concentrations.

Expected Phosphate Concentration (mg/ml)	Calculated Phosphate Concentration ± SE (mg/ml)	Sample Size (n)
100	125.7 ± 0.9	2
200	220.3 ± 14.1	8

Table 3.3: Phosphate assay results. Calculated lipid concentrations for liposome samples.

Liposome Batch	Hydration Buffer	Lipid Concentration (mmol/L)
L5	NaCl	18.7
L5	NaCl/sucrose	17.6
L5	NaCl/trehalose	16.0
L6	NaCl	33.9
L6	NaCl/sucrose	30.6
L6	NaCl/trehalose	36.7
L7	NaCl	56.3
L7	NaCl	45.0
L7	NaCl/sucrose	28.8
L7	NaCl/trehalose	42.5
L8	KCl	86.4
L8	KCl	73.7
L8	KCl	79.4
L8	KCl	85.4
L8	KCl	96.7
L8	KCl	41.9
L8	KCl	54.2
L9	HBSI	111.2
L9	HBSI	90.7
L9	HBSI	76.3
L9	HBSI	111.3
L9	HBSI	107.8
L9	HBSI/sucrose	118.2
L9	HBSI/trehalose	126.8
L10	SFM/trehalose	44.0
L10	SFM/trehalose	87.1
L10	SFM/trehalose	93.7
L10	SFM/trehalose	107.0
L11	SFM/trehalose	133.5
L11	SFM/trehalose	104.5
L12	SFM/trehalose	87.3
L12	SFM/trehalose	63.8
L12	SFM/trehalose	60.1

Table 3.4: Mean size distributions for synthetic beads used for standardization.

Expected Bead Size (nm)	Average Measured Bead Size ± SE (nm)	Sample Size (n)
200	136 ± 0.7	7
400	306 ± 5.3	6
800	757 ± 3.7	7

Table 3.5: Statistical analysis of mean size distributions between groups of liposomes.

P-values	No Sugar	Sucrose	Trehalose
No Sugar	—	0.000*	0.000*
Sucrose	0.000*	—	0.308
Trehalose	0.000*	0.308	—

* The mean difference is significant at the 0.05 level

Table 3.6: Mean liposome size distributions. Measured, standardized, and average (± SEM) size of liposomes prepared (a) without sugar, (b) with trehalose or (c) with sucrose.

(a) Sugar-free Liposomes

Mean Liposome Size Distribution (nm)	
Measured	**Standardized**
566	626
523	584
461	525
437	502
565	625
537	598
556	616
563	623
548	608
546	606
544	605
583	642
574	633
573	632
559	619
530	591
542 ± 10.0 (n=16)	**602 ± 9.5 (n=16)**

(b) Trehalose Liposomes

Mean Liposome Size Distribution (nm)	
Measured	**Standardized**
469	533
376	444
381	449
361	430
436	501
430	496
394	461
401	468
395	462
415	481
406 ± 10.2 (n=10)	**473 ± 9.7 (n=10)**

(c) Sucrose Liposomes

Mean Liposome Size Distribution (nm)	
Measured	**Standardized**
393	460
353	422
373	441
362	431
370 ± 8.6 (n=4)	**439 ± 8.2 (n=4)**

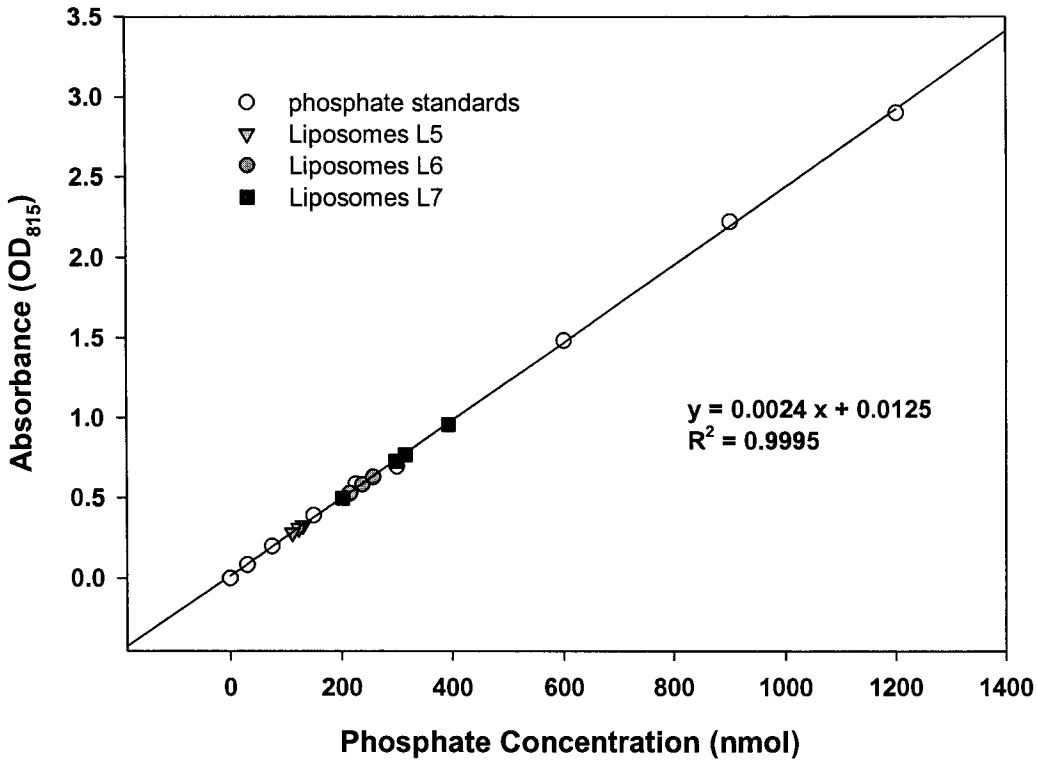

Figure 3.1: Phosphate assay standard curve. Calculated phosphate concentration of liposome samples based on absorbance at 815 nm.

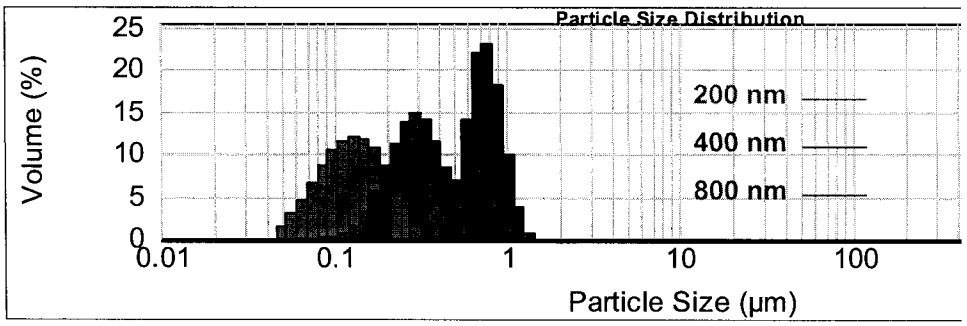

Figure 3.2: The microsphere size standard distribution curves generated from the Mastersizer.

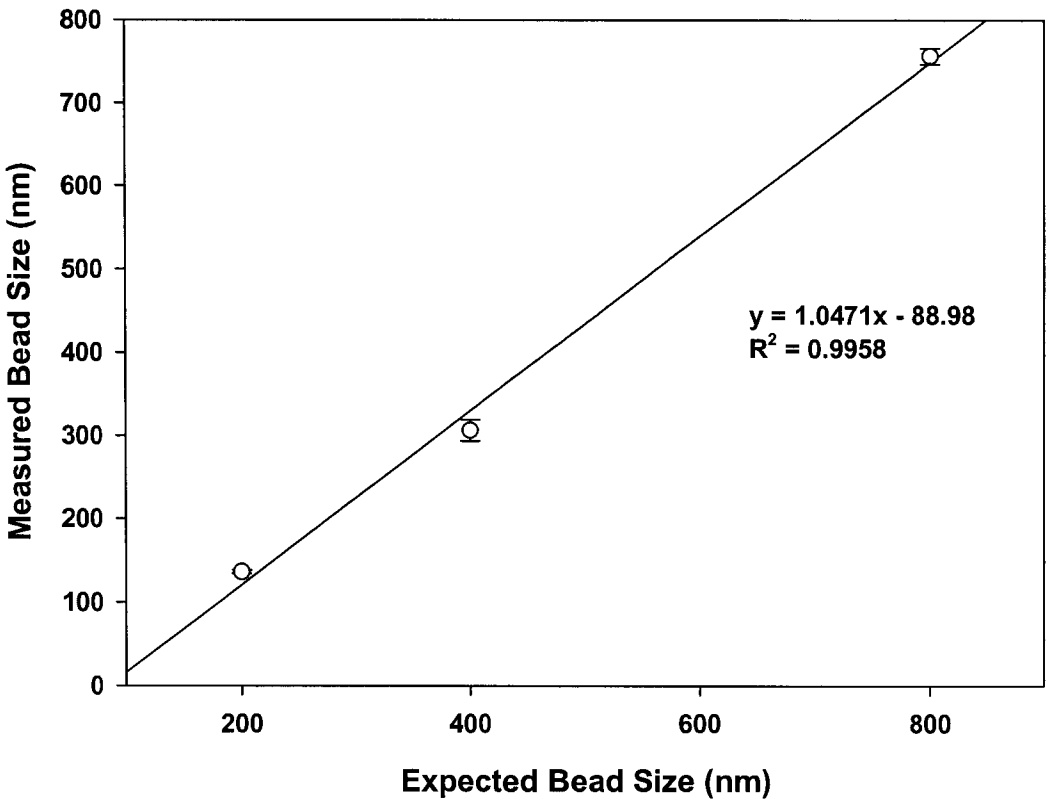

Figure 3.3: Sizing standard curve. A comparison between the mean measured size of synthetic size standards with the mean expected size.

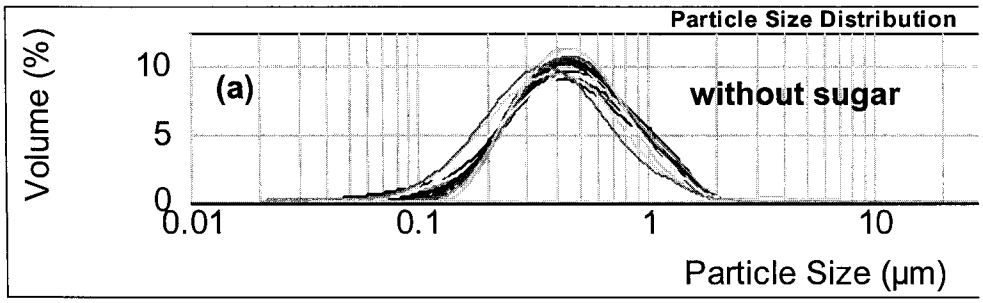

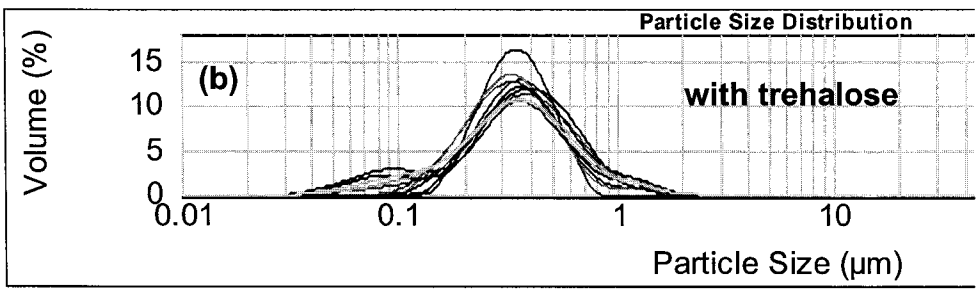

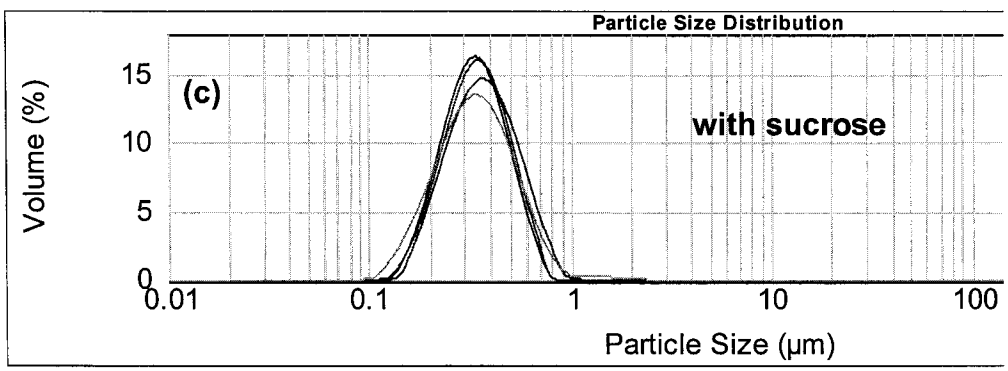

Figure 3.4: Size distribution curves between batches of liposomes synthesized (a) without sugar, (b) with trehalose, and (c) with sucrose.

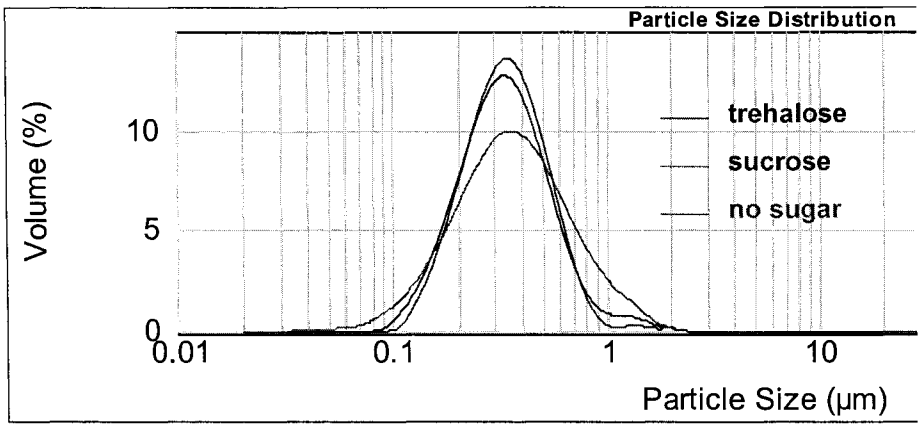

Figure 3.5: The size distributions of different types of liposomes.

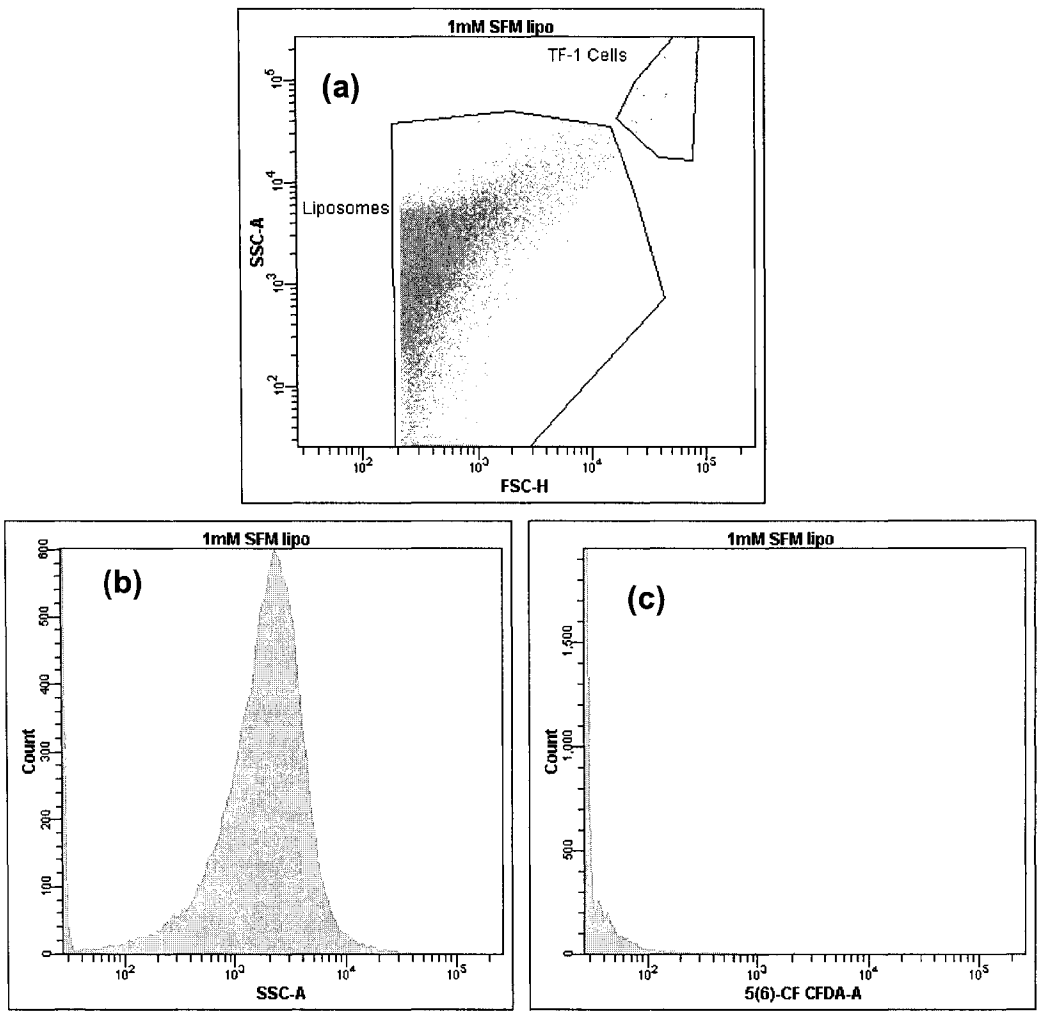

Figure 3.6: Scatter plot (a) and flow histograms (b), (c) for liposomes synthesized to contain SFM (no CF).

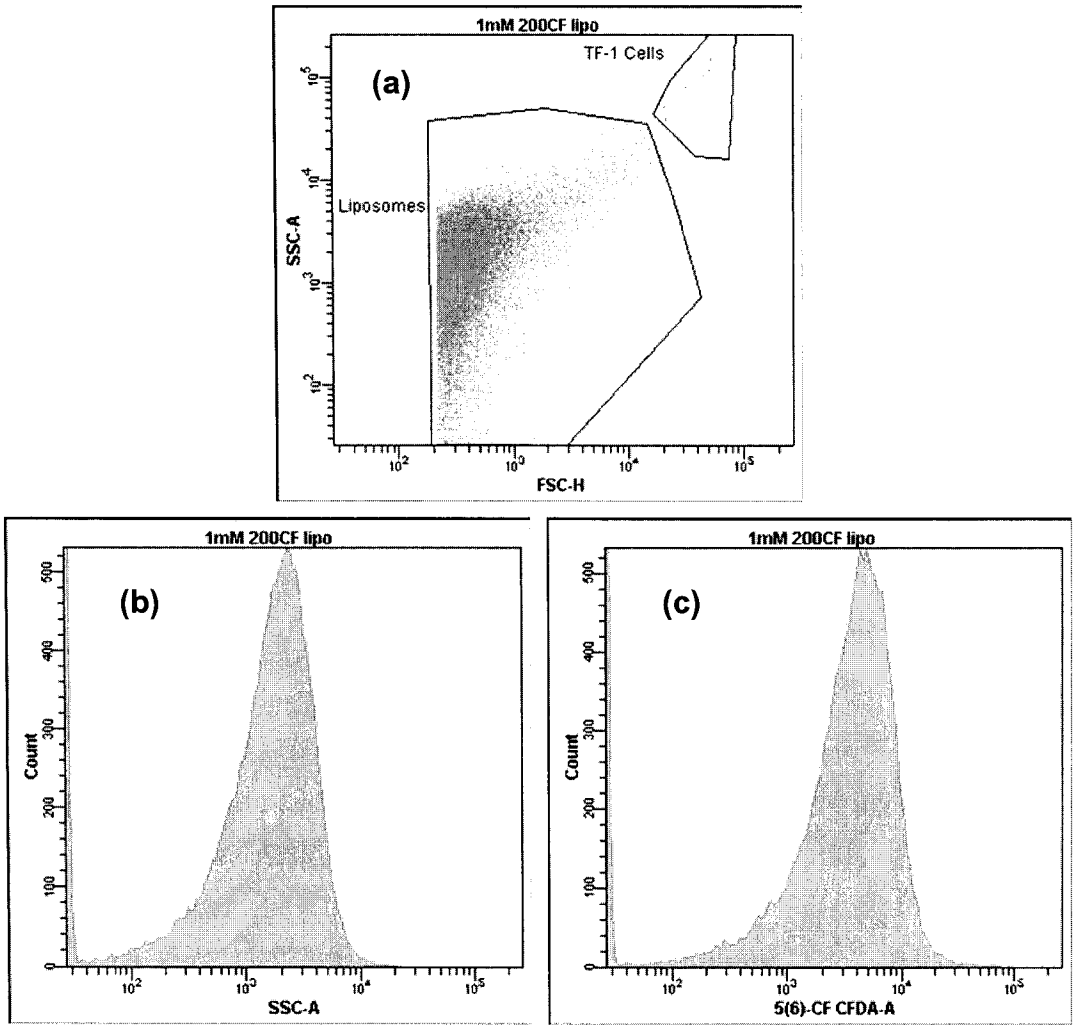

Figure 3.7: Scatter plot (a) and flow histograms (b), (c) for liposomes synthesized to contain 200 µmol/L 5(6)-CF and 0.2 mol/L trehalose.

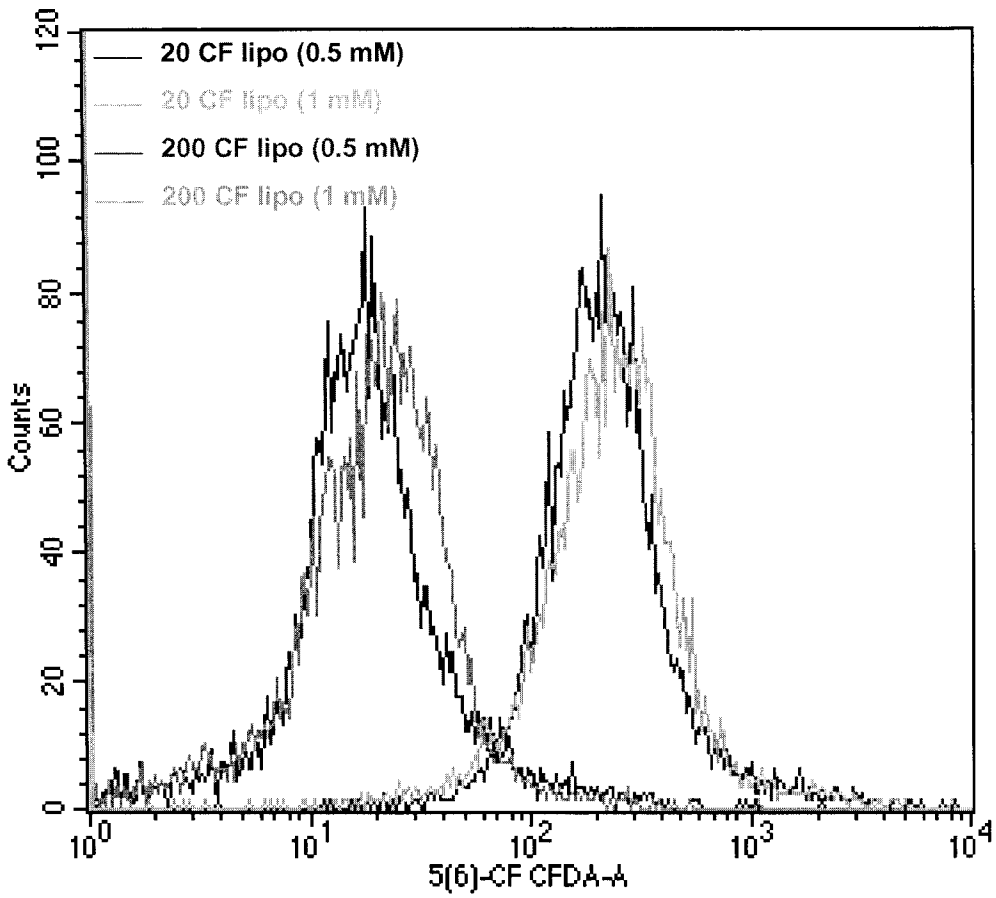

Figure 3.8: Fluorescence intensity of variable concentrations of liposomes synthesized with 20 µmol/L and 200 µmol/L CF.

CHAPTER 4

CHARACTERIZING THE RESPONSE OF TF-1 CELLS TO LIPOSOMES

4.1 INTRODUCTION

In the previous chapter techniques were established to synthesize and characterize liposomes containing trehalose. This was a fundamental precursor to the investigation into the interaction between cells and liposomes *in vitro* because the methods developed allow for the controlled synthesis of a reproducible product with measurable characteristics. Quantifiable properties are a necessary component to ensure a standard of quality between preparations and to provide a means to allow for experimental comparisons.

In order to determine if liposomes are an effective tool for the intracellular delivery of the membrane impermeable molecule trehalose, it is necessary to identify the parameters which influence liposome-cell interactions. An increase in cellular fluorescence intensity is detectable by flow cytometry and therefore was used as the primary indicator of liposome-cell association. Although measuring cellular fluorescence intensity is an indirect approach to gage the liposomal delivery of trehalose, the shared properties of trehalose and carboxyfluorescein provided the rationale for the experimental approach. The merit of using fluorophores as surrogates to trehalose uptake has been demonstrated (1). Trehalose and 5(6)-carboxyfluorescein are similar in molecular weight, both have neutral charge densities, are soluble in aqueous solutions, and considered membrane impermeable which would facilitate

retention of both molecules within the intraliposomal compartment. The purpose of this study was twofold: to assess the effect of time, temperature and liposome concentration on liposome-cell interaction and to characterize the effect of liposome-cell interaction on cell membrane integrity and the expression of surface antigens involved in differentiation and proliferation.

4.2 METHODS

Cell Handling

TF-1 cells were cultured according to a standard protocol (see Appendix A) and maintained between 2 x 10^4 cells/ml and 4 x 10^5 cells/ml. All cell suspensions used in liposome experiments were washed 3 times with SFM by centrifugation (Sorvall 5810R, Eppendorf, Hamburg, Germany) at 100 x g for 5 minutes each at room temperature (RT, 22 °C). Washed cell suspensions from separate flasks were combined and concentrated to between 2 x 10^7 cells/ml - 5 x 10^7 cells/ml. All experimental samples were prepared in 35 mm non-tissue culture treated Petri dishes (Becton Dickinson (BD) Biosciences, CA, USA) by dilution of concentrated cell suspensions to a final working concentration of about 2 x 10^6 cells/ml in SFM supplemented with 0.2 mol/L trehalose. Following experimental manipulation cell suspensions were transferred to 1.5 ml microtubes and centrifuged at 300 x g and 4 °C for 5 minutes. After the initial centrifugation step, cell supernatant was decanted and the cells re-suspended in cold (4 °C) SFM and washed by centrifugation. Cold spins were found to improve the formation of a cell pellet at low cell numbers (2 x 10^6 cells) and

small volumes. Low temperatures also slow metabolic and other biochemical processes such as endocytosis. Endocytosis has been correlated with the uptake of fluid neutral liposomes (similar to those used in this study) by nucleated mammalian cells (2, 3), therefore cold spins were employed to essentially stop or a least slow liposome-cell interactions at the end of the experimental period. Washing by centrifugation was repeated a total of 3 times to ensure removal of liposomes from the cell suspension. Due to cell loss during processing (centrifugation/washing), cells were re-suspended to a final volume of 500 µl with SFM so cell concentrations were adequate for analysis by flow cytometry. All samples were kept in the dark on ice and assessed for change using flow cytometry (FACSCanto, BD Biosciences, CA, USA) (see Appendix A). All liposomes used in these experiments were synthesized to contain 0.2 mol/L trehalose and either 20 µmol/L or 200 µmol/L CF unless stated otherwise. Measurements for liposome concentrations (mmol/L lipid) used in the following experiments were based on the phosphate assay (Chapter 3). Any deviations from this procedure are indicated. TF-1 cells maintained in SFM under the same conditions with respect to incubation time and temperature but without exposure to liposomes, were run in parallel for each experiment and are referred to as untreated controls.

Temperature

For temperature analysis experiments, all buffers were chilled on ice prior to use. Liposomes, containing either 20 µmol/L or 200 µmol/L CF, were added to the cell suspensions in non-tissue culture treated Petri dishes at lipid

concentrations of 0.5 mmol/L or 1 mmol/L. All experimental preparations were mixed well by pipetting. Samples were incubated for 3 hours at 0 °C, 22 °C or 37 °C then processed according to the above protocol.

Liposome Concentration

To look at the effect of liposome concentration on fluorescence transfer into cells, working concentrations of TF-1 cells were prepared in duplicate with liposomes containing either 20 µmol/L or 200 µmol/L CF at lipid concentrations of 0.5, 1, 2, 3, or 4 mmol/L. Samples were incubated at 37 °C for 4 hours before processing.

Immunophenotyping

In a separate experiment the effect of increasing liposome concentration (0.5 – 4 mmol/L) on TF-1 cell antigen expression and membrane integrity was determined following incubation at 37 °C for 2 hours. The rationale for antigen selection is discussed in Appendix A. Liposomes were synthesized to contain 0.2 mol/L trehalose and were devoid of CF marker. Liposomes devoid of CF were required because the monoclonal antibody for CD34 used in this experiment alone was conjugated to fluorescein isothiocyanate (FITC) and is not compatible with other fluorescein molecules such as CF. The CD34 monoclonal antibody used in all other immunophenotyping experiments was conjugated to peridinin chlorophyll protein (PerCP), however PerCP cannot be used in conjunction with the membrane integrity marker 7-amino-actinomycin D (7-AAD) due to spectral overlap. At the end of the incubation period cells were processed as usual but washed only once after the initial centrifugation step.

Cell washing by centrifugation following incubation with liposomes was minimized in order to reduce the stress imposed on the cells prior to immunophenotyping analysis, which requires additional washing by centrifugation a minimum of two times. A pre-determined concentration of monoclonal antibodies for CD33-PE, CD34-FITC and CD71-APC was then added to each sample (see Appendix A). Cell suspensions were incubated on ice for 30 minutes then washed by centrifugation 2 times at 300 x g for 5 minutes each to remove unbound antibody. For a detailed description of the immunophenotyping protocol refer to Appendix A. Membrane integrity was determined by the addition of 20 µl of 7-AAD just prior to flow cytometric assessment.

TF-1 cell antigen expression following 5 hour incubation with 3 mmol/L lipid at either 22 °C or 37 °C was also determined by immunophenotyping. Liposomes used in this experiment contained 200 µmol/L CF. Processed samples were labeled with CD33-PE, CD34-PerCP and CD71-APC.

Temporal Analysis

The effect of incubation time on cellular fluorescence intensity was assessed following incubation at 37 °C with liposomes containing 200 µmol/L CF. Cell suspensions for each time point were prepared in duplicate and incubated with 3 mmol/L lipid for 5 minutes, 30 minutes, 1, 2, 3, 4, or 5 hours before processing. Duplicate samples were also prepared with liposomes and held at 0 °C for 5 hours. Processed samples were kept on ice in the dark until samples

for all time points had been collected, at which point cellular fluorescence was assessed using flow cytometry.

Cellular Response to Free CF

The response of TF-1 cells to free CF was determined following a 5 hour incubation of cells at 37 °C in decreasing concentrations of extracellular, free CF. Incubation solutions were prepared by serial dilution (1:1) of SFM supplemented with 0.2 mol/L trehalose and 20 µmol/L CF. Controls were also prepared to look at the effect of incubation temperature (0 °C, 22 °C and 37 °C) on cells exposed to 20 µmol/L CF for 5 hours. Cells were processed as usual and cellular fluorescence intensity assessed using flow cytometry.

Liposome Leakage

In order to determine whether free CF remains in the extraliposomal buffer following liposome synthesis and washing, liposomes containing 200 µmol/L CF were diluted to 3 mmol/L lipid in SFM and incubated at 0 °C, 22 °C or 37 °C for 5 hours. Another sample of liposomes diluted to 3 mmol/L lipid in SFM was plunged into liquid nitrogen until frozen then thawed in a 70 °C water bath. The freeze-thaw procedure was repeated a total of six times to facilitate the release of intraliposomal contents. When the incubation period was complete all samples, including the freeze-thaw sample, were transferred to 1.5 ml centrifuge tubes and centrifuged for 15 minutes at 13,332 x g. The supernatant was collected and centrifuged for another 15 minutes at 13,332 x g. This process was repeated until there was no visible sign of a liposome pellet in the supernatant. Concentrated TF-1 cells were added to each liposomal

supernatant so final cell concentrations were 2 x 10^6 cells/ml. The addition of cells to the liposomal supernatants was required for gating purposes in order to acquire information related to the fluorescence intensity of non-particulate matter using flow cytometry (see Appendix A). Cell suspensions were kept on ice in the dark and assessed using flow cytometry. The cellular fluorescence intensity was measured and used as an indication of the fluorescence intensity contributed by the liposomal supernatants.

4.3 RESULTS

For each experiment the autofluorescence of untreated TF-1 cells was subtracted from the mean cellular fluorescence intensity of treated cells. Therefore, the mean cellular fluorescence intensity that is reported is a direct result of the treatment condition.

Temperature Analysis

The cellular fluorescence intensity of TF-1 cells following a 3 hour incubation at 0 °C, 22 °C or 37 °C with liposomes containing 20 µmol/L CF either at lipid concentrations of 0.5 mmol/L or 1 mmol/L lipid is illustrated in Figure 4.1(a). The autofluorescence of untreated TF-1 cells is represented by the shaded histogram and the liposome treated cells are represented by the line histograms. There is no detectable increase in cellular fluorescence intensity following incubation with liposomes containing 20 µmol/L CF, regardless of the incubation temperature. When TF-1 cells are incubated under the same conditions (time, temperature and lipid concentration) but with liposomes

containing 200 µmol/L CF, there is a detectable increase in mean cellular fluorescence intensity with treatment (Figure 4.1(b)). Increasing both the liposome concentration and the incubation temperature contributes to the increase in mean cellular fluorescence intensity (Figure 4.2). There is nearly a 100 fold increase in intensity from 0 °C to 37 °C with 0.5 mmol/L lipid and nearly a 200 fold increase over the same temperature spread with 1 mmol/L lipid. At 0 °C the difference in mean cellular fluorescence intensity between liposomes prepared with 20 µmol/L CF and 200 µmol/L CF is small.

Liposome Concentration

An investigation into the effect of lipid concentration on cellular fluorescence intensity is illustrated in Figure 4.3 and 4.4. Mean cellular fluorescence intensity increases with increasing lipid concentration following a 4 hour incubation of TF-1 cells with liposomes containing either 20 µmol/L CF (Figure 4.3(a)) or 200 µmol/L CF (Figure 4.3(b)). The increase in fluorescence intensity is seen as a right shift in the flow histograms, relative to the untreated control (shaded histogram), as lipid concentration increases. The increase in mean cellular fluorescence intensity of cells incubated with liposomes containing 20 µmol/L CF is small relative to the autofluorescence intensity (Figure 4.3(a)). Lipid concentrations ≥ 2 mmol/L are required for a detectable increase in mean cellular fluorescence above autofluorescence (Figure 4.4). The increase in mean cellular fluorescence intensity of cells incubated with liposomes containing 200 µmol/L CF is easily detectable above the cell autofluorescence (Figure 4.3(b)) and the intensity increases with each increase in lipid concentration

(Figure 4.4). There is a strong positive correlation between lipid concentration and mean cellular fluorescence intensity. The magnitude of the increase is also dependent on the concentration of CF inside the liposomes.

Temporal Analysis

The effect of liposome-cell incubation time on cellular fluorescence intensity is depicted in Figure 4.5 and 4.6. The mean cellular fluorescence intensity of cells incubated with liposomes containing 200 μmol/L CF at a concentration of 3 mmol/L increases with incubation time at 37 °C. The increase in intensity above the cells autofluorescence with time is illustrated in Figure 4.5 where cellular autofluorescence is indicated by the shaded histogram. Figure 4.6 is the graphical representation of the temporal response. The cellular fluorescence intensity reaches 50 % of the maximum value in less than 1 hour and starts to plateau around the 4 hour mark. Cells exposed to 3 mmol/L lipid at 37 °C for 5 hours have a mean cellular fluorescence intensity about 7 times greater than cells exposed to 3 mmol/L lipid at 0 °C for 5 hours, reiterating that cell-liposome interaction is temperature dependent.

The Effect of Liposomes on Antigen Expression

TF-1 cell antigen expression following incubation with increasing concentrations of liposomes is illustrated in Figure 4.7. There is no visible change in the expression of CD34, CD33 or CD71 antigens following a 2 hour incubation of cells with unmarked (no CF) liposomes, regardless of lipid concentration (0.5 mmol/L - 4 mmol/L). Cell membrane integrity was also assessed following treatment with increasing lipid concentration and the results are summarized in

Table 4.1. The average percentage of cells with intact membranes following liposome treatment at concentrations up to 4 mmol/L, is > 95 ± 0.7. Antigen expression and cell membrane integrity does not change following short term (2 h) incubation with liposomes, regardless of the lipid concentration.

TF-1 cell antigen expression following incubation at 22 °C or 37 °C with liposomes containing 200 μmol/L CF for 5 hours at a concentration of 3 mmol/L lipid, is illustrated in Figure 4.8. When compared to untreated cells there is an increase in mean cellular fluorescence intensity along the CF axis with increasing temperature, indicating CF is associated with the cell population. The increase in intensity is greater for cells incubated with liposomes at 37 °C compared to cells incubated with liposomes at 22 °C. There is a decrease in the expression of CD71 cell proliferation marker and CD34 differentiation marker in a small percentage of the population. The percentage of the cell population not expressing CD71 increases from 0.7 % in the control group, to 4.5 % and 4.9 % following exposure to liposomes for 5 hours at 22 °C and 37 °C, respectively. Under the same conditions, the percentage of the cell population not expressing CD34 increases from 3.3 % in the control group to 4.2 % and 10.2 % in cells incubated at 22 °C and 37 °C, respectively. While ≥99 % of the cell population expresses the CD33 cell lineage marker, regardless of the condition, there is clearly the appearance of a small second population in the 37 °C treatment group which has decreased CD33 antigen expression. This is indicated by the decrease in intensity along the CD33 axis so that a small portion of the cell population is situated within the second log phase of the

quadrant histogram. This discrete but small cell population is only apparent in the 37 °C treatment group but not in the 22 °C treatment group or the untreated control group.

The Response of TF-1 Cells to Free Fluorophore

When cells are incubated at 37 °C with SFM containing 20 μmol/L CF, there is a rapid increase in mean cellular fluorescence intensity with time (Figure 4.9). The intensity reaches 50 % of the maximum value within 10 minutes and starts to plateau around the 30 minute mark. There is also a corresponding increase in mean cellular fluorescence intensity with increasing concentration of free fluorophore (Figure 4.10) which is highly linear, $R^2 = 0.9974$ (Figure 4.11).

Flow cytometric analysis of TF-1 cells suspended in liposomal supernatants is illustrated in Figure 4.12. A detectable increase in mean cellular fluorescence intensity above the level of autofluoresence, in cells suspended in liposomal supernatant, is an indication that some unencapsulated CF remains in the extraliposomal buffer following liposome synthesis and washing, or that liposomes are not stable and leakage of intraliposomal contents is occurring over time. The amount of CF in the extraliposomal buffer does not appear to be strongly temperature dependent because there is only a small detectable increase in the mean cellular fluorescence intensity when comparing the supernatants of liposomes incubated at increasing temperature for 5 hours. There is a 20 fold increase in the fluorescence intensity in cells suspended in liposomal supernatant following freeze-thaw when compared to the

fluorescence intensity in cells suspended in the liposomal supernatant of unfrozen liposomes.

4.4 DISCUSSION

Temperature Response

Parameters that influence the interaction between liposomes and TF-1 cells are incubation time and temperature as well as liposome concentration. Cell-associated fluorescence increased with increasing incubation temperature. At 0 °C cell-associated fluorescence is markedly reduced, increases at 22 °C and is highest following incubation with liposomes at 37 °C (Figure 4.2). Factors which may be contributing to the observed temperature dependence are changes in the lipid membranes of cells and liposomes as well as changes in biochemical processes as temperature increases. A temperature sensitive response to cellular uptake of liposomes has been observed in 3T3 fibroblasts which incorporate liposomes almost exclusively by endocytosis (3). With evidence in the literature to support the observed temperature dependence of liposomal uptake into nucleated mammalian cells (3), it is clear that incubation temperature is an important variable affecting liposome-cell interaction.

Temporal Response

The temporal analysis shows that cell associated fluorescence increases with incubation time following exposure to liposomes (Figure 4.6). The observed temporal response is slower with liposomes (Figure 4.6) than with free CF (Figure 4.9). The difference in temporal response may be attributed to a

concentration effect, when comparing CF concentrations in a solution of free fluorophore (20 µmol/L) to the relatively small volume assumed to be encapsulated within each liposome. However, the difference in temporal response between the two groups may be considered evidence in support of the hypothesis that liposomes are contributing to the observed increase in cellular fluorescence intensity and the response is not just an artifact of free CF. A temporal response which correlates well with the results of this study has been observed in cultured mammalian cells, with rapid uptake of liposomes within 2 hours, after which uptake leveled off and reached a plateau within 3 to 8 hours depending on cell type (2). The time sensitive nature of liposome-cell interaction observed here and elsewhere, reiterates the importance of defining the parameters which influence the interaction in order to design protocols which promote enhanced delivery of the target molecule.

Liposome Concentration

Another variable which influences liposome-cell interaction is the liposome concentration. As the concentration of liposomes increases there is a corresponding increase in the cell associated fluorescence which is an indication that when the liposome to cell ratio increases, the number of liposome-cell associations also increase. Cultured mammalian cells have been described by Poste, et al. as "display[ing] a remarkable appetite for lipid vesicles" (2).

Antigen Expression and Cytotoxicity

Differences in antigen expression of TF-1 cells incubated with liposomes were seen after 5 hours (Figure 4.8) but not after 2 hours (Figure 4.7). Due to the small sample size, we cannot conclude that the slight decrease in CD34 and CD71 expression following a 5 hour liposome treatment was in response to liposome-cell interaction. Expression of the CD71 transferrin receptor protein, which is essential for cell growth, has been shown to increase or decrease during different phases of the cell cycle (4, 5). Experimental evidence of this has been observed in TF-1 cells during routine immunophenotyping (Appendix A, Figure A.4). The observed loss of CD34 expression may be attributed to the less than ideal incubation conditions in the absence of growth factor and serum protein, however the untreated samples were also incubated for 5 hours in SFM without growth factor or serum with no evident changes in CD34 expression. SFM media was required because the presence of sera have been shown to interact with liposomes causing loss of stability, leakage of liposomal contents and an alteration in the pattern of liposome-cell interactions (6, 7).

Reasons for the appearance of a small population of cells with reduced expression of CD33 can only be speculated. Liposomes are known to interact readily with proteins (2, 8, 9) and the exchange of liposome and cell membrane components has been observed (9). These interactions may result in the masking of surface antigens or a loss of antigen receptor proteins from the cell membrane. The observed differences in expression may also be explained in response to changes in cell membrane surface area, caused by the invagination

and pinching off of the cell membrane as liposomes are engulfed by the cell during endocytotic processes. Further experimentation is clearly necessary to support any of these explanations or even confirm that the observed changes are liposome related.

Immunophenotypic analysis (Figures 4.7 and 4.8) shows that the majority of the TF-1 cell population can tolerate incubation with high concentrations (4 mmol/L) of liposomes over a relatively short period of time (5 hours) without loss of membrane integrity or the expression of important antigens involved in determining cell fate in relation to cell lineage and the capacity to proliferate and differentiate. Cultured mammalian cells have been shown to easily incorporate $1 \times 10^6 - 5 \times 10^6$ liposomal vesicles/cell without cell viability or proliferation being impaired (2). While we are unable to compare this dose response in relation to lipid concentrations used in this study, at lipid concentrations of 4 mmol/L there is no observed difference in cell membrane integrity when comparing untreated cells to liposome-treated cells after 2 hours. It is possible that cells could tolerate even higher concentrations of liposomes, however, there is likely a fine balance between maximum tolerable lipid concentrations and cytotoxicity, which would need to be determined. Another important observation from the immunophenotyping analysis is that the cells which exhibit normal antigen expression are also positive for CF (Figure 4.8), suggestive of liposome-cell association.

The interaction between lipid vesicles and cultured mammalian cells, as summarized by Poste and Papahadjopoulos (10), may involve any or a

combination of the following mechanisms: (i) fusion of vesicles with the plasma membrane; (ii) incorporation of intact vesicles by endocytosis; (iii) exchange of phospholipids between the vesicle membrane and the plasma membrane; and (iv) adsorption of vesicles or fragments of vesicle membrane to the cell surface without true incorporation. The mechanism(s) of interaction between liposomes and cells used in this study is unkown and requires further experimentation.

Intraliposomal Concentration

Another observed response that merits discussion is the increase in cellular fluorescence intensity with liposomes synthesized to contain 200 µmol/L CF in comparison to liposomes containing 20 µmol/L CF. In general, the higher concentration of CF was required for detection using flow cytometry. This is a result of the cellular autofluorescence which interferes with detection of the CF fluorophore at lower concentrations. The increased cell-associated fluorescence observed with liposomes containing high concentrations of intra-liposomal CF is not a result of an increase in liposome-cell association because there is a consistent relationship between lipid concentration and intraliposomal CF concentration (Figure 4.4). Based on this outcome an obvious way of increasing delivery of the target molecule would be to increase the concentration of the target molecule contained inside the liposomes. This is another important factor that requires consideration when trying to optimize delivery.

Incorporation of Free Fluorophore

One important factor that cannot be ignored is the observed uptake of free CF by TF-1 cells (Figure 4.9 and 4.10). To further complicate this matter it is clear that free fluorophore remains in the extraliposomal buffer following liposome synthesis and washing (Figure 4.12). The amount of free fluorophore in the extraliposomal buffer does not appear to be strongly temperature dependent. There is only about a 1 % increase in the amount of CF found in the extraliposmal buffer with each temperature increase. This provides evidence that the increase in cellular fluorescence intensity with increasing incubation temperature is not due to a sudden release of CF from the aqueous core of the liposomes resulting from a change in lipid membrane permeability at higher temperatures. It is possible for trapped aqueous markers to leak from liposomes with the effect being most prominent around the T_m (9). The T_m of fluid neutral liposomes containing DPPC and CL is around 57 °C (11) so a rapid loss of intraliposomal contents at 37 °C would not be expected. In addition, the inclusion of CL in the lipid formulation broadens the Tm of phospholipids (9) and decreases the fluidity and permeability of the lipid membranes above their T_m (12), adding to the stability of liposomes and the retention of their aqueous contents. Although detectable concentrations of free CF are found in the extraliposomal buffer, the majority of the CF is entrapped and contained within the liposomes. This is clearly demonstrated by the fluorescence intensity of the freeze-thaw supernatant which is nearly 20 times greater than that found in the extraliposomal buffer (Figure 4.12).

Based on the amount of CF found in the liposomal supernatant, the contribution is potentially significant when considering the cell associated fluorescence following liposome treatment. That being said, the mean cellular fluorescence intensity is greater in washed cells following exposure to 3 mmol/L lipid for 5 hours (Figure 4.4) than the fluorescence intensity found in the supernatant alone (Figure 4.12). This observation provides evidence that the liposomes must be contributing to the cell associated fluorescence. Considering the size of the liposomes and the small aqueous volume they are capable of entrapping, it is not surprising that this difference is small relative to the total fluorescence. While there is still the confounding factor of free uptake, the observed results support the possibility of liposomal delivery into TF-1 cells.

4.5 CONCLUSIONS

Parameters that influence liposome-cell interaction have been identified. The transfer of fluorescence from liposomes to TF-1 cells is a temperature-, time- and concentration-dependent process. Increasing both the concentration of liposomes and the concentration of the target molecule contained within the liposomes results in an increase in cellular fluorescence. TF-1 cell membrane integrity and the expression of surface antigens involved in cell proliferation and differentiation is well maintained following incubation with specified concentrations of liposomes and for a period of time which is conducive to cellular uptake. The presence of residual CF in the extraliposomal buffer in addition to the cells ability to take up free CF makes it difficult to discern

between cellular fluorescence resulting from free CF and cellular fluorescence resulting from liposome-cell interaction. The temporal analysis and the increase in cell-associated fluorescence above that contributed by free CF in the extraliposomal buffer, provides supporting evidence that liposomes are the dominant factor contributing to cellular fluorescence. However, because the uptake of free CF is also a factor, it is difficult to determine the concentration directly related to liposomes. The extent of liposome-cell interaction, the mechanism(s) of interaction and the liposome encapsulation efficiency is yet to be determined and is not possible with the methods employed here. It is not unreasonable to suspect that if membrane impermeable solutes in the aqueous solution can be taken into the cells that liposomes within the extracellular milieu can also be taken into the cells, whether the mechanism of entry be the same or different is unclear and surpasses the exploration of this study.

4.6 REFERENCES

1. Oliver AE, Jamil K, Crowe JH, Tablin F. Loading human mesenchymal stem cells with trehalose by fluid-phase endocytosis. Cell Preserv Technol 2004;2(1):35-49.
2. Poste G, Papahadjopoulos D, Vail WJ. Lipid vesicles as carriers for introducing biologically active materials into cells. In: Methods Cell Biol: Academic Press; 1976. p. 33-71.
3. Poste G, Papahadjopoulos D. Lipid vesicles as carriers for introducing materials into cultured cells: Influence of vesicle lipid composition on

mechanism(s) of vesicle incorporation into cells. Proc Natl Acad Sci U S A 1976;73(5):1603-1607.

4. Sposi NM, Cianetti L, Tritarelli E, Pelosi E, Militi S, Barberi T, et al. Mechanisms of differential transferrin receptor expression in normal hematopoiesis. Eur J Biochem 2000;267(23):6762-6774.

5. Hedley D, Rugg C, Musgrove E, Taylor I. Modulation of transferrin receptor expression by inhibitors of nucleic acid synthesis. J Cell Physiol 1985;124(1):61-66.

6. Tyrrell DA, Richardson VJ, Ryman BE. The effect of serum protein fractions on liposome-cell interactions in cultured cells and the perfused rat liver. Biochim Biophys Acta 1977;497(2):469-480.

7. Zborowski J, Roerdink F, Scherphof G. Leakage of sucrose from phosphatidylcholine liposomes induced by interaction with serum albumin. Biochim Biophys Acta 1977;497(1):183-191.

8. Philippot JR, Schuber F. Liposomes as tools in basic research and industry. Boca Raton: CRC Press; 1994.

9. Pagano RE. Interactions of liposomes with mammalian cells. Ann Rev Biophys Bioeng 1978;7:435-68.

10. Poste G, Papahadjopoulos D. The influence of vesicle membrane properties on the interaction of lipid vesicles with cultured cells. Ann N Y Acad Sci 1978;308:164-184.

11. McMullen TPW, McElhaney RN. New aspects of the interaction of cholesterol with dipalmitoylphosphatidylcholine bilayers as revealed by

high-sensitivity differential scanning calorimetry. Biochim Biophys Acta 1994;1234:90-98.

12. Oldfield E, Chapman D. Effects of cholesterol and cholesterol derivatives on hydrocarbon chain mobility in lipids. Biochem Biophys Res Comm 1971;43(3):610-616.

Table 4.1: TF-1 cell membrane integrity: post-liposome treatment. TF-1 cell membrane integrity (7-AAD) following a 2 hour incubation with increasing concentrations of liposomes containing 0.2 mol/L trehalose.

Lipid Concentration (mmol/L)	Cell Membrane Integrity (%)
0	95.9
0.5	94.2
1	95.2
2	94.2
3	95.5
4	95.3
average	**95.1 ± 0.70**

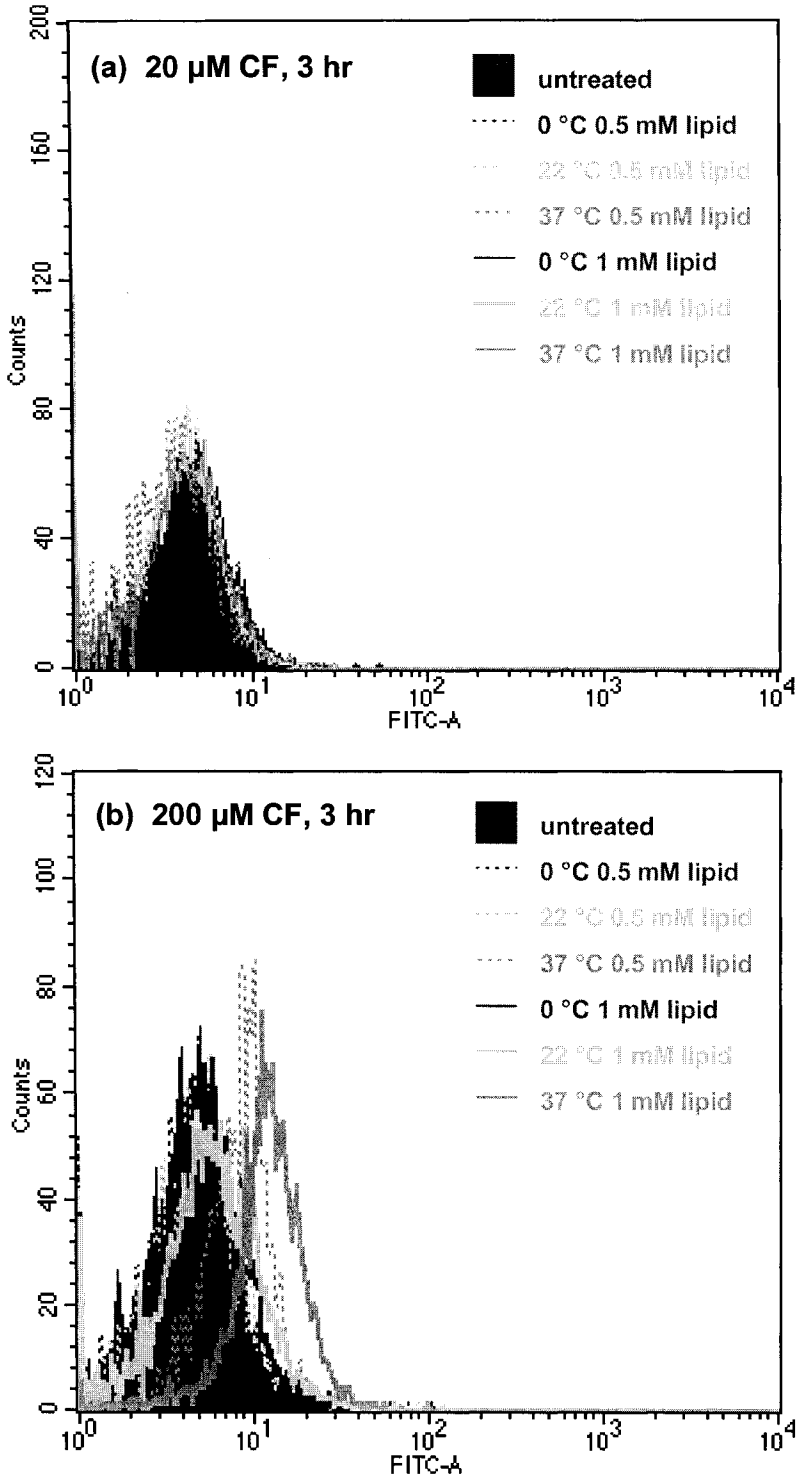

Figure 4.1: Temperature response histograms. Cellular fluoresence intensity of TF-1 cells following a 3 hr incubation at 0, 22, or 37 °C with two different concentrations of liposomes (0.5 or 1 mmol/L lipid) containing (a) 20 µmol/L or (b) 200 µmol/L 5(6)-CF and 0.2 mol/L trehalose.

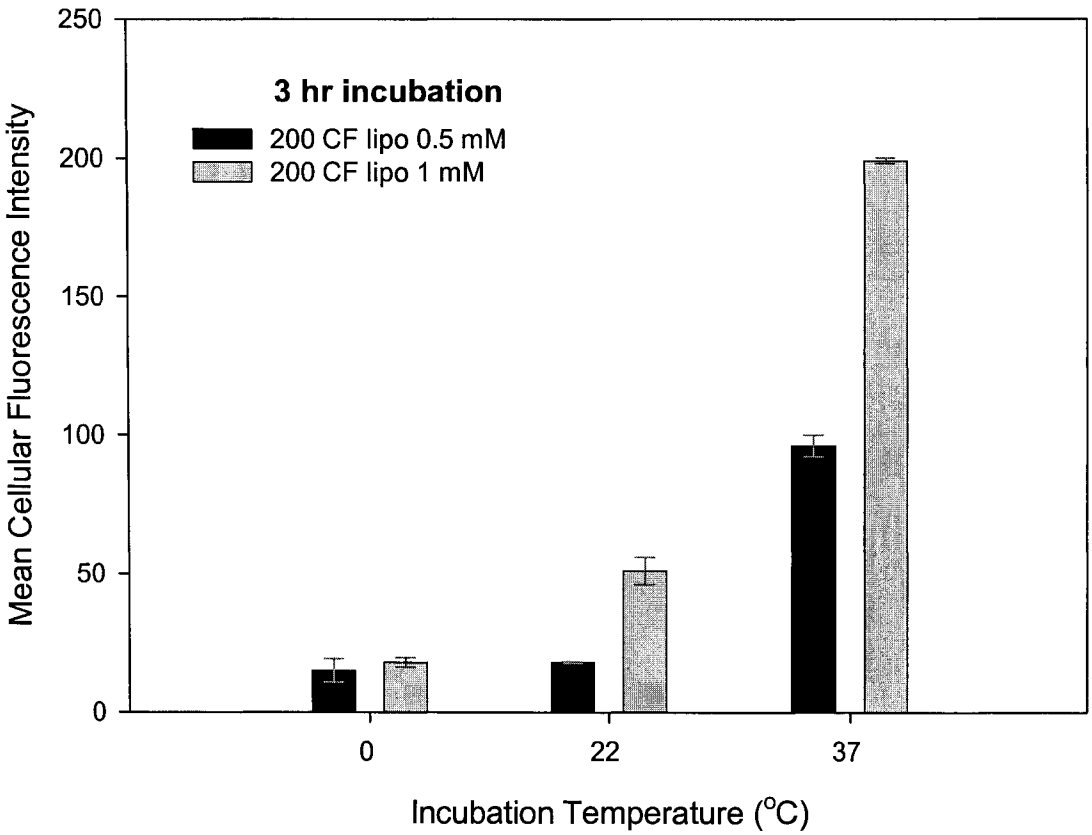

Figure 4.2: Temperature response graph. The mean cellular fluorescence intensity of TF-1 cells following a 3 hour incubation at 0 °C, 22 °C or 37 °C with liposomes containing 200 µmol/L CF either at lipid concentrations of 0.5 mmol/L or 1 mmol/L.

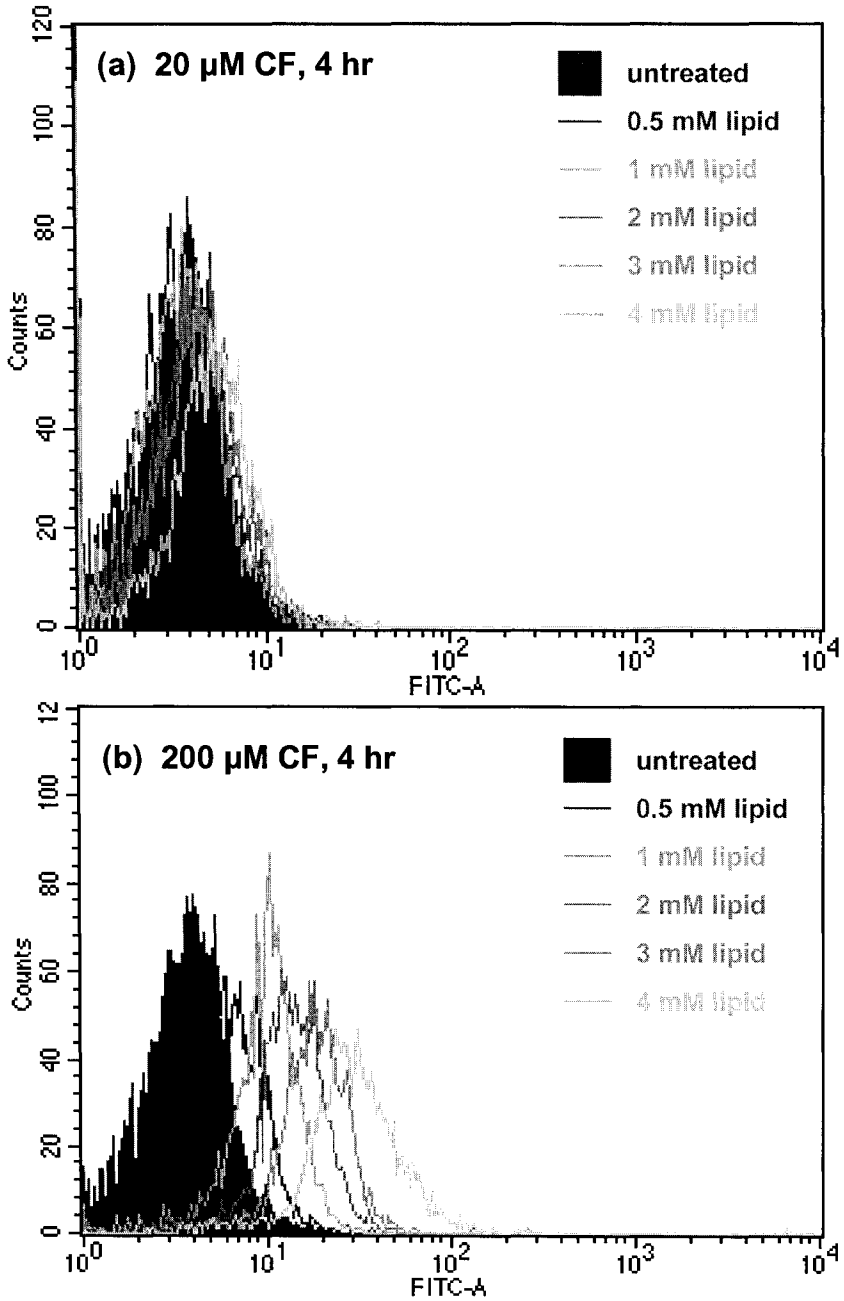

Figure 4.3: Liposome concentration histograms. Cellular fluoresence intensity of TF-1 cells following a 4 hr incubation at 37 °C with increasing concentrations of liposomes (0.5 - 4 mmol/L lipid) containing (a) 20 µmol/L and (b) 200 µmol/L 5(6)-CF and 0.2 mol/L trehalose.

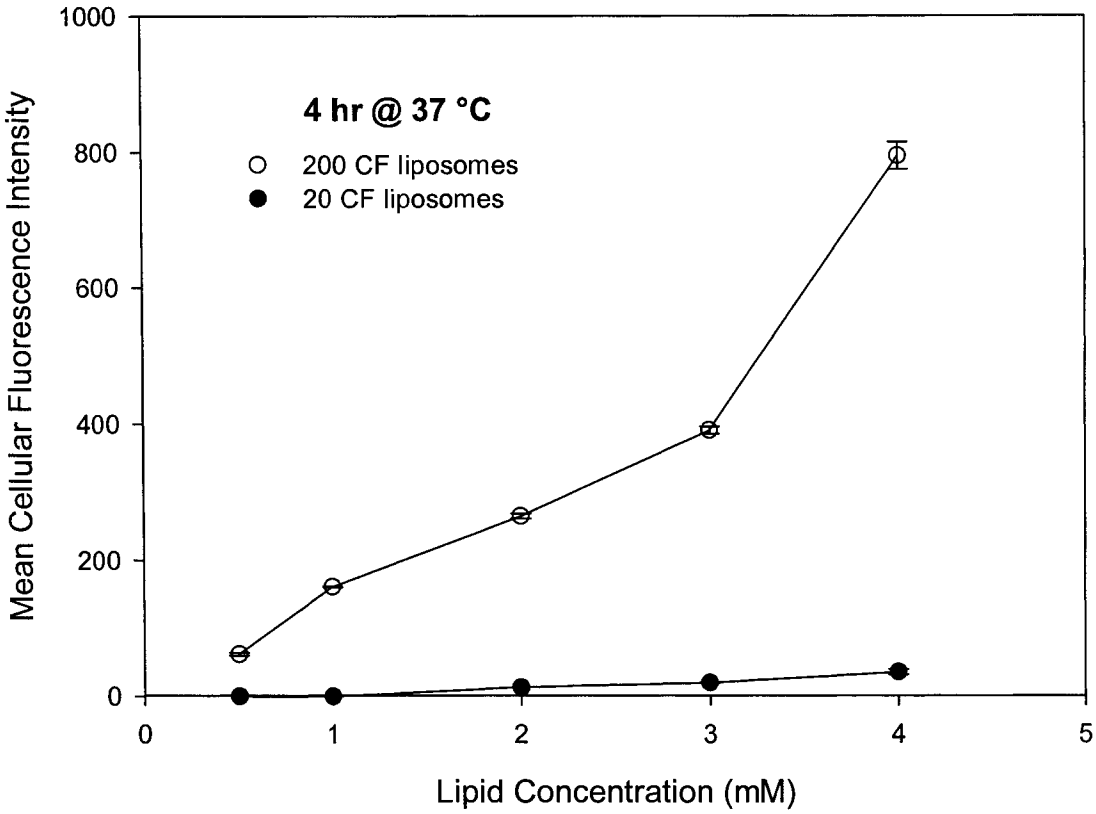

Figure 4.4: Liposome concentration graph. Mean cellular fluorescence intensity of TF-1 cells following 4 hr incubation with liposomes containing 20 µmol/L or 200 µmol/L 5(6)-carboxyfluorescein and 0.2 mol/L trehalose, at 37 °C, with increasing concentrations of liposomes (0.5 mmol/L-4 mmol/L).

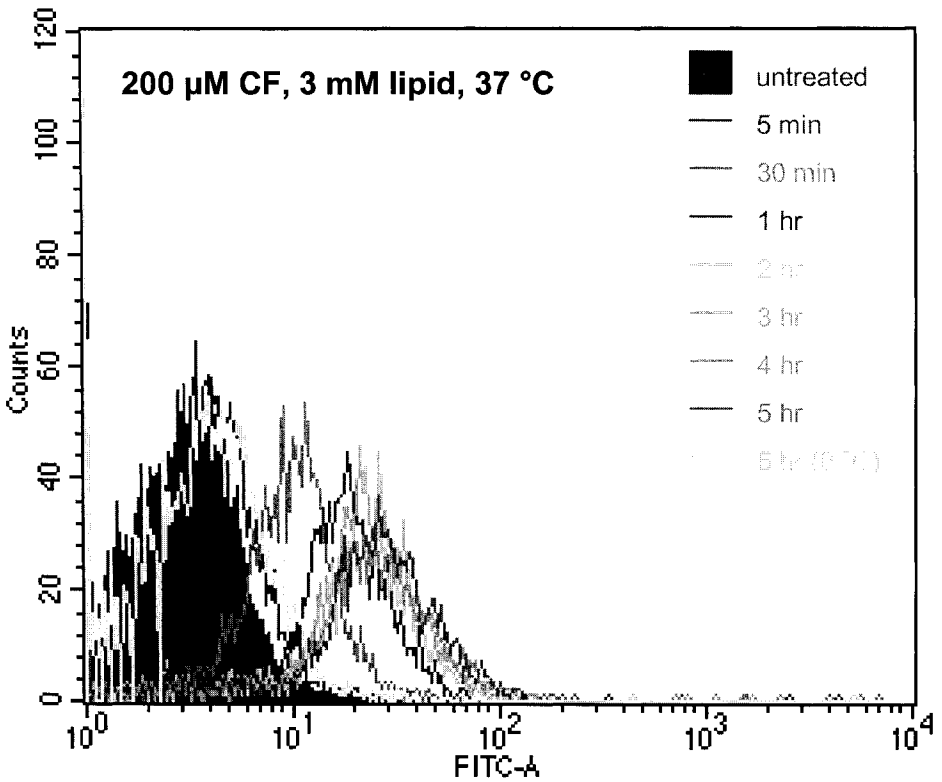

Figure 4.5: Temporal response histograms. Cellular fluoresence intensity of TF-1 cells incubated for up to 5 hours at 37 °C with liposomes containing 200 µmol/L 5(6)-CF and 0.2 mol/L trehalose, at a concentration of 3 mmol/L lipid. The cellular fluorescence intensity of cells incubated with the same liposomes for 5 hours at 0 °C is included for comparison.

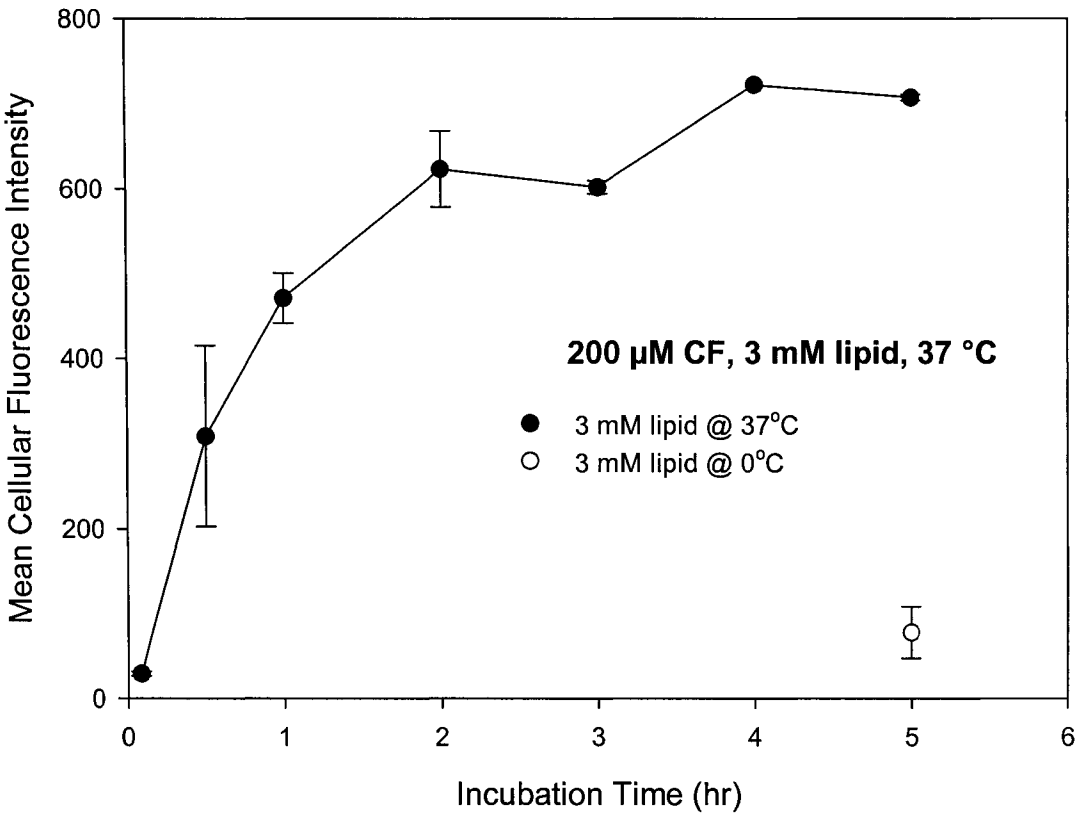

Figure 4.6: Temporal response graph. The mean cellular fluorescence intensity of TF-1 cells incubated at 37 °C with liposomes containing 200 µmol/L 5(6)-CF and 0.2 mol/L trehalose, at a concentration of 3 mmol/L for up to 5 hours. The cellular fluorescence intensity of cells incubated with the same liposomes for 5 hours at 0 °C is included as a control.

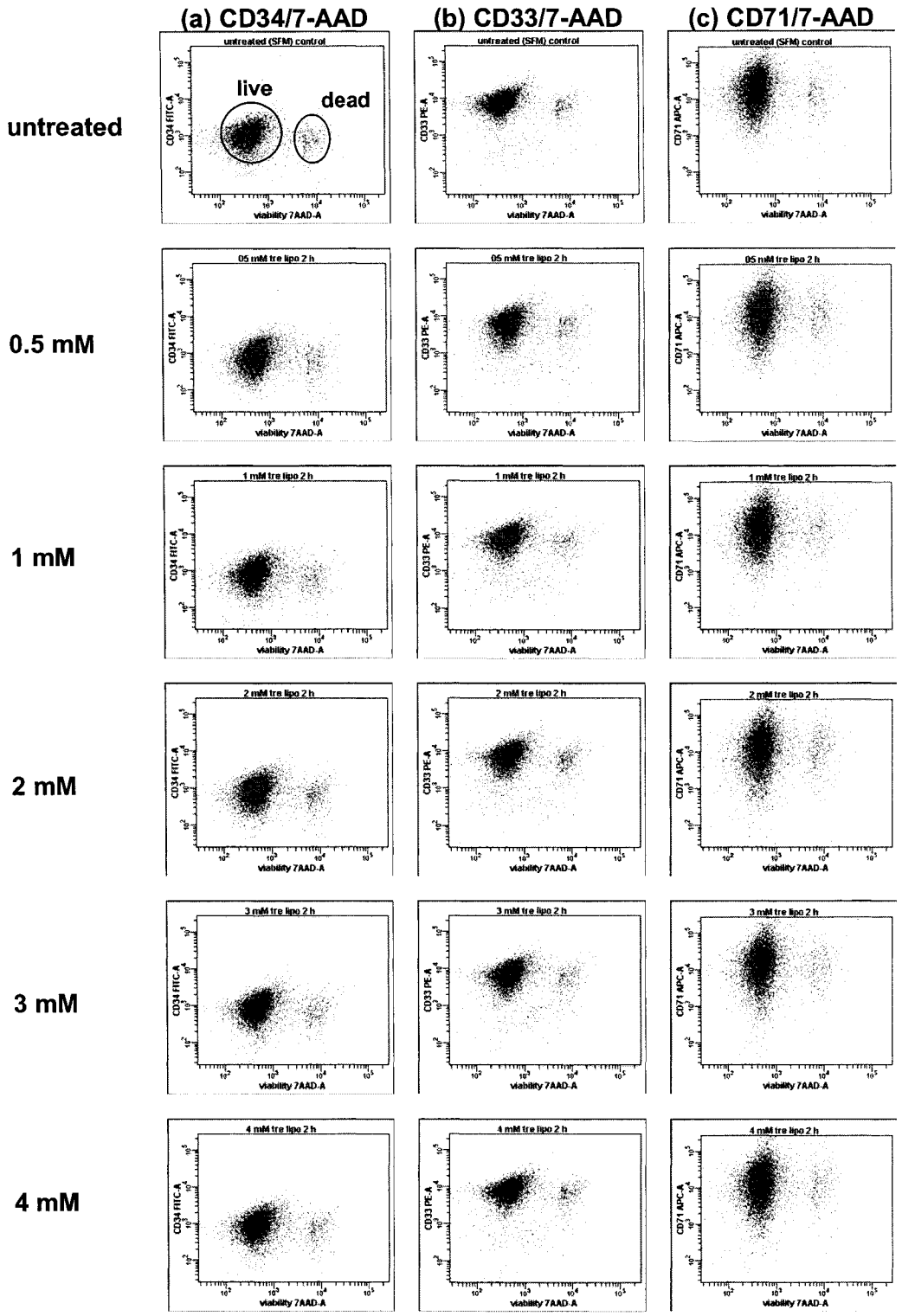

Figure 4.7: Antigen expression and membrane integrity: liposome concentration effect. (a) CD34, (b) CD33 and (c) CD71 TF-1 cell antigen expression and 7-AAD viability following incubation at 37 °C for 2 hours with increasing concentrations of liposomes containing 0.2 mol/L trehalose.

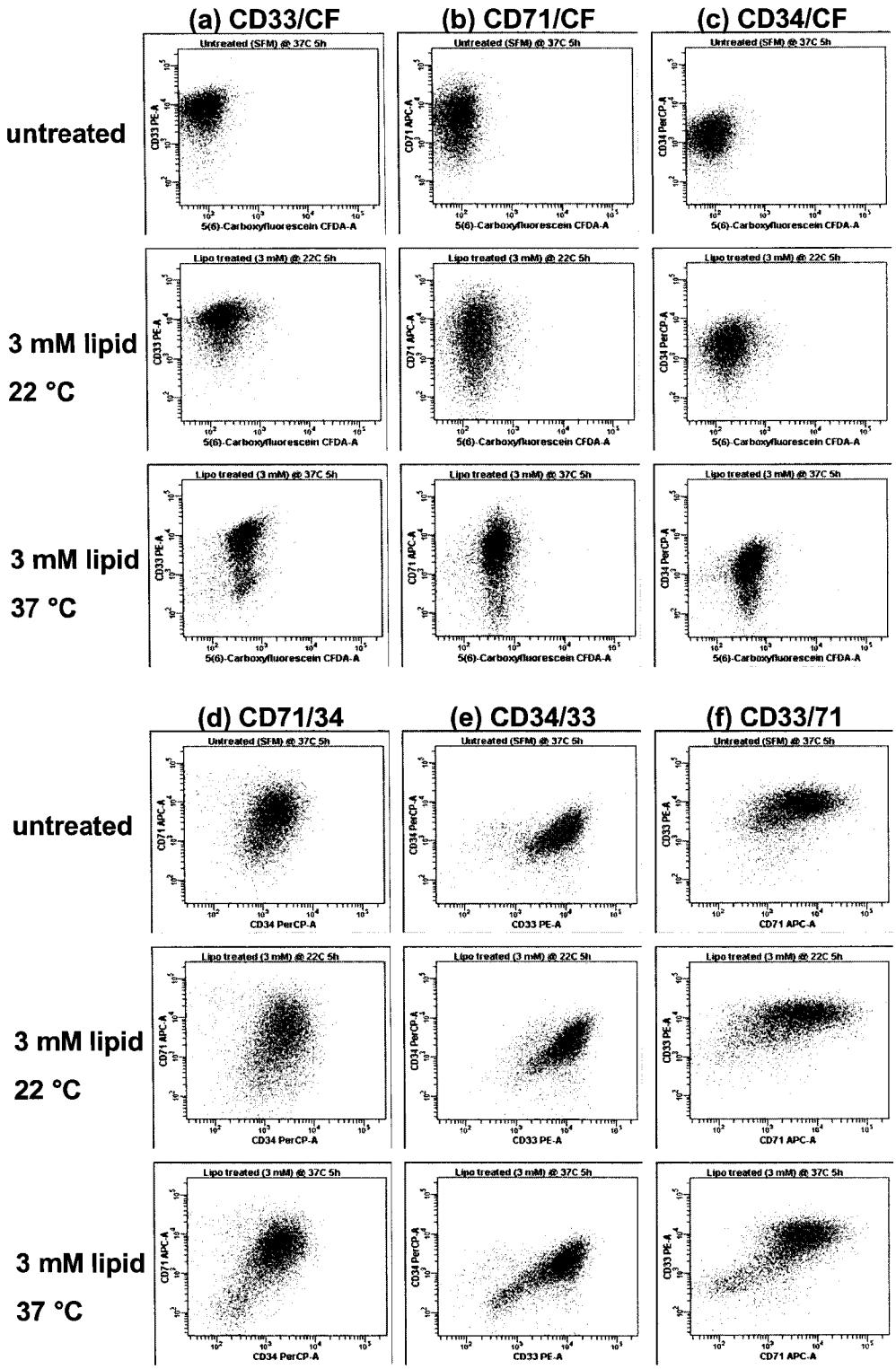

Figure 4.8: Antigen expression: temperature effect. (a) CD33/CF, (b) CD71/CF, (c) CD34/CF, (d) CD71/34, (e) CD34/33, and (f) CD33/71 TF-1 cell antigen expression and CF fluorescence of untreated cells and following incubation at 22 °C or 37 °C for 5 hours with 3 mM lipid containing 0.2 mol/L trehalose and 200 µmol/L 5(6)-carboxyfluorescein.

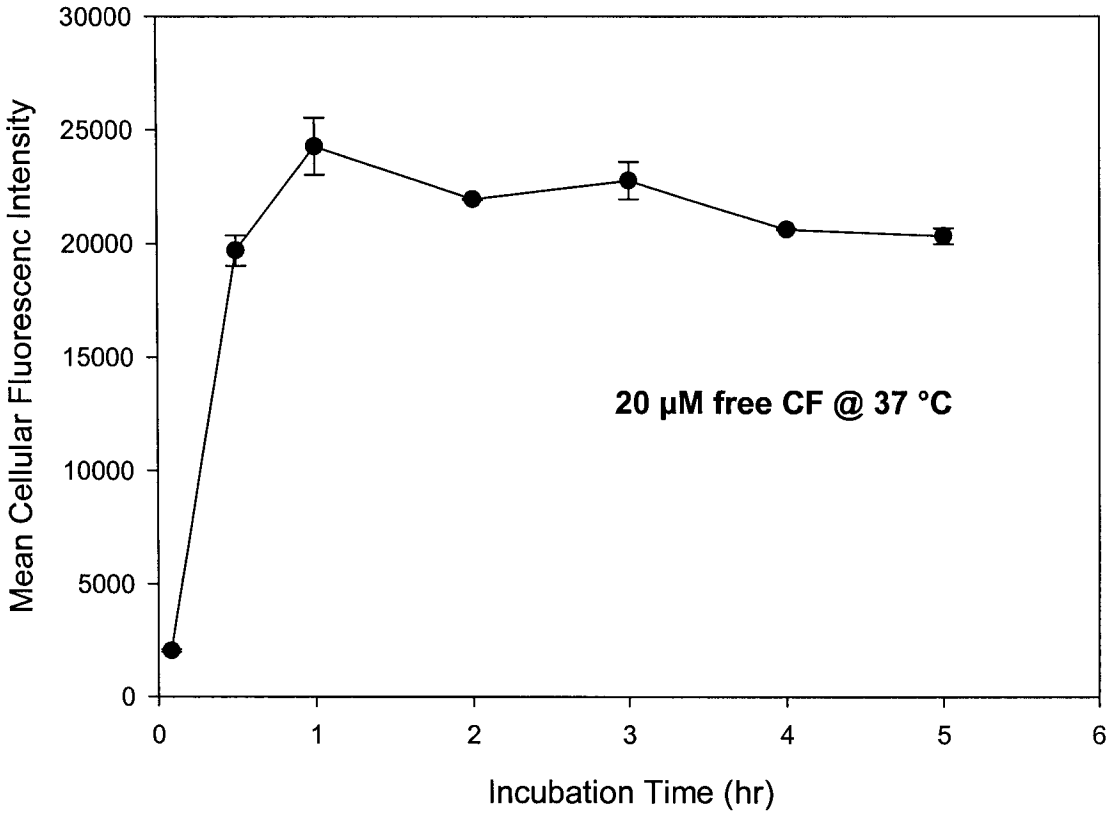

Figure 4.9: Temporal response to free CF. Mean cellular fluorescence intensity of TF-1 cells incubated at 37 °C in SFM containing 20 µmol/L free 5(6)-carboxyfluorescein for up to 5 hours.

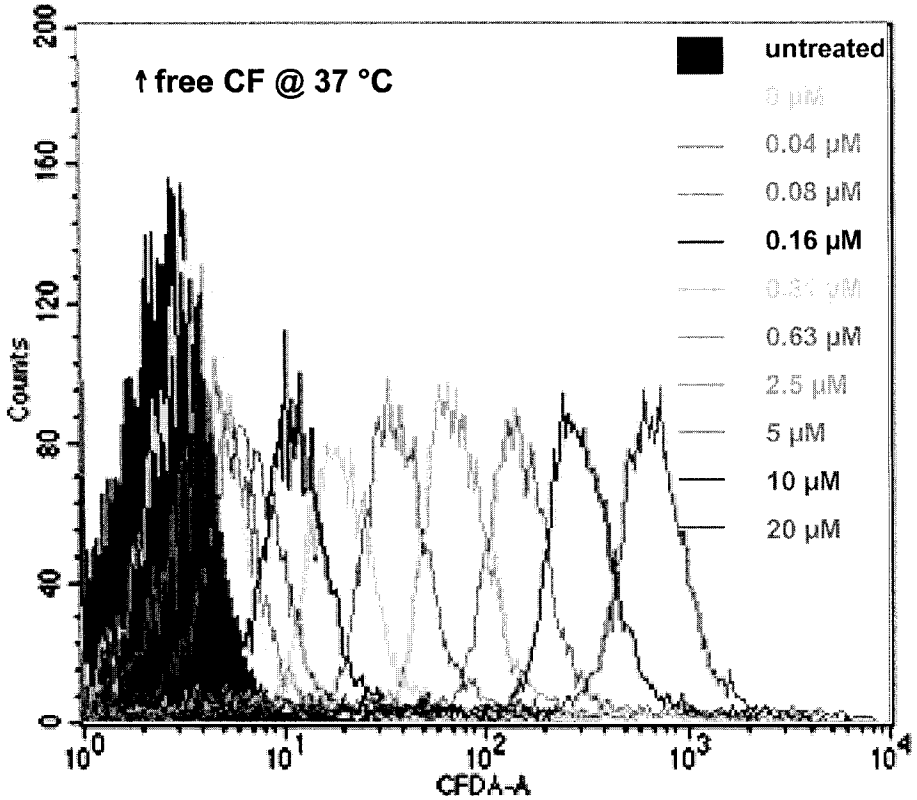

Figure 4.10: Cellular response to increasing concentrations of free CF. Cellular fluorescence intensity of TF-1 cells incubated for 5 hours at 37 °C with increasing concentrations (0-20 µmol/L) of free 5(6)-carboxyfluorescein prepared in SFM.

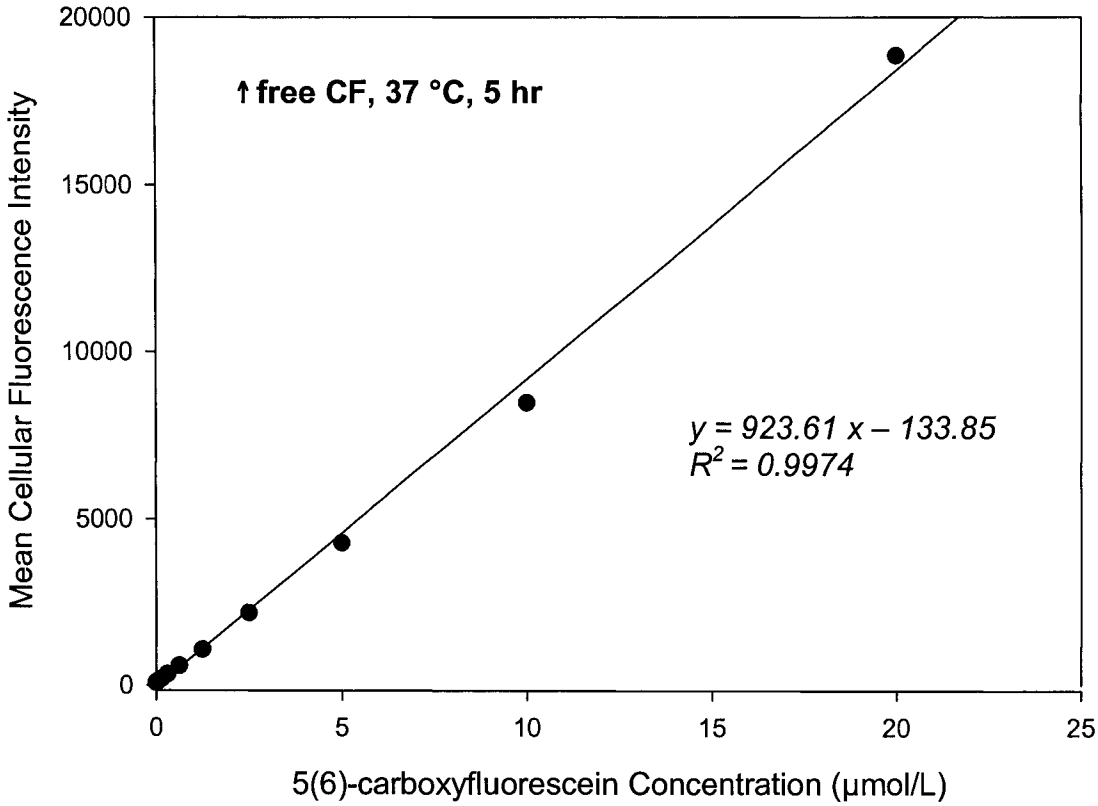

Figure 4.11: Linear response to increasing concentrations of free CF. The mean cellular fluorescence intensity of TF-1 cells following incubation at 37 °C for 5 hours with increasing concentrations of free 5(6)-carboxyfluorescein prepared in SFM.

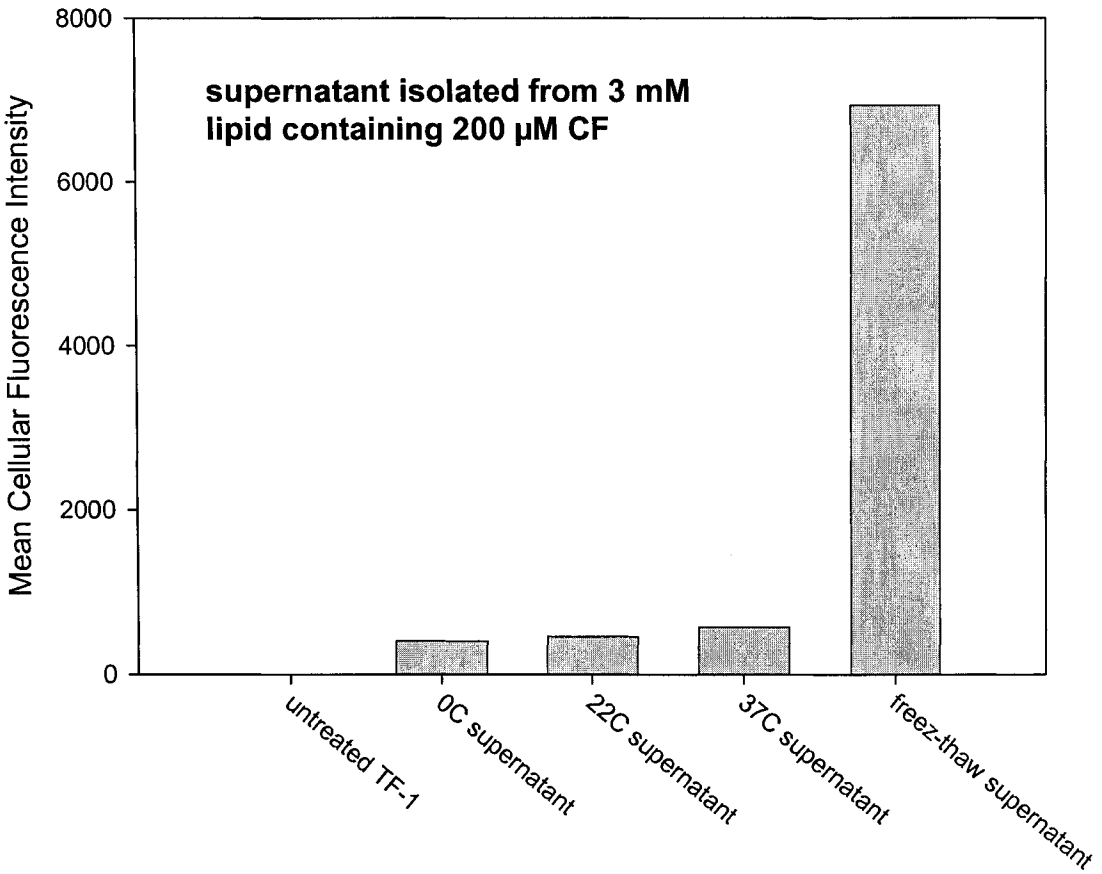

Figure 4.12: Extraliposomal supernatant: associated fluorescence. The mean cellular fluorescence intensity of TF-1 cells that have been re-suspended in extraliposomal supernatant isolated from 200 µmol/L CF liposomes (3 mmol/L lipid) stored at 0 °C, 22 °C and 37 °C for 5 hours, and following freeze-thaw to release intraliposomal contents. Cells were required for gating purposes and fluorescence intensity represents the amount of 'free CF' in the liposome preparation.

CHAPTER 5

FREEZING RESPONSE

5.1 INTRODUCTION

The relatively low concentrations (< 0.2 mol/L) of intra- and extracellular trehalose reported (1-3) for protection against cryoinjury, compared to traditional CPAs like DMSO (1.4 mol/L) and glycerol (30 % w/v), and its relatively non-toxic nature and glass forming tendencies at high subzero temperatures (4, 5), provides the rationale for the development of a clinically acceptable cryopreservation technique involving trehalose. Since the cryoprotective stabilizing properties of trehalose can only be achieved if it is available intracellularly and this molecule is essentially impermeable to mammalian cells, a technique for loading trehalose into the intracellular compartment is required.

The results of Chapter 4 provided evidence that liposomes interact with TF-1 cells and parameters influencing this process were identified. The interaction between liposomes and cells were found to be dependent on incubation temperature and time, as well as the concentration of intraliposomal contents and total lipid. Using 5(6)-carboxyfluorescein as a reporter molecule we were unable to unequivocable demonstrate intracellular delivery of liposomal contents because some free CF remained in the extraliposomal buffer following liposome preparation (Chapter 4, Figure 4.14) and TF-1 cells were able to take up this molecule in the absence of liposomes. While flow cytometry can be used to

detect cellular fluorescence it is incapable of discerning between fluorescence which is associated with the cell surface and intracellular fluorescence.

The goal of this study is to determine the effect low concentrations of trehalose loaded liposomes have on the freezing response of TF-1 cells, alone or in combination with extracellular trehalose. The freezing response provides an alternative measure to assess the intracellular loading of tehalose using liposomes. Liposomes containing trehalose were prepared following the methods used in Chapter 3. The parameters identified in Chapter 4 which were found to increase liposomal-cell association were applied to investigate the feasibility of using liposomes for the delivery of cryoprotective concentrations of trehalose.

5.2 METHODS

TF-1 Cell Preparations

TF-1 cells cultured according to protocol (Appendix A) were lightly centrifuged at 100 x g for 5 minutes at RT, the supernatant removed and warm (37 °C) SFM added back to wash the cells. Centrifugation and washing was repeated an additional two times and the cells concentrated to 2 x 10^7 cells/ml in SFM.

Experimental Conditions

Concentrated cells were prepared to a final concentration of 2 x 10^6 cells/ml in either SFM or SFM modified with 0.2 mol/L trehalose. The SFM prepared with trehalose was adjusted by decreasing the initial volume of SFM by two thirds, adding the desired concentration (g/L) of trehalose, and bringing the solution

back to the original volume with distilled water. A freezing point osmometer (Precision Systems Inc., Massachusetts, USA) was used to ensure the final solution was near physiological osmolality (280 mOsm/kg). Dilution of the SFM decreased the total salt content prior to the addition of trehalose and ensured the osmolality remained near physiological conditions (280 mOsm/kg) in order to prevent cellular osmotic changes prior to the onset of cooling. This approach has been shown to improve the recovery of cryopreserved bull (6) and mouse (7) sperm as well as desiccated murine fibroblasts (8). Liposomes were synthesized to contain SFM or SFM modified with 0.2 mol/L trehalose (iso-osmotic) using the methods described in Chapter 3. Cells were incubated in non-tissue culture treated Petri dishes at 37 °C, 5 % CO_2 and > 95 % relative humidity for 5 hours in cell media prepared with or without trehalose and in the presence or absence of liposomes. Liposomes were added at concentrations of either 3 mmol/L or 4 mmol/L lipid. The incubation time, temperature and lipid concentrations were selected based on the results of the liposome-cell interaction study (Chapter 4), as conditions observed to enhance cell-associated fluorescence. The final composition of each incubation buffer is summarized in Table 5.1. Samples were prepared in duplicate unless stated otherwise.

At the end of the 5 hour incubation period cells were transferred to 1.5 ml microtubes and washed by centrifugation at 300 x g for 5 min at 4 °C. Centrifugation and washing was repeated a total of 3 times. The buffer used for washing and final re-suspension was either SFM or SFM modified with 0.2 mol/L trehalose depending on what was used during the initial incubation period

(Table 5.1). Unwashed samples and washed samples from each test group were maintained on ice and pre-freeze cell membrane integrity was determined using 7-amino actinomycin D (7-AAD).

Freeze-thaw Procedure

Washed samples were transferred to cryotubes and frozen at 1 °C/min to -80 °C using a controlled rate freezer (PLANAR kryosave 30-SV, T.S. Scientific) then transferred to liquid nitrogen for storage. Ice nucleation temperature during cooling was not controlled using this cryopreservation procedure. The freezing profile was the same used for establishment of the cell bank (Appendix A). Samples were stored for two weeks at -196 °C. On removal from liquid nitrogen samples were thawed in a 37 °C water bath and membrane integrity assessed within 30 minutes.

Viability Assessment

The fluorescent nucleic acid marker, 7-AAD (Becton Dickinson Biosciences) was chosen as the viability probe for dead cell exclusion. Living cells with intact membranes and active metabolism exclude 7-AAD, while cells with damaged membranes or impaired metabolism are unable to prevent the dye from entering the cells (9). 7-AAD intercalates within the DNA of non-viable cells resulting in cellular fluorescence which is detectable using flow cytometry. Membrane integrity of washed and unwashed samples was measured within 30 minutes following liposomal treatment, prior to freezing and after cryopreservation (washed samples only), by the addition of 20 µl 7-AAD. All samples were kept on ice in the dark prior to flow analysis. 7-AAD analysis of unwashed samples

was measured to determine the effect of washing and removal of liposomes on membrane integrity. A 7-AAD/DNA complex has a maximum absorption in the green spectral region with an excitation wavelength of 488 nm and red fluorescence emission of 635-675 nm. Flow cytometric analysis of cell membrane integrity was assessed using the FACSCanto (BD, Biosciences, CA, USA). For each sample 1,000,000 total events and 10,000 cellular events were collected over one minute at a low flow rate that consisted of forward scatter (FSC, 488 nm/10 bandpass (BP)), side scatter (SSC, 488 nm/10 BP) and fluorescence emission centered at 650 nm (FL3-7AAD). The live cell population gate was established using fresh untreated control cells. FACSDiva™ 4.*0* (BD Biosciences, NJ, USA) was used for acquisition and analysis.

Statistical Analysis

A Student's t-test (Excel 2003, Microsoft Office) was used for single comparisons to determine if the mean post-thaw recovery of TF-1 cells with intact membranes following treatment with liposomes and trehalose was significantly different (α = 0.05) from cells frozen without a CPA.

5.3 RESULTS

Pre-freeze Membrane Integrity

The pre-freeze membrane integrity of TF-1 cells following treatment is summarized in Table 5.2. The majority of the cells have intact membranes following 5 hour incubation at 37 °C in trehalose enriched SFM and trehalose containing liposomes at concentrations up to 4 mmol/L. The percentage of

washed and unwashed cells with intact membranes is 91 ± 1.9 and 89 ± 1.1, respectively. These results confirm that pre-freeze treatment conditions have no effect on cell membrane integrity when compared to cells incubated in SFM, and the majority of the cell population has intact membranes prior to freezing. In fact, cell membrane integrity is lower for cells incubated in SFM than cells incubated with lipsosomes or trehalose. In addition, repeated washing by centrifugation to remove liposomes following treatment had no affect on cell membrane integrity.

Post-thaw Membrane Integrity

The post-thaw membrane integrity of TF-1 cells following treatment is summarized in Table 5.3 and represented graphically in Figure 5.1. In comparison to TF-1 cells frozen without a CPA there is a trend towards increased post-thaw recovery of TF-1 cells with intact membranes in all treatment groups. The post-thaw outcome is statistically significant (α = 0.05) for cells treated with 3 mmol/L trehalose-containing liposomes (p=0.014, df=2), 4 mmol/L trehalose containing liposomes in 0.2 mol/L extracellular trehalose (p=0.001, df=3) and with extracellular trehalose alone (p=0.005, df=3) when compared to cells frozen in SFM. The difference in post-thaw outcome of cells treated with 3 mmol/L and 4 mmol/L liposomes (in SFM) is statistically significant (p=0.010, df=3 and p=0.025, df=4) when compared to cells treated with extracellular trehalose alone, with the later providing a more positive outcome. The post-thaw outcome of cells treated with 4 mmol/L trehalose loaded liposomes in extracellular trehalose is the only condition which results in

a statistically significant difference when compared to all other treatment conditions. Results of the statistical analysis are summarized in Table 5.4. The average percentage of cells with intact membranes following cryopreservation with 10 % DMSO is 85 ± 4.6. TF-1 cells cryopreserved with DMSO provided the positive control for this experiment and verified that the routinely used freezing protocol was successful.

5.4 DISCUSSION

Pre-freeze Assessment

The pre-freeze assessment of membrane integrity confirms that cells have intact membranes at the onset of freezing so any loss of cell viability post-thaw is directly attributed to freezing or thawing. The average pre-freeze viability is about 90 % for all treatment groups. The high pre-freeze viability following treatment is not surprising as the conditions chosen with respect to liposome concentration, incubation time and incubation temperature were selected based on the results of the liposome-cell interaction study (Chapter 4). These results correlate well with the previous study (Chapter 4) showing that TF-1 cells can tolerate incubation with up to 4 mmol/L lipid at 37 °C for 5 hours without loss of membrane integrity. Higher membrane integrity was observed for cells incubated with trehalose or trehalose containing liposomes compared to cells incubated in SFM suggesting that the former conditions may even be beneficial to the cells in the absence of serum and growth factors. There is very little variability in membrane integrity of washed and unwashed cells following

liposome treatment. Survival of the majority of the cell population post-liposome treatment and following a series of washes by repeated centrifugation verify that cells treated with liposomes have intact membranes and can withstand the strenuous conditions imposed by centrifugation in the absence of serum proteins. In addition, washing is not merely eliminating dead cells from the population and inflating the percent viability of the washed cell population. Liposome-cell interaction studies (Chapter 4) required using washed cells to measure cell-associated fluorescence therefore samples in this study were also washed to remain consistent. The pre-freeze removal of liposomes may not be necessary since liposomes are relatively non-immunogenic and eliminated *in vivo* by cells of the reticuloendothelial system (10, 11). Furthermore, the beneficial effects of liposomes during biopreservation have been demonstrated by Kheirolomoom *et al.* who observed a substantial reduction in hemolysis after rehydration of red blood cells lyophilized in the presence of phospholipid vesicles (12).

Post-thaw Response

The results of the post-thaw membrane integrity assessment show that cell viability is higher when cells are frozen with low concentrations of extracellular trehalose (no liposomes) than cells frozen following liposomal treatment in the absence of extracellular trehalose. There is evidence in the literature that human mesenchymal stem cells can take up trehalose from the extracellular milieu by the process of fluid-phase endocytosis, however the concentrations of trehalose taken up are low relative to that required for protection during freezing

(13). While fluid-phase endocytosis may be a contributing factor to the observed post-thaw outcome in the presence of extracellular trehalose, the outcome more likely is a direct response to changing extra- and intracellular solute concentrations during freezing in the presence of extracellular trehalose. The 23 % cell survival in the presence of extracellular trehalose is consistent with that observed by Buchanan *et al.* who achieved a 27 % post-thaw survival of TF-1 cells using 0.2 mol/L extracellular trehalose. These results address the limited protective capabilities of extracellular trehalose alone and re-enforce the importance of penetrating CPAs to combat solute toxicity. Considering the small volume and low concentration (0.2 mol/L) of trehalose encapsulated within each liposome, the concentration of trehalose being delivered inside the cell is expected to be very low in relation to total cell volume therefore the observed outcome is not surprising.

The results observed using increasing concentrations of liposomes have a significant effect on post-thaw membrane integrity when extracellular trehalose is also present during freezing. This concentration effect is a positive outcome which supports the hypothesis that liposomal delivery of intracellular trehalose has potential applications in cryobiology. The results are also in agreement with previous studies which determined trehalose is most effective when available on both sides of the cell membrane during freezing (3, 14) and freeze-drying (15-17) and reinforces the importance of achieving a threshold level of intracellular trehalose specific to each cellular system, before a substantial improvement in post-thaw viability is apparent. A recent study found sugar concentrations

effective at preventing leakage in model membrane systems during lyophilization were much higher than that required to prevent phase transitions and membrane fusion (18).

Limitations of the Study

The major limitations to this freezing study which must be addressed are the small sample size and the method of post-thaw assessment. Repetition and an increase in sample size are required to determine if statistically significant differences are real or simply occurred by chance and have been influenced by the within group variability. Flow cytometric assessment of immediate post-thaw cell membrane integrity using 7-AAD is a widely used method of assessment however a more rigorous measure of cell viability which includes post-thaw clonogenic output of the TF-1 cell population would be the logical next step to ensure validity of the observed results (19). The importance of cell handling and the method selected for post-thaw assessment of cryopreserved HPCs has been demonstrated (20) which reiterates the importance of a reliable functional assay to accurately determine post-thaw viability and cell loss during cryopreservation (21). Cell membrane integrity assays which are traditionally used immediately post-thaw are also limited by their inability to detect cellular changes which lead to cryopreservation-induced apoptosis (22). The development of a freezing protocol specific for conditions where cryoprotective concentrations of trehalose are present would also be required to improve post-thaw survival.

Clearly an important limiting factor observed is a result of low intracellular concentrations of trehalose achieved using liposomes synthesized in this study. As demonstrated in Chapter 4 using cellular fluorescence to measure liposome-cell interactions, it is possible to increase cell-associated fluorescence by increasing the initial concentration of the target molecule synthesized within the liposomes. Intraliposomal concentrations of trehalose will be limited by the ability to maintain iso-osmotic equivalence between the endogenous and extracellular liposomal environment that will also prevent substantial changes in cellular osmotics. This is required because liposomes respond osmotically to anisotonic conditions (23). While HPCs can tolerate cell volume excursions during exposure to anisotonic conditions ranging from 180 mOsm/kg - 1200 mOsm/kg (24), the effect of changes in surface area on liposome-cell interaction and intracellular delivery of liposomal contents are yet to be determined.

The versatility of liposomes does provide additional approaches to increasing intracellular delivery of trehalose in that the lipid formulation can also be altered to introduce charge and the ease at which liposome and cellular membrane lipids interact, and even the mechanism of interaction (25, 26). While the size selected for liposomes synthesized in this study is based on data in the literature concerning stability and retention of trapped solutes in LUVs, size can be easily altered using the freeze-thaw extrusion technique by changing the pore size of the filter used during extrusion. Since trehalose containing liposomes are significantly smaller than liposomes synthesized without sugars, an increase in size could potentially result in increased intraliposomal

concentrations of trehalose. Entrapment efficiency and stability with respect to liposome size would need to be determined experimentally in order to validate this theory. Like intraliposomal concentrations of trehalose, liposome size is also limited, as demonstrated by electrofusion of trehalose loaded (300 mOsm/kg) giant unilamellar liposomes with Jurkat cells, which cause changes to cell surface area and osmotic effects resulting in cell lysis (27). To conclude this study, a method for measuring intracellular trehalose concentrations following liposomal treatment would reduce experimentation based exclusively on empirical observations and is a technique which is currently being developed in our laboratory by Jelena Holavati. Using a commercially available Megazyme spectrophotometric method to evaluate the encapsulation efficiency of the liposome synthesis process is the first step toward quantifying intracellular trehalose concentrations (28).

5.5 CONCLUSIONS

The feasibility of using liposomes for the intracellular delivery of trehalose for applications in cryobiology has been demonstrated. The highest concentration of liposomes tested increased post-thaw membrane integrity significantly when extracellular trehalose was also present in the cryoprotective media. The low freeze-thaw recovery of liposome-treated cells relative to cells cryopreserved with 10 % DMSO reinforces the importance of achieving a threshold concentration of intracellular trehalose before a substantial improvement in post-thaw viability is apparent. The potential exists to increase intracellular trehalose

concentrations by altering the carrier properties of the liposomes and the internal aqueous composition. This is the first documented account of using liposomes for the intracellular delivery of trehalose into nucleated human cells in an attempt to improve post-thaw cell survival.

5.6 REFERENCES

1. Buchanan S, Gross S, Acker J, Toner M, Carpenter J, Pyatt D. Cryopreservation of stem cells using trehalose: Evaluation of the method using a human hematopoietic cell line. Stem Cells Dev 2004;13:295-305.
2. Buchanan SS, Menze MA, Hand SC, Pyatt DW, Carpenter JF. Cryopreservation of human hematopoietic stem and progenitor cells loaded with trehalose: Transient permeabilization via the adenosine triphophate-dependent P2Z receptor channel. Cell Preserv Technol 2005;3(4):212-222.
3. Eroglu A, Russo MJ, Bieganski R, Fowler A, Cheley S, Bayley H, et al. Intracellular trehalose improves the survival of cryopreserved mammalian cells. Nature Biotechnol 1999;18:163-167.
4. Green JL, Angell CA. Phase relations and vitrification in saccharide-water solutions and the trehalose anomaly. J Phys Chem 1988;93:2880-2882.
5. Chen T, Fowler A, M T. Literature review: Supplemented phase diagram of the trehalose-water binary mixture. Cryobiology 2000;40:277-282.

6. Woelders H, Matthijs A, B E. Effects of trehalose and sucrose, osmolality of the freezing medium, and cooling rate on viability and intactness of bull sperm after freezing and thawing. Cryobiology 1997;35:93-105.

7. Koshimoto C, Gamliel E, Mazur P. Effect of osmolality and oxygen tension on the survival of mouse sperm frozen to various temperatures in various concentrations of glycerol and raffinose. Cryobiology 2000;41(3):204.

8. Acker JP, Fowler A, Lauman B, Cheley S, Toner M. Survival of desiccated mammalian cells: Beneficial effects of isotonic media. Cell Preserv Technol 2002;1(2):129-140.

9. Schmid I, Krall WJ, Uittenbogaart CH, Braun J, Giorgi JV. Dead cell discrimination with 7-amino-actinomycin D in combination with dual color immunofluorescence in single laser flow cytometry. Cytometry 1992;13:204-208.

10. Chonn A, Semple SC, Cullis PR. Association of blood proteins with large unilamellar liposomes in vivo. Relation to circulation lifetimes. J. Biol. Chem. 1992;267(26):18759-18765.

11. Rao M, Alving CR. Delivery of lipids and liposomal proteins to the cytoplasm and Golgi of antigen-presenting cells. Adv Drug Deliv Rev 2000;41(2):171.

12. Kheirolomoom A, Satpathy GR, Torok Z, Banerjee M, Bali R, Novaes RC, et al. Phospholipid vesicles increase the survival of freeze-dried human red blood cells. Cryobiology 2005;51:290-305.

13. Oliver AE, Jamil K, Crowe JH, Tablin F. Loading human mesenchymal stem cells with trehalose by fluid-phase endocytosis. Cell Preserv Technol 2004;2(1):35-49.

14. Chen T, Acker JP, Eroglu A, Cheley S, Bayley H, Fowler A, et al. Beneficial effect of intracellular trehalose on membrane integrity of dried mammlian cells. Cryobiology 2001;43:168-181.

15. Leslie S, Israeli E, Lighthart B, Crowe J, Crowe L. Trehalose and sucrose protect both membranes and proteins in intact bacteria during drying. Appl Environ Microbiol 1995;61(10):3592-3597.

16. Crowe LM, Crowe JH, Rudolph A, Womersley C, Appel L. Preservation of freeze-dried liposomes by trehalose. Arch Biochem Biophys 1985;242(1):240.

17. Cerrutti P, Segovia de Huergo M, Galvagno M, Schebor C, del Pilar Buera M. Commercial baker's yeast stability as affected by intracellular content of trehalose, dehydration procedure and the physical properties of external matrices. Appl Microbiol Biotechnol 2000;54:575-580.

18. Cacela C, Hincha DK. Low amounts of sucrose are sufficient to depress the phase transition temperature of dry phosphatidylcholine, but not for lyoprotection of liposomes. Biophys J 2006;90:2831-2842.

19. Bank HL, Schmehl MK. Parameters for evaluation of viability assays: accuracy, precision, specificity, sensitivity, and standardization. Cryobiology 1989;26(3):203-11.

20. Yang H, Acker JP, Cabuhat M, McGann LE. Effects of incubation temperature and time after thawing on viability assessment of peripheral hematopoietic progenitor cells cryopreserved for transplantation. Bone Marrow Transplant 2003;32(10):1021-6.

21. Yang H, Acker JP, Cabuhat M, Letcher M, Larratt B, McGann LE. Association of post-thaw viable CD34+ cells and CFU-GM with time to hematopoietic engraftment. Bone Marrow Transplant 2005;35(9):881-7.

22. Baust JM, Baust JG. The role of membrane-mediated apoptosis in cryopreservation failure. Cryobiology 2006;53 (*in press*).

23. Reeves JP, Dowben RM. Water permeability of phospholipid vesicles. J Membr Biol 1970;3:123-141.

24. Hunt CJ, Armitage SE, Pegg DE. Cryopreservation of umbilical cord blood: 1. Osmotically inactive volume, hydraulic conductivity and permeability of CD34+ cells to dimethyl sulphoxide. Cryobiology 2003;46:61-75.

25. Poste G, Papahadjopoulos D. Lipid vesicles as carriers for introducing materials into cultured cells: Influence of vesicle lipid composition on mechanism(s) of vesicle incorporation into cells. Proc Natl Acad Sci U S A 1976;73(5):1603-1607.

26. Poste G, Papahadjopoulos D. The influence of vesicle membrane properties on the interaction of lipid vesicles with cultured cells. Ann N Y Acad Sci 1978;308:164-184.

27. Shirakashi R, Yamauchi K, Reuss R, Zimmermann U, Sukhorukov VL. Electrofusion of Jurkat cells and giant unilamellar liposomes loaded with trehalose. Cryobiology 2006;53 (*in press*).

28. Holovati JL, Acker JP. Spectrophotometric measurement of intra-liposomal trehalose. Cryobiology 2006;53 (*in press*).

Table 5.1: Buffer compositions used in freezing experiment.

Treatment Group	Designation	Liposome Concentration (mmol/L lipid)	Intraliposomal Trehalose (mol/L)	Extracellular Trehalose (mol/L)
1	10% DMSO	0	0	0
2	No CPA	0	0	0
3	Extracellular trehalose only	0	0	0.2
4	SFM liposomes	3	0	0
5	Intracellular trehalose only	3	0.2	0
6	Intra- and extracellular trehalose	3	0.2	0.2
7	Intracellular trehalose only	4	0.2	0
8	Intra- and extracellular trehalose	4	0.2	0.2

Table 5.2: Pre-freeze membrane integrity following 5 h treatment.

Treatment Group	Treatment	Cell Membrane Integrity (%)	
		washed	unwashed
2	Untreated (SFM)	88	84
3	Trehalose OUT	94	91
4	SFM liposomes (no trehalose)	95	92
5	Trehalose IN (3 mM lipid)	93	88
6	Trehalose IN/OUT (3 mM lipid)	81	88
7	Trehalose IN (4 mM lipid)	91	92
8	Trehalose IN/OUT (4 mM lipid)	95	91
	Average Viability ± SE	**91 ± 1.9**	**89 ± 1.1**

Table 5.3: Post-thaw TF-1 cell membrane integrity.

Treatment Group	Treatment	Membrane Integrity Average ± SE (Range, Sample Size)
1	10 % DMSO	85.0 ± 4.6 (80.4 - 89.6, n=2)
2	no CPA	6.3 ± 0.2 (6.1 – 6.4, n=2)
3	0.2 M trehalose outside	23.4 ± 1.7 (20.8 – 26.7, n=3)
4	SFM liposomes	15.9 ± 4.1 (9.6 – 23.5, n=2)
5	trehalose liposomes (3 mmo/L)	10.3 ± 0.5 (9.8-10.7, n=2)
6	trehalose liposomes (3 mmol/L) + 0.2 mmol/L trehalose outside	17.3 ± 3.0 (14.3 – 20.2, n=2)
7	trehalose liposomes (4 mmol/L)	11.6 ± 2.9 (7.0 – 17.0, n=3)
8	trehalose liposomes (4 mmol/L) + 0.2 mol/L trehalose outside	32.5 ± 1.7 (30.7 – 36.0, n=3)

Table 5.4: Statistical analysis of TF-1 cell post-thaw membrane integrity following treatment. * Shaded regions denote statistically significant p-values.

P-values	No CPA	Trehalose Out	SFM Liposome (3 mM)	Trehalose In (3 mM lipid)	Trehalose In/Out (3 mM lipid)
No CPA		*0.005 df=3	0.163 df=3	*0.014 df=2	0.065 df=2
Trehalose Out	*0.005 df=3		0.165 df=4	*0.010 df=3	0.145 df=3
SFM Liposome (3 mM lipid)	0.163 df=3	0.165 df=4		0.361 df=3	0.828 df=3
Trehalose In (3 mM lipid)	*0.014 df=2	*0.010 df=3	0.361 df=3		0.144 df=2
Trehalose In/Out (3 mM lipid)	0.065 df=2	0.145 df=3	0.828 df=3	0.144 df=2	
Trehalose In (4 mM lipid)	0.253 df=2	*0.025 df=4	0.435 df=4	0.751 df=3	0.284 df=3
Trehalose In/Out (4 mM lipid)	*0.001 df=3	*0.020 df=4	*0.020 df=4	*0.002 df=3	*0.017 df=3

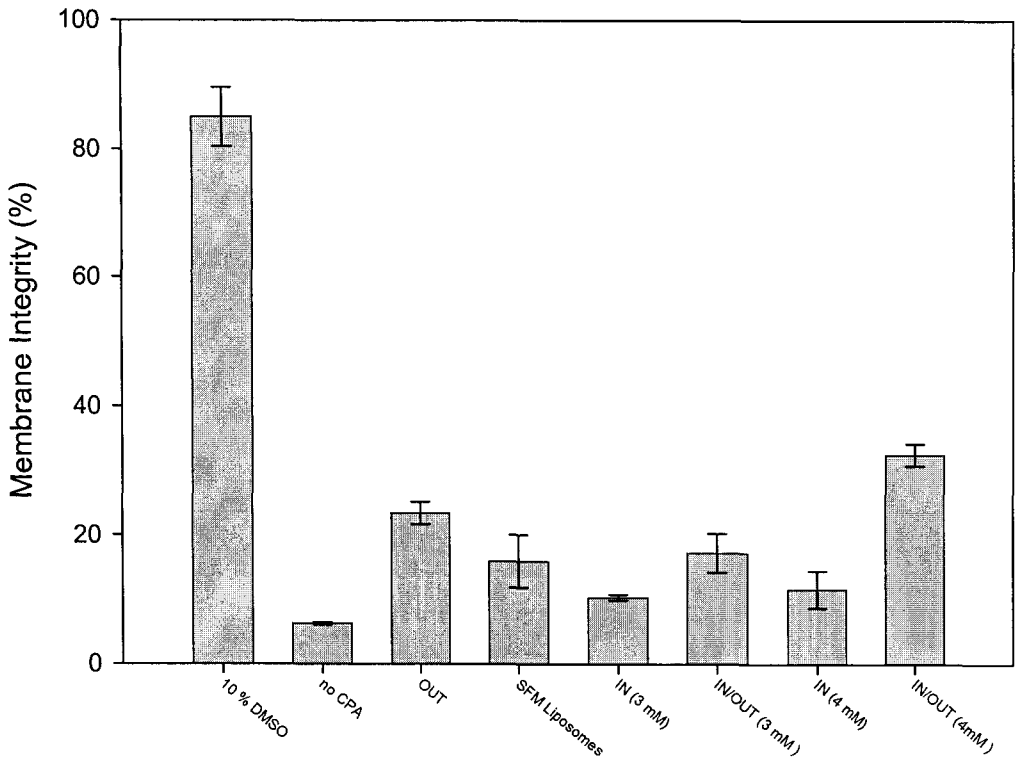

Figure 5.1: Post-thaw response graph. Post-thaw membrane integrity of TF-1 cells stored in LN_2 following treatment with liposomes (3 mmol/L or 4 mmol/L) and/or 0.2 mol/L trehalose.

CHAPTER 6

GENERAL DISCUSSION AND CONCLUSIONS

6.1 REVIEW OF THESIS OBJECTIVES

The objective of this thesis was to investigate the use of liposomes as a delivery vehicle for the intracellular loading of the membrane impermeant molecule trehalose into a nucleated mammalian cell line. The hypothesis stated that liposomal delivery of intracellular trehalose would provide protection to cells during freezing and thawing. Computer simulations were used to model the osmotic response of TF-1 cells to low temperature exposure in the presence of variable concentrations of intra- and/or extracellular trehalose (Chapter 2). Methods were developed to synthesize and characterize liposomes encapsulating low (0.2 mol/L) concentrations of trehalose (Chapter 3). These liposomes were then utilized to identify parameters which influence the transfer of liposomal contents into the cell population (Chapter 4). To conclude this study, the established parameters were applied to investigate the response of TF-1 cells to freezing conditions and assess the potential of this approach for applications in Cryobiology (Chapter 5).

6.2 SUMMARY OF RESULTS

With the use of computer modeling a theoretical prediction of the osmotic response of TF-1 cells to freezing in the presence of low concentrations of intra- and extracellular trehalose was performed. The simulated results provide

valuable information about how the colligative properties of trehalose affect intra- and extracellular solution properties during different rates of linear cooling, and reiterate the importance of a compatible solute on both sides of the cell membrane to limit cell volume excursions. Simulations of cellular osmotic responses to low temperatures demonstrated predictive capabilities with respect to the events that influence cell recovery during cryopreservation. However, the assumption used to define injury caused by exposure to concentrated solutes appears to be the limiting assumption since solute toxicity is not only concentration dependent but is also influenced by exposure time and temperature. Using the upper tolerable limit of 1 mol/kg $[KCl]_i$, the simulations do not predict low concentrations (< 0.3 mol/L) of intra- and extracellular trehalose to be effective at protecting against slow cooling injury. There is experimental evidence in the literature that has proven otherwise, therefore it is important that when using theoretical modeling to predict responses in living systems there exists a clear understanding of the limitations surrounding the model and the assumptions used to interpret the results.

The first step required to investigate the feasibility of using liposomes for the intracellular delivery of trehalose involved the synthesis of liposomes specific for the application. The freeze-thaw extrusion technique was found to be a reliable method for the synthesis of neutral fluid liposomes of a reproducible size. Sizing of the final product using a laser diffraction method proved to be an effective method for characterizing liposome size, determining the reproducibility of the extrusion technique, and discerning between size discrepancies related to

the aqueous composition. The phosphate assay provided a method for the quantitative measure of total lipid and given the size reproducibility between batches we can assume, with some degree of certainty, that the lipid concentration between batches is also comparable. Flow cytometric analysis of the final product confirms the synthesis of a homogenous population and with the inclusion of 5(6)-CF, confirms encapsulation of the aqueous contents and the log normal distribution of the population. We cannot discount the limitations of the characterization techniques discussed earlier, however, eliminating batch to batch variability by controlling liposome size, identifying conditions that result in size variability, and providing a method of quantitative measure to control the amount of liposomes used experimentally, the established techniques enable experimental comparison.

The liposome-cell interaction study was a valuable study for identifying conditions which enhance liposome-cell interactions and for characterizing the effect liposomes have on cell membrane integrity and the expression of antigens invoved in cell proliferation and differentiation. The observed results correlate well with evidence in the literature that liposomes interact with cells in a temperature-, time- and concentration-dependent manner. The identified conditions can be easily manipulated to enhance liposome-cell interactions and do not require time-consuming and exhaustive measures to achieve. The results of this study provide evidence that supports the proposed hypothesis that liposomes can be used to delivery their contents intracellulary without adversely effecting the target population.

The freezing response of TF-1 cells following liposomal treatment confirmed that trehalose-loaded liposomes contribute to an increase in intracellular trehalose which could be indirectly correlated with an increase in the recovery of cells with intact membranes following freezing and thawing. The results of this study demonstrate proof of principle that trehalose loaded liposomes can be used to exert a cryoprotective response in mammalian cells, and describes the first account of using liposomes to load trehalose into 'stem cells' for applications in cryobiology.

6.3 SIGNIFICANCE TO CRYOBIOLOGY

The properties of trehalose have been extensively studied in an attempt to reveal the reasons for its widespread use in natural systems capable of withstanding exposure to adverse environmental conditions. Trehalose along with other saccharides are commonly used as components of extracellular cryoprotective cocktails, where they contribute to freezing protection in the traditional manner by acting as compatible solutes and by promoting cellular dehydration. Many believe that the characteristic properties of trehalose make it the ideal CPA however, the full potential of trehalose as a CPA cannot be attained unless it is present on both sides of the membrane during cryopreservation. Even when considering the high molecular weight of trehalose in comparison to most permeating CPAs and osmotic changes that would inevitably take place *in vivo*, this has not deterred Cryobiologists from attempting to facilitate its use as an intracellular CPA.

Liposomes are an attractive vehicle for the delivery of impermeant molecules into cells mainly because of their versatility. By changing the composition of the liposome bilayer, membrane fluidity and charge can be altered which can have a pronounced effect on the attraction of liposomes to the target cell population and the mechanism by which they interact. The aqueous contents can also be adjusted with relative ease. Liposome size alterations which maintain stability and retention of aqueous contents should also be considered. Phospholipids and CL are major components of biological membranes and do not elicit an immunogenic response *in vivo* and in general are non-cytotoxic. While the experimental approach used here dealt specifically with washed samples where the majority of the liposomes are removed, the potential exists to eliminate pre-freeze washing if direct post-thaw transfusion of cells and liposomes is proven to be clinically acceptable.

Based on the results of the liposome-cell interaction study and the response of cells to freezing following liposomal treatment, it is clear that neutral fluid liposomes containing 0.2 mol/L trehalose are not sufficient to deliver cryoprotective concentrations of intracellular trehalose. Alteration of the above mentioned parameters, combined with a freezing protocol designed specifically to capture the characteristic properties of trehalose, provides a means of enhancing delivery of liposomal contents into mammalian stem cells; the application of liposomes in cryobiology has intriguing potential and further investigation is warranted.

APPENDIX A

TF-1 CELL CULTURE AND CHARACTERIZATION[1]

A.1 INTRODUCTION

The TF-1 cell line used in this study was established by Kitamura and collegues from a heparnized bone marrow aspiration from a patient with erythroleukemia (1). This cell line is dependent on the hematopoietic growth factors interleukin-3 (IL-3), granulocyte-macrophage colony-stimulating factor (GM-CSF) and erythropoietin (EPO) for proliferation. These cells proliferate as single cells in suspension and have morphological characteristics which resemble immature erythroblasts. They are round and about 15-20 μm in diameter, with a villous surface. The appearance of a few very large multinucleated cells is not uncommon. These cells show stable expression of CD33 (99 %) and CD34 (100 %) antigens (1). CD33 is a lineage-specific transmembrane glycoprotein expressed on monocytes and myeloid progenitors but absent in normal erythrocytes and hematopoietic stem cells (2). While these cells express the myeloid lineage marker, they have the ability to undergo differentiation into either more mature erythroid cells or into macrophage-like cells (1). The CD34 antigen is associated with human hematopoietic progenitor cells (HPCs) and is differentiation-stage specific (3). The CD71 transferrin receptor antigen, another lineage specific antigen, is expressed at a high level in immature erythroid cells (4) and HPCs (5). The transferrin receptor binds iron which is necessary for

[1]Adaptations to the cell culture procedure and methods used to characterize TF-1 cells were based on the advice of Dr. Sandhya Buchanan at the University of Colorado.

active metabolism, rapid cell growth, and proliferation (5). Because of the widespread distribution of the transferrin receptor on cultured cells and its association with cell growth, CD71 was chosen as a proliferation marker. Immunophenotypic analysis involving CD34, CD33 and CD71 cell surface antigens was performed periodically during cell culture to ensure that the cell line remained pure and cells retained their capacity to proliferate and differentiate. The TF-1 cell line was chosen for this study as a model system for HPCs.

The purpose of this chapter is to outline the methods developed for the proper handling of TF-1 cells in culture and during experimental manipulation. These methods ensure the cells are established and maintained in culture under conditions that prevent contamination or the alteration of TF-1 cell specific characteristics and morphology.

A.2 METHODS

TF-1 Cell Culture

The human TF-1 cell line was prepared for culture from a frozen stock purchased from American Type Culture Collection (CRL-2003, ATCC, VA, USA). The 1 ml frozen aliquot was thawed in a 37 ˚C waterbath immediately upon arrival because transfer to liquid nitrogen after shipment at -80 ˚C decreases cell recovery. Using strict aseptic techniques the contents were transferred to a 15 ml sterile conical tube and diluted 1 in 10 by dropwise addition of complete growth medium (RPMI 1640, ATCC) which contained 2

mmol/L L-glutamine, 18 mmol/L sodium bicarbonate, 25 mmol/L glucose, 10 mmol/L HEPES, and 1.0 mmol/L sodium pyruvate and 10 % v/v fetal bovine serum (FBS, ATCC). Cell culture media was warmed to 37 °C in a waterbath prior to use. The cell suspension was centrifuged (Sorvall 5810R, Brinkman, Eppendorf, Germany) at 100 x g for 5 minutes at room temperature (RT, 22 °C). The supernatant was aspirated and the cells re-suspended in 5 ml fresh cell culture media. A total cell count was calculated (Eq A.1) from the cell concentration of a measured aliquot (0.5-1 ml) diluted in 10 ml of isoton, using a Coulter Counter (Z2, Coulter Electronics, INC, FL, USA):

$$\text{total cell count} = C_1 \cdot V_f / V_s \cdot V_{total} \qquad \text{(Eq A.1)}$$

where C_1 is the concentration (cells/ml) output from the Coulter, V_f (ml) is the total volume in the Coulter vial, V_s (ml) is the cell volume used in the count and V_{total} (ml) is the total volume in the culture flask.

Initial cultures contained 2 x 10^4 cells/ml in a total volume of 20 ml and were prepared in 250 ml non-tissue culture treated filter top flasks (BD Falcon, MA, USA). Recombinant human granulocyte macrophage colony stimulating factor (Sigma-Aldrich, ON, Canada) was prepared by dissolution in sterile distilled water (dH_20) to a final concentration of 1 µg/ml from a 5 µg lyophilized stock. Each flask was supplemented with 2 ng/ml GM-CSF and 10 % Penicillin G (10, 000 units/ml) and Streptomycin sulfate (10,000 µg/ml) in 0.85 % saline (Gibco, Invitrogen Corporation, NY, USA) and incubated (370 Series Steri-Cycle, Thermo Electron Corporation, OH, USA) at 37 °C in 5 % CO_2 and > 95 %

relative humidity. Cell suspensions were maintained at densities between 2 x 10^4 cells/ml to 4 x 10^5 cells/ml by subculturing.

Subculturing

Flasks were subcultured every 48 to 72 hours depending on the desired cell concentration. Cultures were visually assessed at 20X and 40X magnification using brightfield microscopy (Nikon Eclipse TE 2000-U, Japan) to ensure morphology appeared normal and suspensions remained free of contaminants prior to passaging. Morphology was recorded periodically using a digital camera (Digital Sight DS-U1, Nikon, Japan) and imaging software (ACT-2U 2004, Nikon, Japan). Contents of each flask were mixed well by gentle pipetting and a 0.1 ml aliquot removed aseptically followed by a 1 in 1 dilution with 0.4 % trypan blue in phosphate buffered saline (Sigma-Aldrich, MO, USA). A 10 µl aliquot of the mixture was added to each of two counting chambers of a hemacytometer and the number of cells within each counting square was tallied and used to calculate total cell concentrations (Eq A.2) and % viability (Eq A.3):

$$\text{cell concentration} = \text{cell count} / \#\text{ squares counted} \cdot d_f \cdot 10^4 \qquad \text{(Eq A.2)}$$

$$\%\text{ viability} = \#\text{ live} / (\#\text{ live} + \#\text{ dead}) \qquad \text{(Eq A.3)}$$

where d_f is the dilution factor.

The Coulter counter was used periodically to verify hemacytometer cell counts and assess population distribution. Subcultures were prepared by splitting the contents of each flask by at least half the initial volume followed by dilution in warm (37 °C) fresh cell culture media prepared with 10 % FBS. GM-CSF and Penicillin-Streptomycin were added to the final volume as detailed above.

Centrifugation between subcultures was avoided to minimize stress on the cells and prevent clumping.

Prior to experimental use TF-1 cells were prepared by centrifugation at 100 x g for 5 minutes at RT, the supernatant decanted and the cells re-suspended in warm (37 °C) RPMI 1640 SFM and centrifugation and washing repeated. After the first wash the contents of each flask were combined and centrifugation and washing repeated a second time and the cells re-suspended to a final concentration of between 2 x 10^7 cells/ml and 5 x 10^7 cells/ml in SFM. Cells used for experimental purposes were passaged between 6 and 18 times.

Establishing the TF-1 Cell Bank

A TF-1 cell bank was established once the initial culture was expanded sufficiently to grow enough cells to freeze about 20-25 vials at a concentration of 5 x 10^6 cells/ml each. Cell suspensions from each flask were transferred to 50 ml sterile conical test tubes (BD Falcon) and centrifuged at 100 x g for 5 min at RT. Freezing media was prepared with RPMI 1640 supplemented with 10 % FBS and 10 % dimethyl sulphoxide (DMSO, Cryoserv, Edwards Lifesciences Corporation, CA, USA). Cells were re-suspended to freezing concentrations with freezing media and 1 ml aliquoted into 1.5 ml sterile cryotubes marked with the TF-1 cell lot number, cell concentration, date prepared in culture, and date frozen. Tubes were sealed tightly, secured in aluminum canes and placed in a controlled rate freezer (PLANAR kryosave 30-SV, T.S. Scientific). The PLANAR was programmed to freeze cells at 1 ˚C/min to -80 ˚C at which point they were transferred to liquid nitrogen for long term storage.

Immunophenotyping

CD33 R-phycoerythrin (R-PE)-conjugated mouse anti-human monoclonal antibody; R-phycoerythrin (R-PE)-conjugated mouse IgG_1, κ monoclonal immunoglobulin isotype control; CD71 allophycocyanin (APC)-conjugated mouse anti-human monoclonal antibody; allophycocyanin (APC)-conjugated mouse IgG2a, κ monoclonal immunoglobulin isotype control; CD34 (8G12), peridinin chlorophyll (Per CP)-conjugated mouse anti-human monoclonal antibody; peridinin chlorophyll (Per CP)-conjugated mouse IgG_1, κ monoclonal immunoglobulin isotype control; and CD34 fluorescein isothyocyanate (FITC)-conjugated mouse anti-human monoclonal antibody were all purchased from Becton Dickinson Pharmingen (ON, Canada).

TF-1 cells were washed twice and concentrated to 2 x 10^7 cells/ml as outlined previously (see subculturing). Between 1 x 10^6 and 2 x 10^6 cells were incubated at 4 ˚C in the dark (ice bucket) for 30-45 minutes in microtubes containing cold (4 °C) stain buffer and a pre-titrated optimal concentration of fluorescent monoclonal antibody or immunoglobulin isotype-matched control, prepared to a final volume of 0.5 ml. RPMI 1640 prepared either with or without 10 % FBS was used as the stain buffer, depending on the application. SFM was always used for applications involving liposomes. Optimal concentrations for monoclonal antibodies were determined by titrations between 2 µl and 20 µl. Cell samples incubated with individual fluorescent antibodies were prepared to determine the level of fluorescence signal overlap and to establish proper compensation during flow cytometry. For isotype controls and liposome treated

cells all three immunoglobulins or monoclonal antibodies were combined in a single tube. At the end of the incubation period cells were pelleted by centrifugation at 300 x g for 5 min at 4 °C (2417R, Eppendorf, Hamburg, Germany). Cells were washed twice with 1 ml volumes of cold stain buffer and re-suspended to a final volume of 0.5 ml. Samples were kept on ice and analyzed by flow cytometry within 30 minutes.

Flow Cytometry

Flow cytometric analysis (FACS analysis) for cellular fluorescence was performed using a six colour FACSCanto (Becton Dickinson, MA, USA) equipped with a helium neon laser exciting at wavelengths of 488 nm and 633 nm. For each sample, 15 000 events were collected at a low flow rate that consisted of forward scatter (FSC, 488 nm/10 bandpass (BP)), side scatter (SSC, 488 nm/10 BP) and fluorescence emission centered at 525 nm (FL1-FITC/fluorescein), 575 nm (FL2-PE), 678 nm (FL3-PerCP), 650 nm (FL3-7AAD), and 660 nm (FL4-APC). FSC and SSC were collected on either a linear or logarithmic scale while fluorescence was collected on a logarithmic scale. Electronic compensation was applied when two or more fluorochromes were present to correct for the spectral overlap of fluorescent emissions during excitation by a single wavelength. FACSDiva 4.0 and CellQuest software (BD Biosiences, CA, USA) was applied for the analysis.

Colony Assay

The MethoCult® Starter Kit contained all the supplies required for the colony assay and was purchased from Stem Cell Technologies (Vancouver, BC).

Methocellulose media supplemented with 10 ng/ml human rhGM-CSF, 10 ng/ml recombinant IL-3, 3 U/ml recombinant EPO, 50 ng/ml recombinant stem cell factor, 2 mmol/L L-glutamine, 10^{-4} mol/L 2-mercaptoethanol, 1 % bovine serum albumin (BSA), and 30 % FBS was used to detect and quantify human hematopoietic progenitor cells. Using aseptic techniques and sterile supplies, cells were diluted to between 200 and 500 cells/ml with Iscove's MDM media modified with 2 % FBS. For a duplicate assay 0.3 ml of diluted cells was added to thawed MethoCult® tubes and the contents vortexed vigorously and left to stand 5 minutes. The cell-methylcellulose mixture was dispensed in 1.1 ml aliquots into two 35 mm culture dishes using a 16-gauge blunt-end needle attached to a 3 cc syringe, distributed evenly by rotating and the lid replaced. Both 35 mm culture dishes were placed inside a single 100 mm culture dish with a third 35 mm dish containing 3 ml of sterile dH_2O left uncovered. The 100 mm dish was covered and incubated at 37 ˚C, 5 % CO_2 in air and > 95 % humidity for 14-16 days. Colonies were enumerated *in situ* at the end of the incubation period under high (40X) and low (10X) power using the inverted microscope.

A.3 RESUTS AND DISCUSSION

TF-1 Cell Morphology and Viability

The average pre-freeze viability determined by trypan blue exclusion for each culture flask prior to banking was 97 %. The average percent recovery of cells thawed from the bank was 50 ± 7.5 (Table A.1). Variability in post-thaw recovery of cells cryopreserved from different culture flasks may be a result of

inaccurate pre-freeze cell count which was calculated as the average between flasks 1 and 2 of each subculture flask (A-D). Cells were maintained on ice following addition of the cryoprotective media in order to minimize DMSO toxicity at RT however this may have affected DMSO permeability across the cell membrane, preventing the desired intracellular CPA concentration from being reached (6). The appearance of bacterial contamination four days from the onset of thawing the initial frozen stock acquired from ATCC may also be a contributing factor. Antibiotics were not used during culture prior to the appearance of bacteria. Bacterial contamination was eliminated by daily centrifugation and washing (2X) of the cell samples at 100 x g and the introduction of Penicillin-Streptomycin (1/100) into the culture flask. Daily washing and centrifugation was repeated until bacterial contamination was no longer visible (~ 1 week) at which time passaging by dilution was resumed. While measures were taken to eliminate bacterial contamination, a low level of contamination which was undetectable prior to banking may explain the low post-thaw recovery. Regardless of the low post-thaw recovery, cells remained healthy, free of bacterial contamination, and normal cell morphology was observed during culture (Figure A.1). Initial cell division occurred 48 to 72 hours post-thaw with doubling times every 24 hours thereafter.

TF-1 Cell Characterization

Titration of TF-1 cells with a single monoclonal antibody conjugated to a discrete fluorophore determined the optimal concentration required for each specific antibody during immunophenotying analysis. Optimal concentrations for CD33-

PE, CD34-PerCp and CD71-APC at a maximum cell concentration of 2 x 10^6 cells/ml are 2 µl, 10 µl and 20 µl, respectively (Figure A.2). For isotype-matched controls and CD34-FITC, 20 µl of each was used. Immunophenotyping analysis at optimal antibody concentrations indicates the TF-1 cell line used in this study is 99 % positive for CD33 and CD34 antigens and highly proliferative (Figure A.3(b, c, d)). Variable expression of the cell proliferation marker CD71 is detectable during immunophenotyping analyses (Figure A.4), however cells in the active phases of the cell cycle have been shown to express a higher density of the transferrin receptor (7), therefore these results are not considered unusual. TF-1 cells incubated with isotype-matched controls are > 99 % negative for fluorescence, eliminating the concern for non-specific binding of antibody isotypes (Figure A.3(f)).

Since TF-1 cells are 99 % positive for the CD34 antigen, colony growth on methylcellulose supplemented with GM-CSF, IL-3 and EPO should yield an equivalent number of colonies to the number of cells plated. When cells were prepared to a concentration of 300 cells/ml or 500 cells/ml and 0.3 ml added to each Methocult tube, the average number of colonies at the end of a 16 day incubation period is 30 ± 0.5 (n = 2) and 47 ± 2 (n = 2), respectively. Immunophenotyping analysis and assessment of clonogenic output for the TF-1 cell line confirmed that TF-1 cells established and maintained in culture 4-5 weeks using the methods outlined, remained pure, were functionally viable, and retained the capacity to proliferate and differentiate.

A.4 CHALLENGES AND WORDS OF ADVICE

Due to tremendous difficulties establishing healthy TF-1 cultures it is important to emphasize a few points. ATCC recommends maintaining TF-1 cultures between 3 x 10^4 and 5 x 10^5 viable cells/ml without exceeding a cell concentration of 7 x 10^5 cells/ml. It was found that maintaining cultures at or below 3 x 10^5 cells/ml without exceeding 4 x 10^5 cells/ml is more conducive to prevent cell clumping. Passaging by dilution with fresh cell culture media rather than by centrifugation and re-suspension is recommended to avoid unnecessary stress on the cells and enables detection of low levels of bacterial contamination that may otherwise be overlooked. Sigma-Aldrich was found to be a reliable supplier for GM-CSF. The lyophilized form is nearly undetectable with the naked eye but is easily reconstituted in sterile dH_20. Other suppliers such as Stem Cell Technologies required reconstitution of GM-CSF in phosphate buffered saline and BSA. The use of BSA is unnecessary as serum in the form of FBS is present in the media preparation. This approach is cumbersome and is a potential source for introducing contamination. Culture flasks with filter top lids were used on a regular basis to prevent contamination from the incubator. Filter top lids are not normally supplied for use with non-tissue culture treated flasks and as a result had to be ordered separately and transferred to the flasks aseptically. Disinfection of the incubator prior to starting up a new culture is highly recommended.

Extensive measures were taken to prevent bacterial contamination in the cell line however bacteria was still detectable. RPMI-1640, GM-CSF and FBS used

in the cell preparations were monitored for microbial contamination using Difco™ Hycheck™ slides (BD Biosciences) and came up negative therefore the cell line itself (direcly from ATCC) could not be eliminated as a possible source of contamination. While ATCC does not recommend using antibiotics for culture of TF-1 cells, antibiotics appeared to be the only solution to preventing contamination, and based on routine immunophenotyping analysis, did not alter defining characteristics.

A.5 REFERENCES

1. Kitamura T, Tange T, Terasawa T, Chiba S, Kuwaki T, Miyagawa K, et al. Establishment and characterization of a unique human cell line that proliferates dependently on GM-CSF, IL-3, or erythropoietin. J Cell Physiol 1989;140:323-334.
2. Freeman SD, Kelm S, Barber EK, Crocker PR. Characterization of CD33 as a new member of the sialoadhesin family of cellular interaction molecules. Blood 1995;85(8):2005-2012.
3. Civin CI, Strauss LC, Brovall C, GFackler MJ, Schwartz JF, Shaper JH. Antigenic analysis of hematopoiesis. III. A hematopoietic progenitor cell surface antigen defined by a monoclonal antibody raised against KG-1a cells. J Immunol 1984;133(1):157-65.
4. Cazzola M, Bergamaschi G, Dezza L, Arosio P. Manipulations of cellular iron metabolism for modulating normal and malignant cell proliferation: achievements and prospects. Blood 1990;75(10):1903-1919.

5. Sutherland R, Delia D, Schneider C, Newman R, Kemshead J, Greaves M. Ubiquitous cell-surface glycoprotein on tumor cells is proliferation-associated receptor for transferrin. Immunology 1981;78(7):4515-4519.

6. Hunt CJ, Armitage SE, Pegg DE. Cryopreservation of umbilical cord blood: 1. Osmotically inactive volume, hydraulic conductivity and permeability of CD34+ cells to dimethyl sulphoxide. Cryobiology 2003;46:61-75.

7. Chitambar CR, Masey EJ, Seligman PA. Regulation of transferrin receptor expression on human leukemic cells during proliferation and induction of differentiation. J Clin Invest 1983;72:1314-1325.

Table A.1: Post-thaw recovery of cryopreserved (10 % DMSO) TF-1 cells from the cell bank.

Thaw Date	Subculture Designation	Post-thaw Cell Membrane Integrity (%)
25-11-05	B1	72
07-02-06	D1	38
08-03-06	D2	42
18-04-06	C2	63
21-04-06	D1	34
	Average ± SE	**50 ± 7.5**

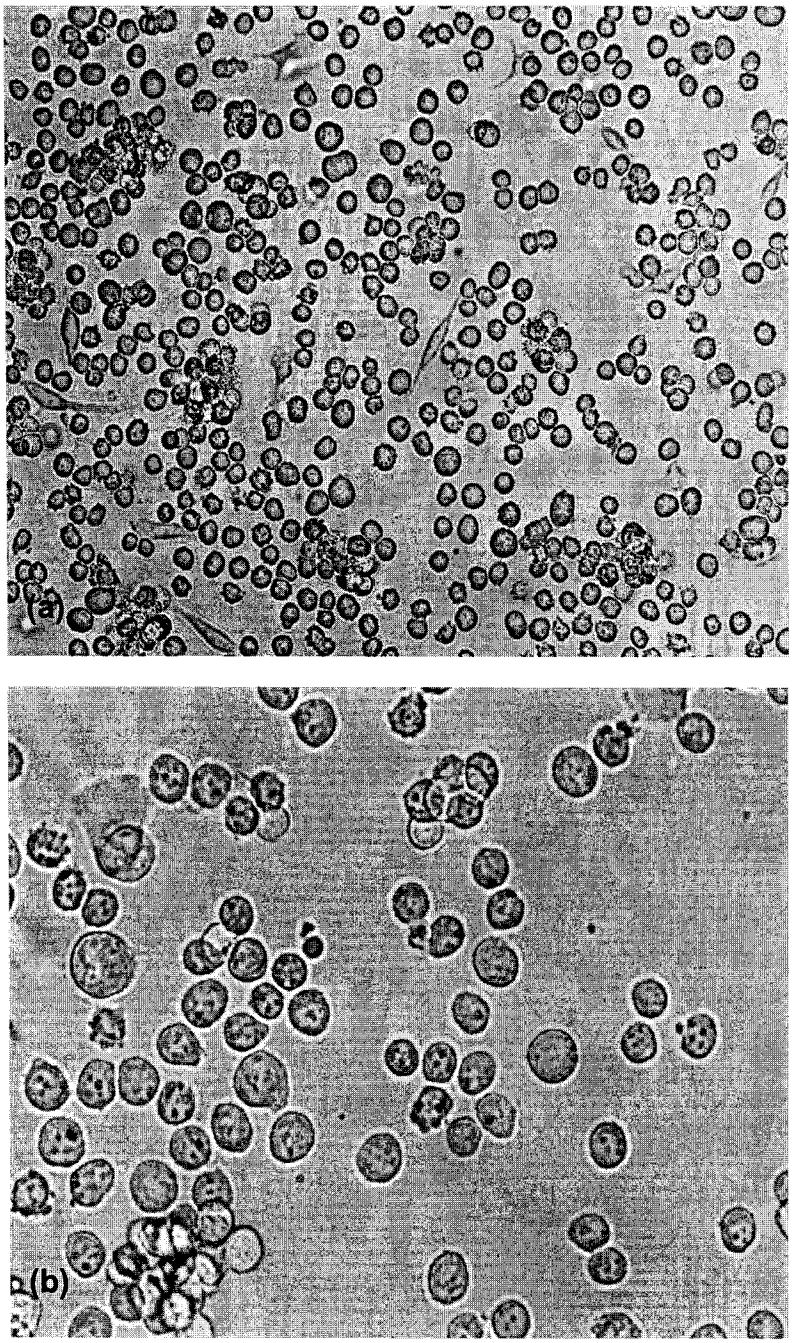

Figure A.1: TF-1 cell morphology during culture at (a) 20X and (b) 40X magnification.

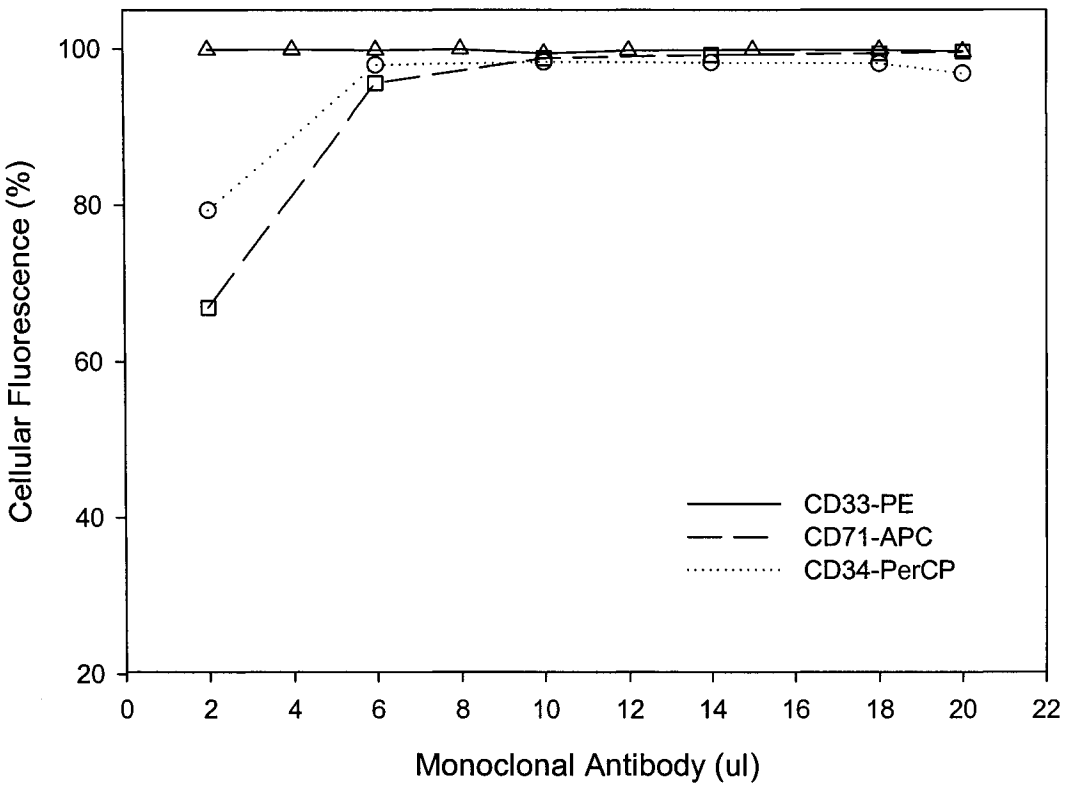

Figure A.2: TF-1 cell monoclonal antibody titration.

(a) untreated

(b) CD33-PE

(c) CD34-PerCP

(d) CD71-APC

(e) CD33/34/71

(f) IgGs

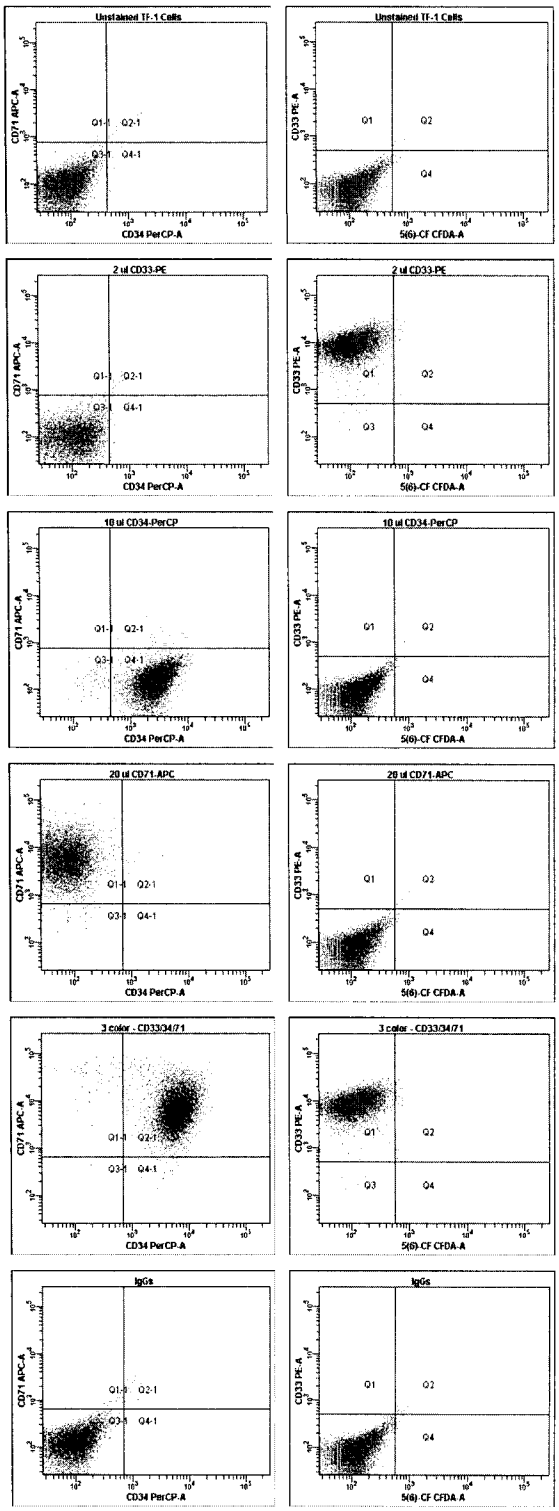

Figure A.3: Immunophenotyping analysis at optimal antibody concentrations: (a) untreated TF-1 cells and TF-1 cell antigen expression following addition of monoclonal antibodies (b) CD33, (c) CD34, (d) CD71, (e) CD33/34/71, and (f) IgG isotype controls.

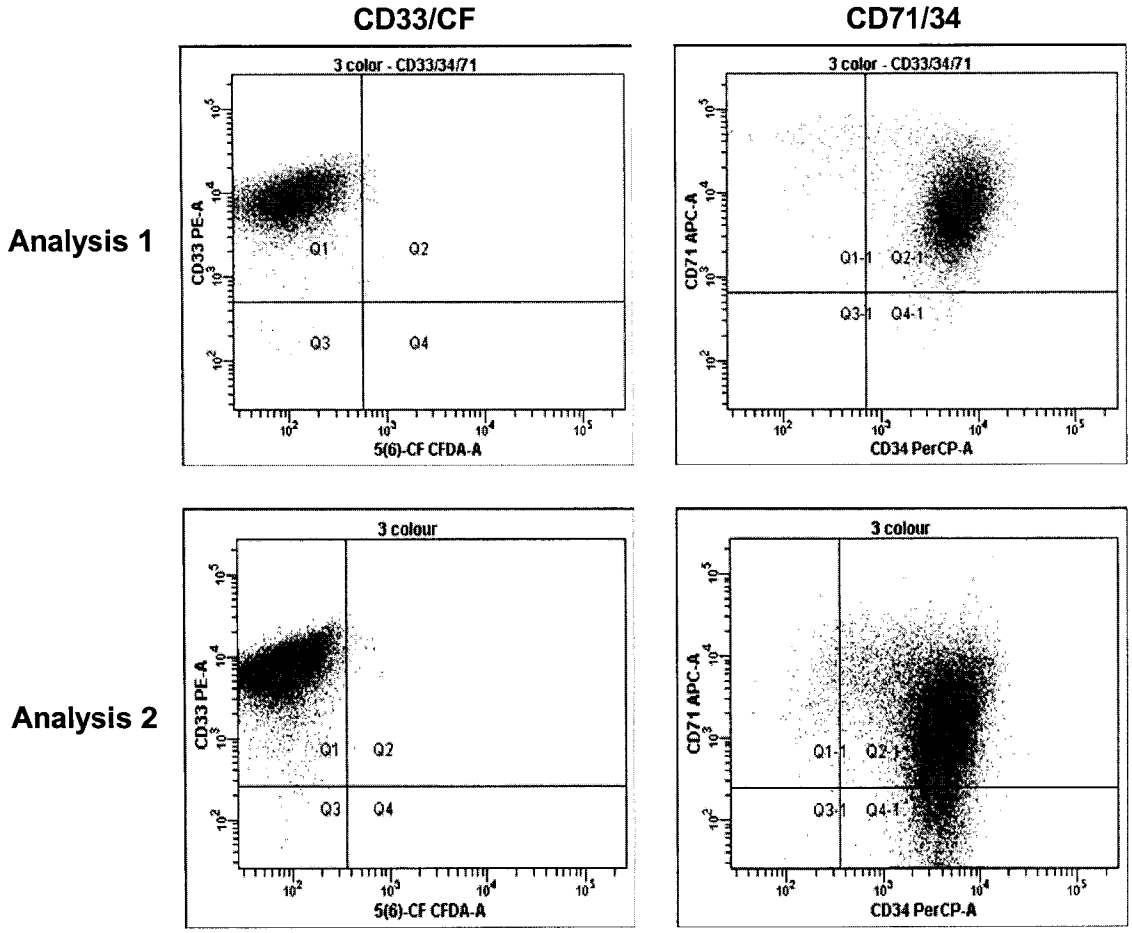

Figure A.4: Variability in TF-1 cell CD71 antigen expression. Following immunophenotyping analysis of TF-1 cells variable CD71 antigen expression is apparent during repeated analysis of a single culture, however, CD33 and CD34 antigen expression remains constant.